AD-A057 330 DAYTON UNIV OHIO RESEARCH INST F/G 6/16
A MATHEMATICAL MODEL OF BONE REMODELING.(U)
MAY 78 D M HEGEDUS F33615-75-C-5054
UNCLASSIFIED AMRL-TR-76-40 NL

1 OF 2
AD A057330

(2) LEVEL II

(18) (19) AMRL-TR-76-40

(6) A MATHEMATICAL MODEL OF BONE REMODELING.

(9) Technical rept. Dec 74-Mar 76,

(10) DAVID M. HEGEDUS
THE UNIVERSITY OF DAYTON RESEARCH INSTITUTE
DAYTON, OHIO 45469

(12) 123 p.

(11) MAY 1978

(15) F33615-75-C-5054

(16) 7231 (17) 05

Approved for public release; distribution unlimited.

AEROSPACE MEDICAL RESEARCH LABORATORY
AEROSPACE MEDICAL DIVISION
AIR FORCE SYSTEMS COMMAND
WRIGHT-PATTERSON AIR FORCE BASE, OHIO 45433

NOTICES

When US Government drawings, specifications, or other data are used for any purpose other than a definitely related Government procurement operation, the Government thereby incurs no responsibility nor any obligation whatsoever, and the fact that the Government may have formulated, furnished, or in any way supplied the said drawings, specifications, or other data, is not to be regarded by implication or otherwise, as in any manner licensing the holder or any other person or corporation, or conveying any rights or permission to manufacture, use, or sell any patented invention that may in any way be related thereto.

Please do not request copies of this report from Aerospace Medical Research Laboratory. Additional copies may be purchased from:

National Technical Information Service
5285 Port Royal Road
Springfield, Virginia 22161

Federal Government agencies and their contractors registered with Defense Documentation Center should direct requests for copies of this report to:

Defense Documentation Center
Cameron Station
Alexandria, Virginia 22314

TECHNICAL REVIEW AND APPROVAL

AMRL-TR-76-40

This report has been reviewed by the Information Office (OI) and is releasable to the National Technical Information Service (NTIS). At NTIS, it will be available to the general public, including foreign nations.

This technical report has been reviewed and is approved for publication.

FOR THE COMMANDER

HENNING E. VON GIERKE
Director
Biodynamics and Bioengineering Division
Aerospace Medical Research Laboratory

AIR FORCE/56780/7 June 1978 — 150

SECURITY CLASSIFICATION OF THIS PAGE *(When Data Entered)*

REPORT DOCUMENTATION PAGE		READ INSTRUCTIONS BEFORE COMPLETING FORM
1. REPORT NUMBER AMRL-TR-76-40	2. GOVT ACCESSION NO.	3. RECIPIENT'S CATALOG NUMBER
4. TITLE *(and Subtitle)* A MATHEMATICAL MODEL OF BONE REMODELING		5. TYPE OF REPORT & PERIOD COVERED Technical Report December 1974 to March 1976 6. PERFORMING ORG. REPORT NUMBER
7. AUTHOR(s) David M. Hegedus		8. CONTRACT OR GRANT NUMBER(s) F33615-75-C-5054
9. PERFORMING ORGANIZATION NAME AND ADDRESS University of Dayton Research Institute 300 College Park Avenue Dayton, Ohio 45469		10. PROGRAM ELEMENT, PROJECT, TASK AREA & WORK UNIT NUMBERS 62202F; 7231-05-18
11. CONTROLLING OFFICE NAME AND ADDRESS Aerospace Medical Research Laboratory, Aerospace Medical Division, Air Force Systems Command, Wright-Patterson Air Force Base, Ohio 45433		12. REPORT DATE May 1978 13. NUMBER OF PAGES 123
14. MONITORING AGENCY NAME & ADDRESS*(if different from Controlling Office)*		15. SECURITY CLASS. *(of this report)* UNCLASSIFIED 15a. DECLASSIFICATION/DOWNGRADING SCHEDULE

16. DISTRIBUTION STATEMENT *(of this Report)*

Approved for public release; distribution unlimited.

17. DISTRIBUTION STATEMENT *(of the abstract entered in Block 20, if different from Report)*

18. SUPPLEMENTARY NOTES

19. KEY WORDS *(Continue on reverse side if necessary and identify by block number)*

Adaptive Elasticity
Biomechanics
Bone Remodeling

20. ABSTRACT *(Continue on reverse side if necessary and identify by block number)*

Living bone is continually undergoing processes of growth, reinforcement and resorption. These processes are termed collectively "remodeling." The remodeling processes in living bone are the mechanisms by which the bone adapts its histological structure to long-term changes in loading. Prolonged straining of a bone tends to make the bone stiffer, stronger and more dense; conversely, a living bone not subjected to its accustomed strain level will, in

→ over

DD FORM 1 JAN 73 1473 EDITION OF 1 NOV 65 IS OBSOLETE

SECURITY CLASSIFICATION OF THIS PAGE *(When Data Entered)*

time, become more compliant, weaker and more porous. An example of this occurs when men are subjected to prolonged weightlessness, such as in the Skylab experiments. Other questions of interest involve the effects of prolonged inactivity on the strength of bones, and therefore on the physical fitness of personnel. For this reason it is useful to construct a mathematical model describing the stress adaptation properties of living bone in order to predict what exercise regimen might be most effective in stopping, or at least controlling, the skeletal degeneration brought on by weightlessness and/or physical inactivity.

This report describes a mathematical model for the stress adaptation of cancellous bone. In Section I, the basic anatomical and physiological properties of bone which bring about remodeling are reviewed. Section II develops a general theory of adaptive elasticity that is capable of describing the trabecular adaptation of cancellous bone. In Section III, the general governing equations developed in the previous section are specialized to the case of two-dimensional adaptation to plane stress and numerical procedures as well as applications are discussed. Finally, Section IV describes the experimental procedures by which the material coefficients discussed in Section II can be measured experimentally.

TABLE OF CONTENTS

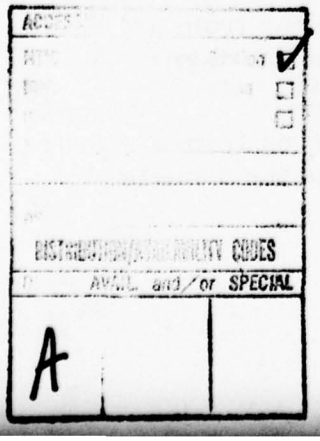

LIST OF FIGURES

LIST OF FIGURES (Continued)

PREFACE

The work described in this report was performed under Contract F33615-75-C-5054, Task Number 723105, Work Unit 7231-05-18 during the period from December 1974 to March 1976.

INTRODUCTION

Living bone is continually undergoing processes of growth, reinforcement and resorption. These processes are termed collectively "remodeling." The remodeling processes in living bone are the mechanisms by which the bone adapts its histological structure to long-term changes in loading. Prolonged straining of a bone tends to make the bone stiffer, stronger and more dense. This is why a person in the later stages of recovery from a broken leg is encouraged to walk on his healing limb. Conversely, a living bone not subjected to its accustomed strain level will, in time, become more compliant, weaker and more porous. An example of this occurs when men are subjected to prolonged weightlessness such as in the recent Skylab experiments. Researchers have noted that after these astronauts were subjected to months of weightlessness, the mineral content of their bones had decreased significantly. They estimate that for longer periods of weightlessness, such as might occur on a flight to Mars, this skeletal degeneration (as well as concomitant atrophy in the cardiovascular system) might become dangerous. Other questions of interest involve the effects of prolonged inactivity on the strength of bones, and therefore on the physical fitness of personnel. For this reason it is useful to construct a mathematical model describing the stress adaptation properties of living bone in order to predict what exercise regimen might be most effective in stopping, or at least controlling, the skeletal degeneration brought on by weightlessness and/or physical inactivity.

This report describes a mathematical model for the stress adaptation of cancellous bone. The model is a generalization of the mathematical theory for the stress-adaptation of cortical bone originally developed by the author in 1971 and first presented publicly at the ASME Biomechanics Symposium in Atlanta, Georgia in June, 1973 (Hegedus, 1973). More detailed development of the cortical bone model can be found in the author's dissertation (Hegedus, 1976) and in two other papers that the author has written in collaboration with Prof. S. C. Cowin (Cowin and Hegedus, 1976, and Hegedus and Cowin, 1976). The development of the theory of adaptive elasticity is in this paper.

In Section I, we will review the basic anatomical and physiological properties of bone which bring about remodeling. In Section II, we develop a general theory of adaptive elasticity that is capable of describing the trabecular adaptation of cancellous bone. In Section III, the general governing equations developed in the previous section are specialized to the case of two-dimensional adaptation to plane stress. We also describe and cite results from a computer program that analyzes problems in two-dimensional adaptive elasticity. Finally, in Section IV, the experimental procedure is described by which the material coefficients, discussed in Section II, can be measured experimentally.

SECTION I

THE BIOLOGICAL PROPERTIES OF LIVING BONE

I. 1 INTRODUCTION

In this Section we will review the physiological and anatomical properties of bone that are of interest in the present study. A more detailed description of the anatomy and physiology of bone is given by McLean (1958). Herrman and Liebowitz (1972) and Kummer (1972) have written comprehensive review articles on the mechanical properties of living bone.

First we will discuss the gross anatomy and histology of bone (pertinent to bone remodeling) and then consider the physiological mechanisms within bone which bring about bone remodeling. In Subsection 4, the external conditions which bring about remodeling and the structural changes by which remodeling manifests itself will be discussed.

I. 2 THE STRUCTURE OF BONE

a. Gross Anatomy

There are two major histological classes of bone tissue which significantly contribute to the structural strength of the skeletal system. They are called cancellous and cortical bone. First, cancellous bone will be described. Figure 1 shows a partial longitudinal section of a thigh bone, or femur. Toward the central axis, in the epiphyseal region (near the joints), there exists a network of hard, interconnected filaments called "trabeculae." Interspersed among the trabeculae are marrow (blood generating tissue) and a large number of small blood vessels. The tissue, consisting of the trabeculae, the marrow, and the blood vessels, is called collectively "cancellous bone," "trabecular bone," or "spongy bone."

Lining the inner surface of the marrow cavities is a thin layer of specialized tissue called endosteum. Similarly, the periosteum covers the entire outer surface of the femur, except for a portion of the femoral neck. The endosteum and periosteum are involved in the regeneration of bone when a fracture occurs. Immediately below the periosteum, on the outer surface of the epiphyseal region, there is a layer of harder, denser tissue called "cortical bone." Cortical bone contains no marrow and its blood vessels are microscopically small. The details of its microstructure will be discussed in the next subsection. As we can see in Figure 1, as one moves from the epiphyseal region into the diaphyseal region (away from the joints), (1) the trabeculae of the cancellous bone become scarcer and thinner and (2) the shaft diameter of the femur decreases, while (3) the layer of cortical bone of the outer surface of the femur becomes thicker. Thus we can conclude that the cancellous bone determines the structural properties of the femur in the epiphyseal regions while the cortical bone determines the structural properties of the femur in the diaphyseal region.

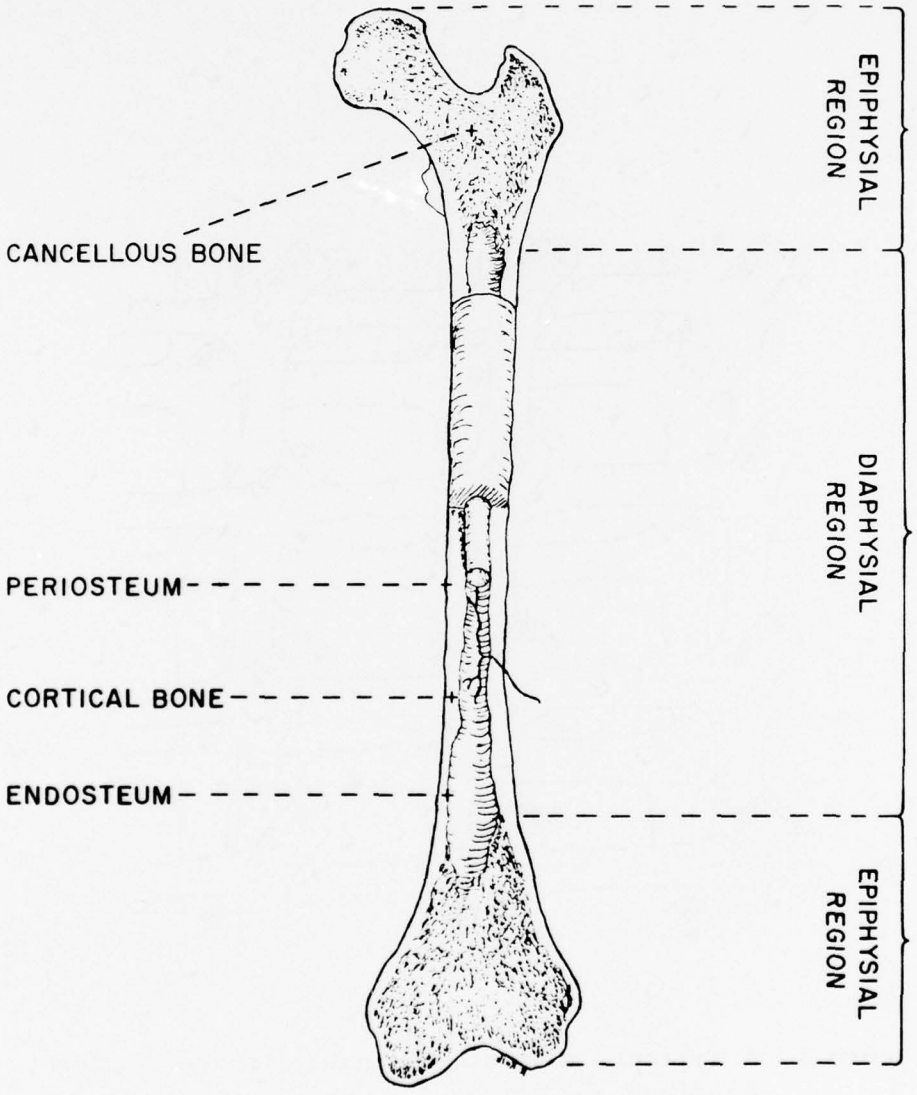

Figure 1. A Longitudinal Section of a Human Femur (redrawn after Kraus (1969)).

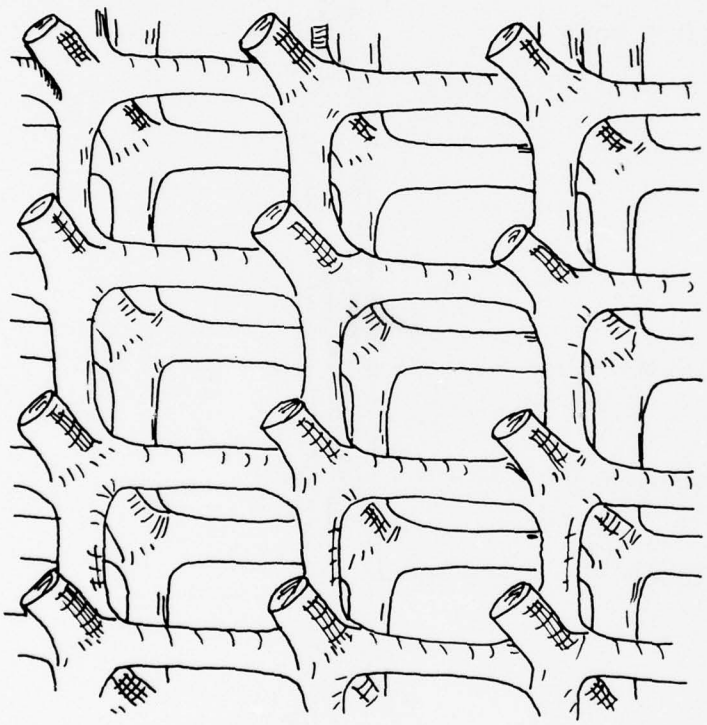

Figure 2. A Typical Trabecular Structure (redrawn after Arnold et al., 1966).

I. 3 THE PHYSIOLOGY OF BONE REMODELING

Remodeling manifests itself as a change in the structural configuration of living bone. By necessity this change of configuration involves a chemical reaction brought about on the microscopic level by the activity of certain cells embedded within the matrix structure.

a. The Bone Cells

Bone remodeling can only take place by the activity of certain cells embedded within its matrix structure. There are three types of bone cells which actively participate in bone remodeling: osteoblasts, osteocytes, and osteoclasts. We will begin by discussing osteoblasts. Osteoblasts synthesize bone material. In the first step of this synthesis, the osteoblast secretes a soluble protein called tropocollagen into the interstitial fluid. The tropocollagen is then polymerized into fibers of bone collagen. Next, the collagen matrix is mineralized by the precipitation of hydroxyapatite crystals into the collagen fibers. According to Frost (1969) this process takes about two weeks.

When an osteoblast completes its building process, it envelopes itself within a hollowing, or lacuna, leaving only a thin cytoplasmic process in contact with the blood supply. Internal changes then occur within the osteoblast and it becomes an ostecyte. The main function of osteocytes is to facilitate the transfer of calcium and other ions between the bone mineral and the blood plasma (McLean, 1958). The osteocytes allow the haversian system of bone to act as a body-wide ion exchange column helping to stabilize the concentration of calcium in the blood plasma.

Neuman and Neuman (1958) have suggested that as an osteon ages, its hydroxyapatite crystals become dehydrated and lose their ability to interact with the plasma. Thus, to maintain the physiological function of bone an old dehydrated osteon must be resorbed, even though its loading remains constant and its anatomical structure remains intact. An osteon is normally resorbed by large multinucleated cells called osteoclasts. It is thought that osteoclasts arise in vivo from the merger of a number of osteocytes or osteoblasts. Such a merger can be observed in vitro by exposing osteocytes or osteoblasts to parathyroid hormone. Chemically, bone resorption is not bone synthesis in reverse; the collagen and the bone mineral are dissolved simultaneously, the protein is hydrolyzed and the mineral is acted on by a chelating agent and possibly a locally high hydrogen ion concentration.

b. The Control of Remodeling

This discussion shows that there are a number of chemical reactions involved in bone remodeling. We turn now to the question of what mechanism controls these chemical reactions. There is no definitive answer to this question; however, there are two phenomena that are likely candidates: one is electrical and the other is chemical.

b. The Microstructure of Bone

Histologically, all bone tissue can be classified as connective tissue (Maximow and Bloom, 1957). One of the distinctive features of connective tissue is thepresence of an abundant extracellular material or matrix. In bone, not only does the matrix account for virtually all the mechanical strength of the bone tissue, but also the volume fraction of the matrix is considerably larger than the volume fraction of the bone cells. In the next section we will discuss the activity and control of the bone cells, and the manner in which they affect remodeling by modifying the microstructure of the bone matrix in which they are embedded.

The primary histological unit of bone structure is the osteon. In cortical bone, the osteons have a cylindrical shape and average 150 micra in diameter and one to two centimeters in length. These osteons have axes, most of which run parallel to the axis of the bone itself, and these osteons are cemented together into bundles by interstitial lamellae. Each osteon has fluid-filled hollowing or lumen along the center of its long axis. The diameter of the lumen is approximately 40 micra. Within each lumen there is a blood vessel that supplies nourishment to the bone cells in the vicinity of that osteon. These blood vessels and lumina are all interconnected into what is called a haversian system. During the development of an osteon, bone generating cells, or osteoblasts, located in the canal deposit a sequence of layers of lamellar bone on the inner wall of the osteon, making the canal successively narrower.

Lamellar bone is a composite material similar in structure to fiberglass. There is a strong but brittle inorganic fraction (crystals of hydroxyapatite) reinforced by a matrix of a tough but flexible organic fraction (mostly the protein collagen). The hydroxyapatite, like the glass filaments in the fiberglass, is oriented in a locally uniform direction or grain. The collagen, unlike the amorphous resin of fiberglass, is also composed of filaments. The collagen fibers run parallel to the long axis of the hydroxyapatite crystals.

In cancellous bone the osteons compose the trabeculae. These osteons do not have any uniform shape. They are often fenestrated plates and sometimes cylinders or truncated cones, connected together into a three-dimensional network called the trabecular structure. A typical trabecular structure is illustrated in Figure 2. The osteons of cancellous bone are, in general, not hollow. The bone cells are nourished by blood vessels outside the trabeculae running within the trabecular structure. Bone resorption and reconstruction can thus be expected to take place from the outside of the osteons rather than from the inside.

In 1953 Fukada (1957) discovered that bone demonstrates a piezoelectric effect. He later went on to demonstrate that this was due to the collagen and he subsequently measured the piezoelectric matrix of both bone and collagen. Thus, there is at least one way in which strain in bone can generate an electric field.

In 1962 Basset and Becker proposed a physiological mechanism for the remodeling of bone in terms of its piezoelectric properties. There are at least two ways in which the presence of an electric field can affect bone growth. Becker and Murray (1970) have recently reported that an electric field is capable of activating the protein synthesizing organelles in osteogenic cells of frogs. The presence of an electric field near polymerizing tropocollagen will cause the fibers to orient themselves perpendicular to the lines of force. Basset and Pawlick (1964) have reported that if a metal plate is implanted adjacent to a living bone, a negative charge on the plate will induce the deposition of new bone material on this negative charged electrode. However, they reported that there was no resorption near the positive electrode. Thus, an electric field may stimulate the activity of osteblasts but have no effect on osteoclasts other than to inhibit their activity.

The second candidate for a controlling mechanism is chemical, the calcium concentration. Calcium has been implicated as a controlling factor in many other biochemical reactions, for instance muscular contraction. Justus and Luft (1970) have demonstrated that straining bone will increase the calcium concentration in the interstitial fluid. He showed that this was due to a change in the solubility of the hydroxyapatite crystals and also demonstrated this mechanochemical effect with inorganic crystals in vitro. A chemical mechanism would be particularly convenient in explaining the stimulation of osteoclastic activity. We mentioned above that there are two different situations which would call for bone resorption and osteoclastic activity: low ambient loading and dehydration of bone mineral. Both of these situations, however, would have the same chemical effect: a lower calcium ion concentration. Thus, if osteoclastic activity were activated by a low calcium concentration both of these effects could be corrected by this same chemical mechanism.

I.4 THE PROCESS OF BONE REMODELING

a. General Observations

We will follow the distinction made by Front (1964) between surface and internal remodeling. Surface remodeling refers to the resorption or deposition of bone material on the surfaces of the endosteum and the periosteum. Surface remodeling can be observed correcting an improperly set fracture in the bones of young children. For instance, if the two ends of a healing femur are set slightly skew to each other, the bone, when it is healed, will tend to bow when a load is placed on it. However, surface remodeling that is particularly pronounced in young children will cause new osteons to

grow on the concave surface, and excess bone material to be eaten away on the convex surface, so as to correct the bowing effect.

Internal remodeling refers to the resorption or deposition of bone material between the surfaces of the periosteum and the endosteum. Because of the rigidity of adjacent matrix material between the periosteal and endosteal surfaces, internal remodeling (in contrast to surface remodeling) cannot change the physical dimensions of a bone. However, there is experimental evidence indicating that internal remodeling can change the porosity, ash content, x-ray opacity and total weight of a living bone, as well as modify its mecahnical properties such as modulus of elasticity and compressive strength.

In this paper, we will limit discussion to the internal remodeling of cancellous bone. A mathematical model of the external remodeling of bone has been suggested by Gjelsvik (1973). The problem of internal remodeling of cortical bone has already been discussed by Hegedus (1976b), Hegedus and Cowin (1973).

b. Remodeling in Cancellous Bone

The general concept of stress-or strain-induced remodeling was first introduced by the German anatomist Julius Wolff (1892) and is often called Wolff's Law. Wolff pointed out that the thickness and orientation of the trabecular plates of cancellous bone seemed to optimize its weight bearing capacity for the particular load configuration to which it was normally subjected.

One of the best examples of this load-optimized structural pattern can be seen in a radiograph of the proximal femur, whose loading configuration is indicated in Figure 3. Koch (1917) analyzed these trabecular patterns and concluded that they could be categorized into tensile and compressive groups which, under ambient loading conditions, carry tensile and compressive loads, respectively. These trabecular groups and their anatomical names are indicated in Figure 4.

The largest load component applied to the human femur is the downward compression applied by the hip to the femoral head. In the femoral head, this compressive load is carried primarily by the Principal Compressive Group of trabeculae that extends from the proximal end of medial diaphysial shaft to the superior surface of the head. Since the loading from the hip is not colinear with the axis of the femur itself, there exists a bending moment in the femoral neck that tends to turn it medially. This bending is opposed by the Principal and Secondary Tensile Groups of trabeculae that extend from the proximal end of the lateral diaphysis, through the neck, to the medial head. The Secondary Tensile Group of trabeculae receives auxiliary support from the Secondary Compressive Group that arises from the medial diaphysial shaft. There exists a fifth trabecular group of lesser structural importance in the vicinity of the Greater Trochanter. This Greater Trochanter Group carries the vertical and medial forces from the muscles which are attached to the Greater Trochanter. In Section V we will

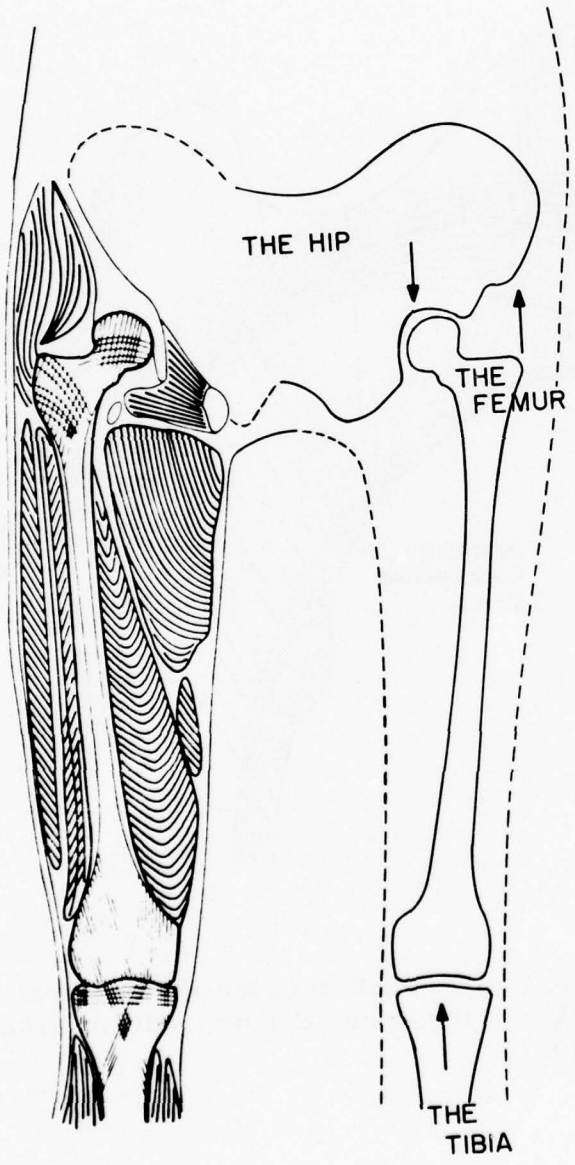

Figure 3. Musculature and Approximate Ambient Loading of a Human Femur (redrawn after Grant (1962), Kummer (1956), and Pauwels (1948)).

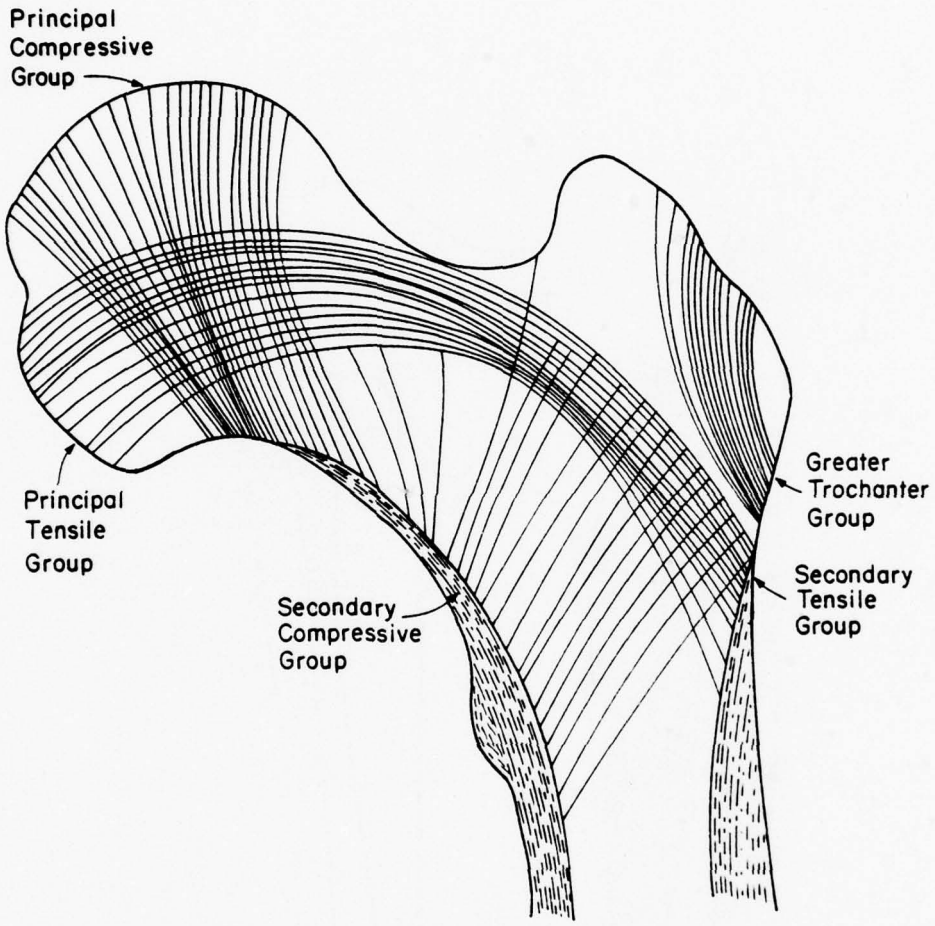

Figure 4. Diagramatic Representation of the Five Normal Groups of Trabeculae of the Upper Femur (redrawn from Singh et al., 1970).

demonstrate a model which will develop these patterns when it is subjected to the loading configuration of a human femur.

c. Immobilization Experiments

One of the earliest quantitative descriptions of internal remodeling in humans was conducted by Dietrick et al (1948). Human volunteers were immobilized from the waist down in plaster casts for periods of from 6 to 8 weeks. During this study their urine, feces, and blood were analyzed for certain organic components such as creatinine as well as certain inorganic components such as calcium and phosphorus. Four days after the plaster casts were removed, they resumed normal activity. The chemical analysis indicated that during the immobilization their bodies suffered a net loss of the bone materials calcium and phosphorus. After normal activity had been resumed, the mineral loss phenomenon was reversed and the body regained calcium and phosphorus. It took approximately six weeks to recover from the effects of this immobilization. When the recovery period had ended, the excretion levels of calcium and phosphorus, had decreased to values indicating that the body had reattained homeostasis with respect to these minerals.

A similar net loss of calcium was reported by Mack et al (1967) for astronauts subjected to weightlessness for periods of four days or more. Mack correlated this calcium loss with a decrease in the x-ray opacity of the bones. It has been pointed out by Brannon et al.(1963) that the skeletal loss in recumbency or weightlessness could be partially reversed if the subject performed certain exercises that apply loading to the bones, which compensates for the loading that would have occurred under conditions of normal gravity. Mack has suggested that the exercises, included in the regimen of the Gemini VII flight, were responsible for the fact that the astronauts of this 14-day mission actually suffered less bone loss than the astronauts of the 8-day Gemini V mission.

Immobilization studies have also been conducted on experimental animals. Kazarian and von Gierke (1967) reported an immobilization study on rhesus monkeys similar to that of Dietrick. The monkeys were divided into two groups. One group was immobilized in whole-body casts, while a control group, given an identical diet, was allowed to have normal activity. After 60 days both groups were sacrificed. An autopsy indicated that the immobilized animals were suffering from osteoporosis, a pathological condition of severely weakened bone. When bone samples from each group were excised, it was observed that the bone from the nonimmobilized animals was stiffer and stronger, and had a higher radiographic density than the bone from the constrained animals. They concluded that the immobilized animals suffered a massive resorption of the trabeculae of their cancellous bone due to the lack of strain stimuli.

d. The Effects of Cyclic Loading

Another significant qualitative study of bone remodeling was inspired by the theoretical work of Pauwels (1948, 1950). Pauwels started with the premise that the diaphysis of the human femur, in normal bipedal activity such as walking or standing, will be subjected to a nonuniform load distribution. As mentioned earlier, the central axis of the femur is not directly over the center of mass of the body and must be pressed medially (inwardly) in order to prevent the leg from buckling outward. Pauwels theorized that this medial bending moment is partially offset on the femur by a constant lateral (outward) bending moment caused by the iliotibial tract. Consequently, a human femur is normally subjected to a periodically medial and lateral bending moment, superimposed on a periodical axial compression. This net loading configuration is illustrated in Figure 5. Pauwels concluded that the adaptive properties of cortical bone would cause the medial and lateral side of the femur to become stiffer and stronger than the anterior and posterior sides (the front and back). Thus the cortical bone of the human femur modifies the distribution of its material strength in a manner that corresponds to its load distribution. This distribution is somewhat analogous to that of an I-beam.

Amtmann (1971), in a study on autopsied human femora, verified such a distribution of material properties. The cortical bone on the medial and lateral sides of the femur was observed to be stiffer, stronger, less porous and more radio-opaque than cortical bone from the posterior and anterior portions. This cyclic loading effect points out an important property of bone remodeling, namely, that bone accretion is not a linear function of the load applied but rather it is some nonlinear function such that cyclic loading causes faster bone accretion than static loading of the same average magnitude.

e. Senile Osteoporosis

As a person ages, the ability of the body to synthesize collagen markedly decreases. Since collagen is an essential component in the synthesis of new bone, aging slows down bone accretion. If bone resorption continues unabated, bone will become weaker and more compliant, even though the loading remains fixed. This disease is called senile osteoporois and is an important cause of debilitation, particularly in elderly women

I. 5 CONCLUSIONS

Living bone, in addition to its structural utility, also fulfills a vital physiological function. It acts as a storage depot for minerals, in particular calcium and phosphorus. Since the body is constantly using calcium and phosphorus, bone is constantly being resorbed. Under normal loading conditions, the excessive removal of bone material in a particular location will induce a greater than normal strain around that point, which will initiate the accretion of new bone material. This constant remodeling of bone has a beneficial effect for the structural utility. It optimizes the distribution of

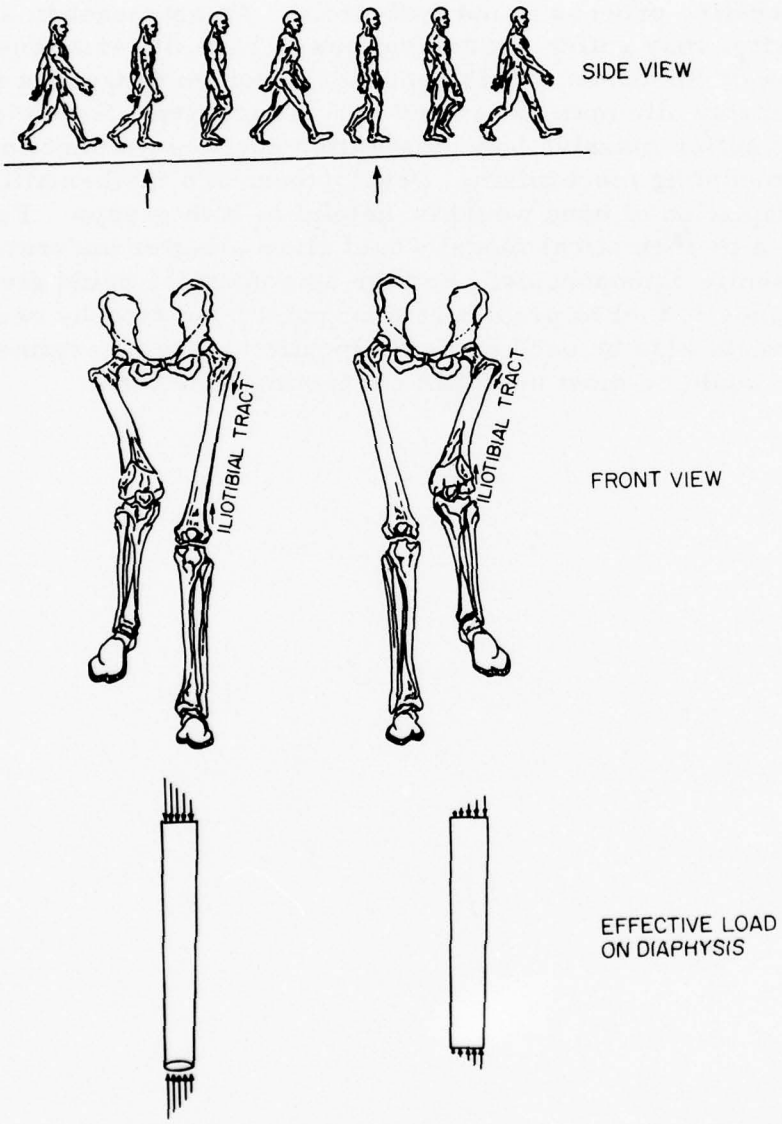

Figure 5. The Effect of Cyclic Loading on the Diaphysis of a Right Femur during Walking (partially redrawn after E. Gardner et al., 1969).

bone material both generally and locally. Generally, if bones are too large or too high in calcium content (and thus too dense), there will be excessive weight and the organism will suffer a competitive disadvantage from the loss of mobility. If, on the other hand, the bone is allowed to be too small or fragile, there is a danger of fracture, in which case the organism would suffer an even more precarious loss of mobility. Locally, this optimization assures that the various regions of a bone undergoing roughly the same average strain carry their proportionate share of the load.

This remodeling process is not fool-proof. An astronaut in space, without normal gravity, may suffer a massive loss of bone material due to a lack of normal stress on his bones. This condition becomes dangerous if he returns to earth and suddenly attempts to resume normal activity. Even elderly people on earth can suffer massive bone resorption due to a malfunction of the normal bone remodeling mechanism. Development of a mathematical model of the stress adaptation of bone would be helpful to both groups. For the elderly patient, a mathematical model would allow a better understanding of the etiology of senile osteoporosis. For the astronaut, it would give medical personnel a diagnostic tool to predict at what point bone atrophy becomes dangerous. It might also be used as a therapeutic tool to determine the types of exercise that would be most useful in correcting bone loss.

SECTION II

THE BASIC GOVERNING EQUATIONS AND THE MODEL

II.1 INTRODUCTION

A mathematical model for the stress-adaption of cancellous bone has been developed in which cancellous bone is represented as a chemically reacting porous medium. The solid constituent of the porous medium represents the matrix structure of the cancellous bone and the perfusant constituent represents the bone cells, the blood vessels, and the interstitial fluid. The strain-adapting properties of bone, caused by the bone cells, is represented by strain-controlled chemical reactions that transfer mass, momentum, energy, and entropy between the solid constituent and the perfusant.

We will begin our analysis by developing a continuum theory of an N-component solid mixture similar to those formulated by Truesdell (1960) and later by Bowen (1968). The next step will be to set the concentration of each of these N "chemical components" equivalent to the thickness of an infinitesimal trabecular plate in an arbitrary direction and consider the limit as N goes to infinity. The resulting General Linear Governing Equations are similar to those characterizing classical linear elasticity except that; (1) there exists a new tensor field representing the trabecular development whose rate of change is a function of the strain; and (2) the compliance in the stress-strain relationship is a function of the trabecular development.

In the next section these generalized governing equations will be specialized to the case of two-dimensional adaptation to plane stress. The conditions of two-dimensional adaptation will be relatively easy to simulate in-vivo, and will allow the collection of experimental data which will be essential in quantitive analysis of bone remodeling.

II.2 THE DESCRIPTION OF THE MODEL

This section presents the basic rationale for the mathematical model of bone remodeling. It begins by summarizing certain basic biological and physical observations of the process of bone remodeling. It then describes how the salient features of these processes can be incorporated into a mathematical model for the stress-adaptation of living bone.

We summarize the salient physical and biological properties as follows:

(1.) There are three basic components of whole bone: the bone cells, the extracellular fluid and the solid extracellular material, which is called the bone matrix.

(2.) The bone matrix is a solid structure with interconnected pores. The mechanical properties of whole bone are essentially the same as the mechanical properties of the matrix.

(3.) The trabecular development of the bone matrix is affected by the ambient long-term strain history of the bone.

(4.) The trabecular development of the bone matrix is changed by the addition of mass or the removal of mass from the bone matrix. This transfer of mass occurs as the result of a chemical reaction which is mediated by the bone cells. Momentum, energy and entropy may also be transferred to or from the matrix structure by these chemical reactions.

(5.) The rates of these chemical reactions depend upon the strain and are very slow. It can be estimated from the studies of Frost (1969), using tetracycline labeling, that the characteristic time for such a reaction normally is in the order of months.

(6.) The extracellular fluid is always in contact with the blood plasma. The plasma supplies the materials necessary for the synthesis of bone matrix.

Considering these observations, we will assume the load-adapting properties of living bone can be modeled by a chemically reacting porous medium in which the rate of reaction is strain-controlled. The porous medium has two constituents: (1) a porous elastic solid representing the matrix structure of bone, and (2) a perfusant, which represents the cells, extracellular fluid and the blood plasma that flow through the matrix structure. A schematic diagram of this model is shown in Figure 6. The fact that living bone is encased in a living organism is reflected in the model by setting the porous structure in a bath of the perfusant. When necessary, we will assume the perfusant bath to be an isothermal heat reservoir, an assumption that appears to be easily justified by common knowledge concerning living organisms. The mechanical load is applied directly to the porous structure across the walls of the perfusant bath as illustrated in Figure 6. The system consisting of the porous structure and its perfusant bath is considered to be closed with respect to mass, heat energy, and entropy transfer, but open with respect to momentum transfer from loading and its associated energy transfer. The system consisting of only the porous structure without its entrained perfusant is open with respect to momentum transfer as well as mass, energy, and entropy transfer. We take the bone matrix as our control system, since the mechanical properties of the bone matrix alone determine the mechanical properties of bone. We shall therefore write balance and constitutive equations for only the bone matrix. The perfusant will be accounted for only insofar as it transfers mass, momentum, energy, or entropy to the bone matrix. The rate at which these transfers of mass, momentum, energy, and entropy occur will depend on the local strain and other independent variables.

The model contains a further simplification. As the porosity of the porous structure changes, the area of the interface between the porous structure and the perfusant will also, in general, change. There is not a direct relation between the porosity and the area of the interface. We shall consider here only porosity changes and we shall not introduce the area of the interface into the model as a

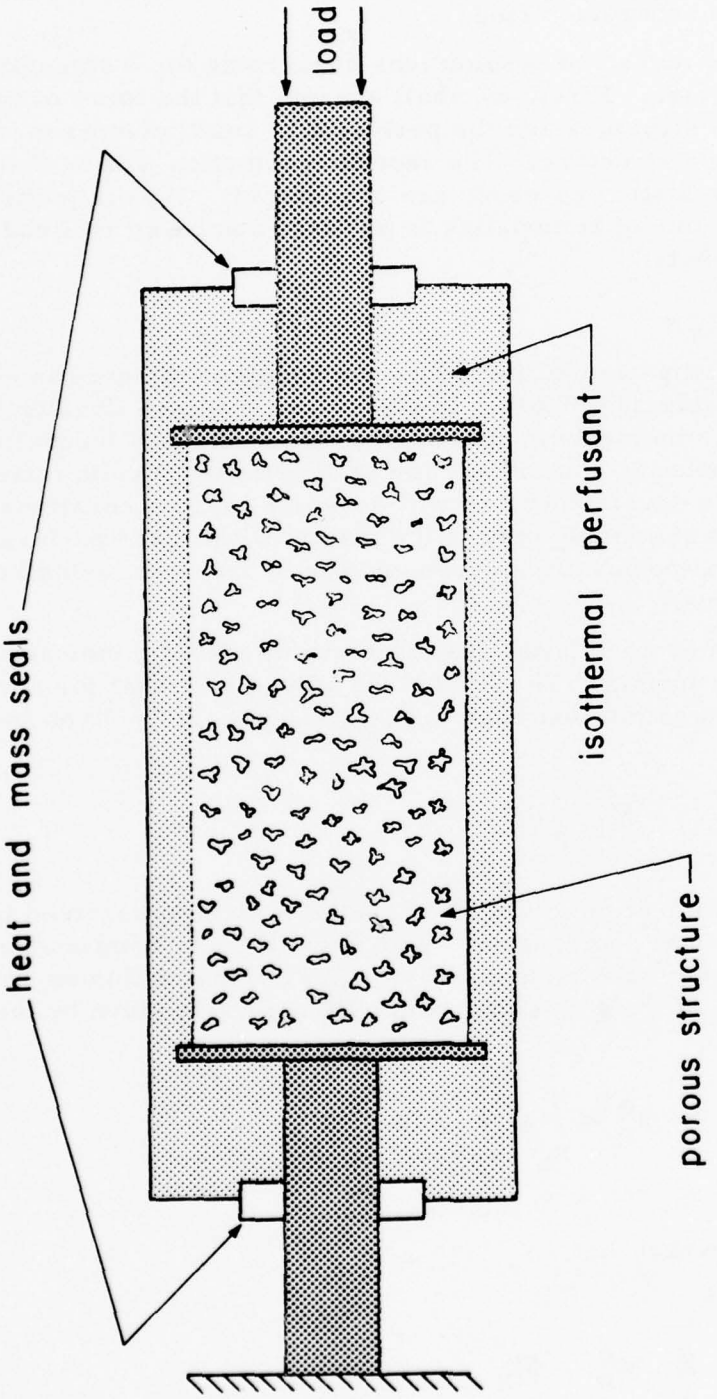

Figure 6. A Schematic Diagram of the Model of Bone Remodeling.

variable. Also, we shall not consider the thermodynamic properties of interior points in the matrix structure. The thermodynamics of the interface in a chemically reacting porous material has been discussed in a recent paper by Bazant (1972) on concrete curing.

We shall also make two assumptions concerning the momentum balance of the porous structure. First, we shall assume that the force of interaction between the porous structure and the perfusant is small compared to the load applied to the porous structure. The second assumption will be that only mechanically quasi-static processes are considered. This is justified because the characteristic time of remodeling is so large compared to a characteristic time for inertia effects.

II. 3 THE NOTATION

In this subsection we will introduce the notation employed in our development of continuum mixture theory. In subsection 4 we will develop balance equations for mass, momentum, and energy and an entropy inequality, and in subsection 5, constitutive constraints for an N component solid mixture will be obtained. In this development we will consider balance equations and governing equations that apply only to the matrix without the perfusant. The effect of the internal perfusant is accounted for by transfer terms in each of the balance equations.

We will begin by postulating the existence of a field ρ indicating the bulk mass density of the matrix. The field ρ has values such that for any arbitrary region, R, the mass within that region, M_R, will always be given by the integral

$$M_R = \int_R \rho \, dv \tag{1}$$

where dv is the element of volume. The solid matrix is assumed to consist of N distinct chemical components. With each of these components we will associate a component bulk mass density, ρ^α, such that within an arbitrary region R, the mass of the α-th component will always be given by the integral.

$$M_R^\alpha = \int_R \rho^\alpha \, dv \tag{2}$$

Of course we can expect that

$$\sum_{\alpha=1}^{N} M_R^\alpha = M_R \tag{3}$$

and thus

$$\sum_{\alpha=1}^{N} \rho^{\alpha} = \rho \cdot \tag{4}$$

Next we will consider the kinematic notation. The position of the particle X_K^{α}, of the α-th component at time, t, will be described by the functional relation

$$x_i^{\alpha} = \chi_i^{\alpha}(X_K^{\alpha}, t) \tag{5}$$

where i = 1, 2, 3 and K = I, II, III are indices labeling the three different coordinate directions in the deformed and reference configurations, respectively. Throughout this entire development we will assume that the N components of a matrix do not move with respect to one another. Thus, in all subsequent development we will consider a single function $x_i = \chi_i(X, t)$ as describing the motion of all components of the mixture. The velocity of the particles is given by

$$v_i = \frac{\partial \chi_i}{\partial t} \tag{6}$$

and the deformation gradients F_{iK} by

$$F_{iK} = \frac{\partial \chi_i}{\partial X_K} \cdot \tag{7}$$

In index notation, a field quantity followed by a subscripted comma and an index, indicates a gradient with respect to the material coordinates. Thus the velocity gradient

$$\underset{\sim}{L} = \text{grad } \underset{\sim}{v}$$

can be written as

$$L_{ij} = v_{i,j} \tag{8}$$

A superimposed dot indicates the material or substantial time derivative. For any arbitrary tensor quantity $\underset{\sim}{f}$ we will have

$$\dot{\underset{\sim}{f}} = \frac{\partial \underset{\sim}{f}}{\partial t} + \underset{\sim}{v} \cdot \text{grad } \underset{\sim}{f}$$

or, in index notation,

$$\dot{f}_i = \frac{\partial f_i}{\partial t} + v_j f_{i,j} \tag{9}$$

Note that in (9) we have employed the summation convention, that is, that over product terms with repeated subscript indices summation is to be performed. This summation convention however will not apply to the superscript indices indicating the chemical component. In this report we will denote this latter index by Greek letters.

Applying (9) to the definition (7), we can see that the time derivative of the velocity gradient will have the form

$$\dot{F}_{iK} = L_{ij} F_{jK} \tag{10}$$

It can also be shown that

$$\text{div } \underset{\sim}{v} \ \det \underset{\sim}{F} = \dot{\overline{\det \underset{\sim}{F}}} \tag{11}$$

or, in index notation,

$$v_{k,k} \det \underset{\sim}{F} = L_{kk} \det \underset{\sim}{F} = \dot{\det \underset{\sim}{F}}, \tag{12}$$

where $\det \underset{\sim}{F}$ is the determinant of the matrix of deformation gradients F_{iK}. The symmetric part of the velocity gradients is called the rate of deformation tensor and is denoted by D_{ij}.

$$D_{ij} = \frac{1}{2}(L_{ij} + L_{ji}) \tag{13}$$

The above notation, as well as that which follows, is generally that employed by Truesdell and Toupin (1960), Truesdell and Noll (1965) and Bowen (1970), with the important exception that we employ Greek superscripts to indicate the index of the chemical component while the previous authors have used Gothic subscripts.

II.4 THE BALANCE EQUATIONS AND THE ENTROPY INEQUALITY

a. Mass Balance

Let us now postulate that the conservation of mass equation for the α-th constituent takes the form

$$\frac{\partial}{\partial t} \int_R \rho^\alpha dv = - \oint_{\partial R} v_i \rho^\alpha n_i \, ds + \int_R \hat{c}^\alpha dv \tag{14}$$

where ∂R is the surface of R, ds is an element of R, and n_i is a unit normal of ∂R and $\hat{c}^\alpha$ is the rate at which constituent α is being generated by the chemical reaction. If we apply the divergence theorem and (9), (14) can be written in the form

$$\rho^\alpha + \rho^\alpha v_{i,i} = \hat{c}^\alpha \tag{15}$$

The conservation of mass for the matrix as a whole can be written to be

$$\frac{\partial}{\partial t} \int_R \rho \, dv = - \oint_{\partial R} v_i \rho \, n_i \, ds + \int_R \hat{c} \, dv \tag{16}$$

where $\hat{c}$ is the total rate at which matter is being generated from all chemical reactions. Again the divergence theorem and (9) give the field equation

$$\dot{\rho} + \rho \, v_{i,i} = \hat{c} \tag{17}$$

If we substitute (15) into (17) and (4), we will have

$$\hat{c} = \sum_{\alpha=1}^{N} \hat{c}^{\alpha} \tag{18}$$

Finally we note that it will be useful for our future development if we define two new sets of field variables which can be used in lieu of ρ and ρ^{α}. These new fields will be called the <u>zero strain bulk matrix mass density</u> and the <u>zero strain bulk component mass density</u>, defined as

$$\gamma = \rho \det \underset{\sim}{F}$$

and (19)

$$\gamma^{\alpha} = \rho^{\alpha} \det \underset{\sim}{F} \, ,$$

respectively. In terms of these new field variables, the conservation of mass equations (17) and (15) can be written as

$$\dot{\gamma} = \hat{c} \det \underset{\sim}{F}$$

(20)

$$\dot{\gamma}^{\alpha} = \hat{c}^{\alpha} \det \underset{\sim}{F} \, ,$$

respectively.

b. Momentum Balance

The conservation of momentum equation for the α-th constituent is given by the relation

$$\frac{\partial}{\partial t}\int_B \rho^\alpha v_i \, dv = -\oint_{\partial B} (\rho^\alpha v_i) v_j n_j \, ds + \oint_{\partial B} T_{ij}^\alpha n_j \, ds + \int_B \rho^\alpha b_i^\alpha \, dv$$

$$+ \int_B (\hat{p}_i^\alpha + \hat{c}^\alpha v_i) \, dv \qquad (21)$$

where T_{ij} denotes the partial stress tensor of the α-th component, b_i is the body force per unit mass of the α-th component, and $\hat{p}_i^\alpha$ is the force applied on the α-th component by all other components and the perfusant. The first three integrals on the right hand side of (8) are customary, the fourth is a departure. The first term in the fourth integrand, $\hat{p}_i^\alpha$, represents the force applied on the α-th component by the (N-1) other components and the perfusant; the second term, $\hat{c}^\alpha v_i$, represents the momentum added to the porous matrix structure due to the addition of mass by the chemical reaction.

Using the divergence theorem, the conservation of mass (15), (21) can be rewritten into the form

$$\rho^\alpha \ddot{x}_i = T_{ij,j}^\alpha + \rho^\alpha b_i^\alpha + \hat{p}_i^\alpha \qquad (22)$$

The conservation of momentum for the matrix as a whole can be postulated to be

$$\frac{\partial}{\partial t}\int_B \rho \, v_i \, dv = -\oint_{\partial B} (\rho v_i) v_j n_j \, ds + \oint_{\partial B} T_{ij} n_j \, ds + \int_B \rho \, b_i \, dv$$

$$+ \int_B (\hat{c} \, v_i + \hat{p}_i) \, dv \qquad (23)$$

where T_{ij} is the total stress tensor for the matrix constituent, defined as

$$T_{ij} = \sum_{\alpha=1}^{N} T_{ij}^{\alpha} \tag{24}$$

b_i is the total body force on the matrix, defined as

$$b_i = \left(\frac{1}{\rho}\right) \sum_{\alpha=1}^{N} \rho^{\alpha} b_i^{\alpha} \tag{25}$$

and $\hat{p}_i$ is the force applied to the matrix by the perfusant. Again use of the divergence theorem and the conservation of mass equation (4) yields the field equation

$$\rho \ \ddot{x}_i = T_{ij,j} + \rho \ b_i + \hat{p}_i \tag{26}$$

Comparison of (22) with (26) gives us

$$\hat{p}_i = \sum_{\alpha=1}^{N} \hat{p}_i^{\alpha} \tag{27}$$

Again, in the special case when $\hat{p}_i^{\alpha} = 0$ for all α, equation (26) reduces to the familiar conservation of momentum equation for a simple continuum.

c. Moment of Momentum Balance

We will next consider balance of moment of momentum. In terms of direct notation, balance of moment of momentum for the α-th component can be postulated to be

$$\frac{\partial}{\partial t}\int_R [\underset{\sim}{x} \times (\rho \ \underset{\sim}{v})] \ dv = -\oint_{\partial R} (\underset{\sim}{x} \times \rho \ \underset{\sim}{v})(\underset{\sim}{v} \cdot \underset{\sim}{ds}) + \oint_{\partial R} \underset{\sim}{x} \times [\underset{\sim}{T} \cdot \underset{\sim}{ds}]$$

$$+ \int_R [\underset{\sim}{x} \times (\rho \ \underset{\sim}{b} + \hat{c} \ \underset{\sim}{v} + \underset{\sim}{\hat{p}}) + \underset{\sim}{\hat{m}}] \ dv \tag{28}$$

where $\underset{\sim}{ds}$ is an element of the surface of ∂R times a unit normal; the binary operand $\times$ denotes the cross product of two vectors; and $\hat{\underset{\sim}{m}}^{\alpha}$ is the momentum supply vector for the α-th component playing a role in (28) analogous to the role of $\hat{\rho}_i^{\alpha}$, in equation (21). Using the divergence theorem, and equations (15) and (22), equation (28) reduces to the form

$$\underset{\sim}{T}^{\alpha} - [\underset{\sim}{T}^{\alpha}]^t = \underset{\sim}{M}$$

or

$$T_{ij}^{\alpha} - T_{ji}^{\alpha} = M_{ij}^{\alpha} \tag{29}$$

where the components of the skew-symetric tensor M_{ij}^{α} are given by

$$M_{11}^{\alpha} = M_{22}^{\alpha} = M_{33}^{\alpha} = 0$$

$$M_{23}^{\alpha} = -M_{32}^{\alpha} = \hat{m}_1^{\alpha}$$

$$M_{31}^{\alpha} = -M_{13}^{\alpha} = \hat{m}_2^{\alpha}$$

and $$M_{12}^{\alpha} = -M_{21}^{\alpha} = \hat{m}_3^{\alpha} \; . \tag{30}$$

We will now postulate a conservation of moment of momentum equation for the matrix as a whole to be

$$\frac{\partial}{\partial t} \int_R \underset{\sim}{x} \times (\rho \underset{\sim}{v}) \, dv = - \oint_{\partial R} (\rho \underset{\sim}{v} \times v)(\underset{\sim}{v} \cdot \underset{\sim}{ds}) + \oint_{\partial R} \underset{\sim}{x} \times [T \cdot ds]$$

$$+ \int_R [\underset{\sim}{x} \times (\rho \underset{\sim}{b} + \hat{p}\hat{c}\underset{\sim}{v}) + \hat{\underset{\sim}{m}}] \, dv \tag{31}$$

where $\hat{\underset{\sim}{m}}$ is the momentum supply vector for the matrix. Equation (18) can be reduced to the field equation

$$T_{ij} - T_{ji} = \hat{M}_{ij} \tag{32}$$

where

$$\hat{M}_{ij} = \sum_{\alpha=1}^{N} M_{ij}^{\alpha} \tag{33}$$

Of course, if all the moment of momentum supply vectors are zero, equation (32) reduces to

$$T_{ij} = T_{ji} \tag{34}$$

which is the conservation of moment of momentum equation for a simple material.

d. *Energy Balance*

In this subsection we consider conservation of energy. The conservation of energy equation of the α-th component has the form

$$\frac{\partial}{\partial t} \int_R \rho^{\alpha} \left(\varepsilon^{\alpha} + \frac{1}{2} v_i v_i\right) dv = - \oint_{\partial R} \rho^{\alpha} \left(\varepsilon^{\alpha} + \frac{1}{2} v_i v_i\right) v_j n_j \, ds + \oint_{\partial R} \left(v_i T_{ij}^{\alpha} - q_j^{\alpha}\right) n_j \, ds$$

$$+ \int_R \rho^{\alpha} \left(b_i^{\alpha} v_i + r^{\alpha}\right) + \int_R \left(\hat{p}_i^{\alpha} v_i + \frac{1}{2} \hat{c}^{\alpha} v_i v_i + c^{\alpha} \varepsilon^{\alpha} + \bar{h}^{\alpha}\right) dv \tag{35}$$

where ε^{α} is the specific internal energy of the α-th component; q_i^{α} is the heat flux vector in the α-th component, r^{α} is the specific heat supply for the α-th component per unit time and $\bar{h}^{\alpha}$ is the energy transfer between the matrix and the (N-1) other components and the perfusant. The first three integrals on the right side of (35) are customary: the first integral is the sum of the

convected internal and kinetic energy; the second is the work done by the surface tractions and the heat flux; and the third represents the heat supply per unit mass plus the work of the body force. The fourth integrand in (35) is associated with the energy transfer to the α-th component from the (N-1) other components and the perfusant. The first term in the fourth integrand is the work done by the force of interaction; the second represents the kinetic energy of the added mass; and the third represents the internal energy of the added mass, assuming its specific internal energy is the same as that in the extant porous structure. The fourth term represents any energy transfer between the α-th component which is not accounted for by the other three terms. For example, $\bar{h}^{\alpha}$ may represent the energy transfer due to the fact that the internal energy of the added mass is not the same as that of the extant material.

Using the divergence theorem, and equations (15) and (26), we can rewrite (35) as

$$\rho^{\alpha} \dot{e}^{\alpha} = T^{\alpha}_{ij} L^{\alpha}_{ji} - q^{\alpha}_{i,i} + \rho^{\alpha} r^{\alpha} + \bar{h}^{\alpha} \tag{36}$$

We will next postulate the energy balance equation for the matrix as a whole to be

$$\frac{\partial}{\partial t} \int_R \rho \left(\varepsilon + \frac{1}{2} v_i v_i\right) dv = - \oint_{\partial R} \rho \left(e + \frac{1}{2} v_i v_i\right) v_j n_j \, ds + \oint_{\partial R} \left(v_i T_{ij} - q_j\right) n_j \, ds$$

$$+ \int_R \rho \left(b v_i + r\right) dv + \int_R \left(\hat{p}_i v_i + \frac{1}{2} \hat{c} v_i v_i + \hat{c}\varepsilon + \bar{h}\right) dv \tag{37}$$

where we have defined

$$\varepsilon = (1/\rho) \sum_{\alpha=1}^{N} \rho^{\alpha} \varepsilon^{\alpha}$$

$$q_i = \sum_{\alpha=1}^{N} q_i^{\alpha}$$

and

$$r = (1/\rho) \sum_{\alpha=1}^{N} \rho^{\alpha} r^{\alpha} \tag{38}$$

We should observe that (38) is made possible by the fact that the N chemical components of the matrix are not moving relative to one another. We can next use the divergence theorem and the equations (17) and (26) to yield the field equation

$$\rho \dot{\varepsilon} = T_{ij} L_{ji} - q_{i,i} + \rho r + \bar{h} \tag{39}$$

where

$$\bar{h} = \sum_{\alpha=1}^{N} \bar{h}^{\alpha} + \sum_{\alpha=1}^{N} \hat{c}^{\alpha} \varepsilon^{\alpha} - \hat{c} \varepsilon \tag{40}$$

e. The Entropy Inequality

With each component α we will associate a component-specific entropy function η^{α}, such that within any region R the entropy of the α-th chemical component is given by

$$S_R^{\alpha} = \int_R \rho^{\alpha} \eta^{\alpha} \, dv \, . \tag{41}$$

Similarly, for the matrix as a whole, we will assume that there exists a matrix-specific density function η such that with any region R the entropy of the matrix is given by

$$S_R = \int_R \rho\eta \; dv = \sum_{\alpha=1}^{N} S_R^{\alpha} \; . \tag{42}$$

These two assumptions place no constraints on the generality of this development. Next we will postulate an entropy inequality for each component such that the partial time derivative of each S_R has the form

$$\frac{\partial}{\partial t} \int \rho^{\alpha} \eta^{\alpha} dv \geq$$

$$- \oint_{\partial R} \rho^{\alpha}\eta^{\alpha} v_i n_i \, ds - \oint_{\partial R} \left[\frac{q_i^{\alpha} n_i}{\theta^{\alpha}} \right] ds + \int_R \left[\frac{\rho^{\alpha} r^{\alpha}}{\theta^{\alpha}} \right] dv + \int_R \left[\hat{c}^{\alpha}\eta^{\alpha} + \frac{\bar{\bar{h}}^{\alpha}}{\theta^{\alpha}} \right] dv \tag{43}$$

where θ^{α} is a positive real scalar, indicating the temperature of the α-th component and $\bar{\bar{h}}^{\alpha}$ is defined in a manner analogous to that of $\bar{h}^{\alpha}$ in equation (35). We distinquish between $\bar{\bar{h}}^{\alpha}$ and $\bar{h}^{\alpha}$ to indicate that all the energy transferred to the α-th chemical component need not contribute to the entropy production in the α-th component. As in the case of the balance equations for energy and entropy, the first three integrals on the right side are traditional and the fourth integral is a departure: The first integral represents the convected entropy, the second is the entropy production associated with the heat flux, the third is the entropy production associated with the specific heat supply and the fourth represents the entropy production due to heat transfer and chemical reactions with the (N-1) other chemical components and the perfusant. The first term in the fourth integrand is the entropy produced by the chemical reaction generating new material in the α-th component assuming that this new material has the same specific entropy as the extant material. The second term in the fourth integrand represents all entropy

production not already accounted for. For example, this term may represent the additional entropy contribution due to the fact that the temperature of the newly formed matrix material has a higher temperature than that of the extant material.

Equation (43) may next be converted into a field equation by the use of the divergence theorem, conservation of mass (15) and (22) giving us

$$\rho^{\alpha}\dot{\eta}^{\alpha} \geq -\left[\frac{q_i^{\alpha}}{\theta^{\alpha}}\right]_{,i} + \left[\frac{\rho^{\alpha} r^{\alpha} + \bar{\bar{h}}^{\alpha}}{\theta^{\alpha}}\right] \tag{44}$$

Using the same motivation as that above, we can postulate that the entropy inequality for the matrix as a whole has the form

$$\frac{\partial}{\partial t}\int_R \rho\eta \, dv \geq \oint_{\partial R} \rho\eta v_i n_i \, ds - \oint_{\partial R} \sum_{\alpha=1}^{N}\left[\frac{q_i^{\alpha} n_i}{\theta^{\alpha}}\right] ds + \int_R \sum_{\alpha=1}^{N}\left[\frac{\rho^{\alpha} r^{\alpha} + \hat{c}\eta^{\alpha}\theta^{\alpha} + \bar{\bar{h}}^{\alpha}}{\theta^{\alpha}}\right] dv \tag{45}$$

which reduces to the field equation

$$\rho\dot{\eta} \geq \sum_{\alpha=1}^{N}\left[-\left(\frac{q_i^{\alpha}}{\theta^{\alpha}}\right)_{,i} + \frac{\rho^{\alpha} r^{\alpha} + \bar{\bar{h}}^{\alpha}}{\theta^{\alpha}}\right] \tag{46}$$

In further discussions, we will limit ourselves to the special case when all N chemical components have the same temperature field θ, in which case inequality (45) can be written in the form

$$\rho\dot{\eta} \geq -\left(\frac{q_i}{\theta}\right)_{,i} + \frac{pr + \bar{\bar{h}}}{\theta} \tag{47}$$

where

$$\bar{\bar{h}} = \sum_{\alpha=1}^{N} \bar{\bar{h}}^{\alpha} + \sum_{\alpha=1}^{N} \hat{c}^{\alpha}\eta^{\alpha}\theta - \hat{c}\eta\theta \tag{48}$$

However, this inequality does not contain any new restrictions that are not already contained in inequalities (44).

f. The Helmholz Free Energy

In this final subsection we will recast the conservation of energy and the entropy inequality in terms of the Helmholz free energy. Let us define the component-specific free energy density as

$$\psi^{\alpha} = \varepsilon^{\alpha} - \eta^{\alpha}\theta^{\alpha} \tag{49}$$

and the matrix-specific free energy as

$$\psi = (1/\rho) \sum_{\alpha=1}^{N} \rho^{\alpha}\psi^{\alpha} \tag{50}$$

Since we have assumed that the temperature fields of all N chemical components of the matrix are the same, we can also write

$$\psi = \varepsilon - \eta\theta \ . \tag{51}$$

Finally we can substitute equation (47) into the energy balance equation (36) and obtain the relation

$$-\rho^{\alpha}(\dot{\psi}^{\alpha} + \eta^{\alpha}\dot{\theta} + \dot{\eta}^{\alpha}\theta) - T^{\alpha}_{ij}L_{ji} + q^{\alpha}_{i,i} - \bar{h}^{\alpha} = \rho^{\alpha}r^{\alpha} \tag{52}$$

for conservation of energy in the α-th component. In addition, equation (52) can be substituted into (44) to give the entropy inequality

$$-\rho^{\alpha}\dot{\psi}^{\alpha} - \rho^{\alpha}\dot{\eta}^{\alpha}\theta + T^{\alpha}_{ij}L_{ji} + \hat{h}^{\alpha} - \left(\frac{1}{\theta}\right) q^{\alpha}_{i}\, g_{i} \geq 0 \tag{53}$$

where

$$\hat{h}^{\alpha} = \bar{h}^{\alpha} - \bar{\bar{h}}^{\alpha} \tag{54}$$

and $$g_i = \theta_{,i}$$

II. 5 THE CONSTITUTIVE CONSTRAINTS AND THE ENTROPY INEQUALITY

a. Introduction

In the previous subsection we discussed the balance equations for mass, momentum, energy, and entropy. Now we make constitutive assumptions appropriate for an elastic material and obtain constraints on the constitutive equations from the entropy inequality and from certain physical and physiological assumptions about the physiological nature of bone remodeling. The resulting equations constitute the governing equations for an N-component, ideal, "non-swelling", linearly elastic solid mixture. In the following subsection we will discuss how this finite element component model might be generalized to simulate cancellous bone.

In the following subsection we will summarize the balance equations and the constitutive constraint that can be built into the balance equations. In the next subsection we will discuss the manner in which the entropy inequality placed further constraints on the constitutive equations. In the fourth subsection we will discuss certain auxiliary constitutive assumptions, based on simple physical and physiological assumptions about the nature of bone and bone remodeling, which will further simplify the governing equations.

b. The Balance Equations

We will recall that in our development of the balance equations, it simplified our discussion to place certain constraints on the governing equations. These constraints were, that

(1) all N components of the matrix have the same motion, i.e.

$$\underset{\sim}{\chi}^{\alpha}(X, t) = \underset{\sim}{\chi}(X, t) \text{ for } \alpha = 1, 2, \ldots N \tag{55}$$

(2) all N components of the matrix have the same temperature

$$\theta = \theta^{\alpha}(X, t) = \theta(X, t) \text{ for } \alpha = 1, 2, \ldots N \tag{56}$$

It would also be physically reasonable to expect further that

(3) all N components of the matrix have the same body force, i.e.

$$\underset{\sim}{b} = \underset{\sim}{\tilde{b}}^{\alpha}(X, t) = \underset{\sim}{\tilde{b}}(X, t) \text{ for } \alpha = 1, 2 \ldots N \tag{57}$$

(4) the matrix is non-polar, i.e.

$$\underset{\sim}{M}^{\alpha} = \underset{\sim}{\tilde{M}}^{\alpha}(X,t) = 0 \qquad \text{for } \alpha = 1, 2, \ldots N \tag{58}$$

and that

5) the matrix-perfusant momentum interaction can be ignored, i.e.

$$\hat{p}^{\alpha} = \tilde{p}^{\alpha}(X,t) = 0 \quad \text{for } \alpha = 1, 2, \ldots N. \tag{59}$$

$$\left.\begin{aligned}
&\gamma^{\alpha} = \hat{c}^{\alpha} \det \underset{\sim}{F} \\
&\gamma^{\alpha}(\ddot{x}_i - b_i) = T_{ij}^{\alpha} \det \underset{\sim}{F} \\
&T_{ij}^{\alpha} - T_{ji}^{\alpha} = 0 \\
&\gamma^{\alpha}[\dot{\psi}^{\alpha} + \eta^{\alpha}\dot{\theta} + \dot{\eta}^{\alpha}\theta - r^{\alpha}] = [T_{ij}^{\alpha} L_{ji} - q_{i,i}^{\alpha} + \bar{h}^{\alpha}] \det \underset{\sim}{F} \\
&-\gamma^{\alpha}[\dot{\psi}^{\alpha} - \eta^{\alpha}\dot{\theta}] + [T_{ij}^{\alpha} L_{ji} + \hat{h}^{\alpha} - \frac{1}{\theta} q_i^{\alpha} \theta_{,i}] \det \underset{\sim}{F} \geq 0
\end{aligned}\right\} \tag{60}$$

By letting

$$\left.\begin{aligned}
\gamma &= \sum_{\alpha=1}^{N} \gamma^{\alpha} \\
T_{ij} &= \sum_{\alpha=1}^{N} T_{ij}^{\alpha} \\
q_i &= \sum_{\alpha=1}^{N} q_i^{\alpha} \\
\gamma r &= \sum_{\alpha=1}^{N} \gamma^{\alpha} r^{\alpha} \\
h &= \sum_{\alpha=1}^{N} h^{\alpha} \\
\gamma \psi &= \sum_{\alpha=1}^{N} \gamma^{\alpha} \psi^{\alpha} \\
\gamma \eta &= \sum_{\alpha=1}^{N} \gamma^{\alpha} \eta^{\alpha}
\end{aligned}\right\} \qquad (61)$$

the conservation of mass, momentum, and energy, for the matrix as a whole takes the form

$$\dot{\gamma} = \hat{c} \det \underset{\sim}{F} \qquad (62)$$

$$\gamma (\dot{v}_i - b_i) = T_{ij} \det \underset{\sim}{F}$$

$$T_{ij} - T_{ji} = 0$$

and

$$-\gamma\left(\dot{\psi} + \dot{\eta}\theta + \eta\dot{\theta} - r\right) \pm \left(T_{ij}L_{ji} - q_{i,i} + h\right) \det \underset{\sim}{F} \geq 0$$

As mentioned previously, given the constraint (56), the entropy inequality for the matrix as a whole does not contain any new constraints not already implied by (60).

c. The Entropy Inequality

Our objective is to model the normal adaptive processes that occur in cancellous bone remodeling as strain-controlled mass deposition and/or resorption which modify the trabecular structure of the porous elastic solid. We shall therefore make constitutive assumptions similar to those made for elastic solids, but with the inclusion of additional independent variables $\{\gamma^1, \gamma^2, \ldots, \gamma^N\}$ which measure the degree of trabecular adaptation. Thus we can write

$$\begin{aligned}
\psi^{\alpha} &= \hat{\psi}^{\alpha}(\theta, \theta_{,i}, F_{iK}, \gamma^{\beta}) \\
\eta^{\alpha} &= \hat{\eta}^{\alpha}(\theta, \theta_{,i}, F_{iK}, \gamma^{\beta}) \\
T_{ij}^{\alpha} &= \hat{T}_{ij}^{\alpha}(\theta, \theta_{,i}, F_{iK}, \gamma^{\beta}) \\
q_i &= \hat{q}_i(\theta, \theta_{,i}, F_{iK}, \gamma^{\beta}) \\
\hat{c}^{\alpha} &= \hat{\underset{\sim}{c}}^{\alpha}(\theta, \theta_{,i}, F_{iK}, \gamma^{\beta}) \\
\bar{h}^{\alpha} &= \hat{\underset{\sim}{h}}^{\alpha}(\theta, \theta_{,i}, F_{iK}, \gamma^{\beta}) \\
\hat{h}^{\alpha} &= \hat{\underset{\sim}{h}}^{\alpha}(\theta, \theta_{,i}, F_{iK}, \gamma^{\beta})
\end{aligned} \tag{63}$$

Where the third argument of (63) symbolizes the set $\gamma^1, \gamma^2, \ldots, \gamma^N$. Substituting (63) into $(60)_5$ gives us the entropy inequality

$$-\gamma^{\alpha}\left\{\frac{\partial\psi^{\alpha}}{\partial\theta}\dot{\theta}+\frac{\partial\psi^{\alpha}}{\partial\theta_{,i}}\dot{\theta}_{,i}+\sum_{\alpha=1}^{N}\left[\frac{\partial\psi^{\alpha}}{\partial\gamma^{\beta}}\hat{c}^{\alpha}\det\underset{\sim}{F}\right]+\frac{\partial\psi^{\alpha}}{\partial F_{iK}}L_{ij}F_{jK}+\eta^{\alpha}\dot{\theta}\right\}$$

$$+\left[T^{\alpha}_{ij}L_{ji}+\hat{h}^{\alpha}-\left(\frac{1}{\theta}\right)q^{\alpha}_{,i}\theta_{,i}\right]\det\underset{\sim}{F}\geq 0 \qquad (64)$$

where equations (62), and (10) have also been employed.

We will now use an argument, initially outlined by Coleman and Noll (1963) and Coleman and Mizel (1964); we will claim that the time derivative terms θ, $\dot{\theta}_{,i}$, and L_{ij} can be specified independently of the independent variables $(\theta, \theta_{,i}, F_{iK}, \gamma^{\beta})$. Note however that $\dot{\gamma}^{\beta}$ is constrained by equations $(60)_1$ and $(63)_5$. The entropy inequality (64) then implies the following restrictions

$$\frac{\partial\psi^{\alpha}}{\partial\theta}+\eta^{\alpha}=0,\quad \frac{\partial\psi^{\alpha}}{\partial\theta_{,i}}=0,\quad \text{and}\quad T^{\alpha}_{ij}=\frac{\gamma}{\det\underset{\sim}{F}}\frac{\partial\psi^{\alpha}}{\partial F_{iK}}F_{jK} \qquad (65)$$

These results show that ψ^{α} is independent of the temperature gradient and the η^{α} and T^{α}_{ij} are related to ψ^{α} by the formulae

$$\psi^{\alpha}=\hat{\psi}^{\alpha}(\theta, F_{iK}, \gamma^{\beta}),$$

$$\eta^{\alpha}=-\frac{\partial\hat{\psi}^{\alpha}}{\partial\theta} \qquad (66)$$

and

$$T^{\alpha}_{ij}=p^{\alpha}\frac{\partial\psi^{\alpha}}{\partial F_{iK}}F_{jK}$$

When the results (66) are substituted back into (65), the reduced entropy inequality becomes

$$-\sum_{\beta=1}^{N} \frac{\partial \psi^{\alpha}}{\partial \gamma^{\beta}} \hat{c}^{\beta} + \hat{h}^{\alpha} - \left(\frac{1}{\theta}\right) q_i^{\alpha} \theta_{,i} \geq 0 \tag{67}$$

From equation $(61)_7$ it follows that the total stress for the matrix material has the form

$$T_{ij} = \left(\sum_{\alpha=1}^{N} p^{\alpha} \frac{\partial \psi^{\alpha}}{\partial F_{iK}} \right) F_{jK} \tag{68}$$

This result will prove to be important in future discussion.

d. Approximations and Additional Constraints on the Governing Equations

The governing equations derived in the previous subsubsection are too general to have immediate practical application and it will be necessary to simplify and specialize them further. These simplifications are justified by certain easily observable physiological properties of living bone. For instance we can assume that

(1) living bone may be regarded as isothermal, i.e.

$$\theta = \theta^{\alpha}(X, t) = \text{constant for} \quad \alpha = 1, 2, \ldots N \quad \text{and all } X \text{ and } t \, . \tag{69}$$

Under these circumstances, the governing equations of the previous subsection reduce to the set

$$\dot{\gamma}^{\alpha} = \hat{c}^{\alpha}(F_{iK}, \gamma^{\beta}) \det \underset{\sim}{F}$$

and

$$\gamma(\dot{v}_i - b_i) = T_{ij,j} \det \underset{\sim}{F} \, ,$$

where

$$\gamma = \sum_{\alpha=1}^{N} \gamma^{\alpha} ,$$

$$T_{ij} = \sum_{\alpha=1}^{N} T_{ij}^{\alpha} \tag{70}$$

and

$$T_{ij}^{\alpha} = T_{ji}^{\alpha} = \frac{\gamma^{\alpha}}{\det \underset{\sim}{F}} \left\{ \frac{\partial}{\partial F_{iK}} \left(\hat{\psi}^{\alpha} (F_{kL}, \gamma^{\beta}) \right) F_{jK} \right\}$$

We will next assume that

(2) <u>bone remodeling occurs in a manner such that bone remains nonswelling</u>.

By <u>nonswelling</u> we mean that as trabecular adaptation proceeds, the geometric configuration of the bone under zero stress (the reference state for strain) remains the same, no matter where the trabecular adaptation takes place. One might imagine a block of cancellous bone containing four equidistant points, the vertices of a tetrahedron marked for the purpose of measuring strain. When adaptation occurs, material is added or taken away from the trabeculae, but if the boundary conditions are ever returned to conditions such that the local stress within the strain-tetrahedron is zero, the distance between the four vertices of the tetrahedron will always return to their initial value. In terms of the stress function in eq. (63) this constraint can be written as

$$0 = \hat{T}_{ij}^{\alpha} (\delta_{iK}, \gamma^{\beta}) \qquad \text{for all } \gamma\beta \tag{71}$$

and in terms of the free energy function we will have

$$0 = \frac{\partial}{\partial F_{iK}} \psi^{\alpha} (F_{iK}, \gamma^{\beta}) \Big|_{F_{iK} = \delta_{iK}} \tag{72}$$

Let us next define the strain tensor by

$$E_{KM} = \tfrac{1}{2}\left[F_{iK}F_{iM} - \delta_{KM}\right] \tag{73}$$

In terms of the displacement gradients $u_{K,M}$, E_{KM} has the representation

$$E_{KM} = \tfrac{1}{2}\left[u_{K,M} - u_{M,K} - u_{P,M}u_{P,K}\right] \tag{74}$$

In addition, the free energy function (63) and the rate of reaction function in eq. (63) can be redefined in terms of these new arguments as

$$\bar{c}^{\alpha}(E_{KM}, \gamma^{\beta}) = \hat{\bar{c}}^{\alpha}(F_{iK}, \gamma^{\beta})$$

$$\bar{\psi}^{\alpha}(E_{KM}, \gamma^{\beta}) = \hat{\psi}^{\alpha}(F_{iK}, \gamma^{\beta}) \tag{75}$$

respectively.

We are now in a position to make the assumption that

(3) <u>bone is subjected only to small strain and this strain is linearly related to the stress</u>.

The constitutive equations for $\hat{c}^{\alpha}$ and $\hat{\psi}^{\alpha}$ can now be approximated by assuming that the displacement gradients $u_{K,M}$ are small and their squares can be neglected. When the squares of the displacement gradients are neglected and the material and spatial coordinate systems are made to coincide, the strain tensor can be approximated as

$$E_{ij} = \tfrac{1}{2}\left[u_{i,j} + u_{j,i}\right], \tag{76}$$

Approximations for $\bar{c}^{\alpha}$ and $\bar{\psi}^{\alpha}$ are obtained by neglecting terms of order three and higher in a Taylor series expansion

$$\bar{c}^{\alpha}(E_{ij}, \gamma^{\beta}) = a^{\alpha}(\gamma^{\beta}) + A^{\alpha}_{ij}(\gamma^{\beta})\,E_{ij} + 1/2\,B^{\alpha}_{ijk\ell}(\gamma^{\beta})\,E_{ij}\,E_{k\ell}$$

$$\bar{\psi}^{\alpha}(E_{ij},\ \gamma^{\beta}) = \bar{\psi}^{\alpha}(0,\ \gamma^{\beta}) + D_{ij}^{\alpha}(\gamma^{\beta}) + \tfrac{1}{2}C_{ijk\ell}^{\alpha}(\gamma^{\beta})\, E_{ij}E_{k\ell} \tag{77}$$

where

$$a^{\alpha}(\gamma^{\beta}) = \bar{c}^{\alpha}(\gamma^{\beta},\ 0)$$

$$A_{ij}^{\alpha}(\gamma^{\beta}) = \frac{\partial}{\partial E_{ij}}\, \bar{c}^{\alpha}(E_{pq},\ \gamma^{\beta}) \Big|_{E_{pq} = 0}$$

$$B_{ijk\ell}^{\alpha}(\gamma^{\beta}) = \frac{\partial^2}{\partial E_{ij}\partial E_{k\ell}}\, \bar{c}^{\alpha}(E_{pq},\ \gamma^{\beta}) \Big|_{E_{pq} = 0}$$

$$\bar{D}_{ij}^{\alpha}(\gamma^{\beta}) = \frac{\partial}{\partial E_{ij}}\, \bar{\psi}^{\alpha}(E_{ij}, \gamma^{\beta}) \Big|_{E_{pq} = 0}$$

$$\bar{C}_{ijk\ell}^{\alpha}(\gamma^{\beta}) = \frac{\partial^2}{\partial E_{ij}\, \partial E_{k\ell}}\, \bar{\psi}^{\alpha}(E_{pq},\ \gamma^{\beta}) \Big|_{E_{pq} = 0} \tag{78}$$

The constraint (72) requires that

$$D_{ij}^{\alpha}(\gamma^{\beta}) = 0 \qquad \text{for all } \alpha \text{ and } \gamma^{\beta} \tag{79}$$

thus when (79) is substituted back into (77), the stress-strain relationship (70) takes the form

$$T_{ij} = \hat{C}_{ijk\ell}\, E_{k\ell} \tag{80}$$

where

$$\hat{C}_{ijk\ell} = \sum_{\alpha=1}^{N} \gamma^{\alpha} \bar{C}^{\alpha}_{ijk\ell} (\gamma^{\beta}) \tag{81}$$

e. Summary of the N-Component Model

The approximations of the current subsection allow us to simplify considerably the governing equations developed in the previous subsection. The approximated governing equations consist of

(1) a definition of the strain tensor in terms of the displacement,

$$E_{ij} = \tfrac{1}{2}\left[u_{i,j} + u_{j,i}\right] ; \tag{82}$$

(2) a stress-strain relationship

$$T_{ij} = \hat{C}_{ijk\ell} (\gamma^{\beta}) E_{k\ell}$$

where

$$\hat{C}_{ijk\ell} (\gamma^{\beta}) = \sum_{\alpha=1}^{N} \gamma^{\alpha} C^{\alpha}_{ijk\ell} ;$$

(3) a rate of reaction equation for each component

$$\dot{\gamma}^{\alpha} = \hat{c}^{\alpha} (E_{ij}, \gamma^{\beta})$$

where

$$\hat{c}^{\alpha} (E_{ij}, \gamma^{\beta}) = a^{\alpha}_{o} + A^{\alpha}_{ij} E_{ij} + \tfrac{1}{2} B^{\alpha}_{ijk\ell} E_{ij} E_{k\ell}$$

, for $\alpha = 1, 2, \ldots N$;

and

(d) a conservation of momentum equation

$$\rho \ddot{u}_i = T_{ij,j} + \rho b_i ,$$

where

$$\rho = \sum_{\alpha=1}^{N} \rho^{\alpha} ; \tag{83}$$

In order to quantify the physical properties of this material it is necessary to specify two sets of constitutive functions, each of which is specified by its own set of material parameters. The first set, composed solely of the function $\hat{C}_{ijk\ell}$, describes the total stiffness of the material as a function of the chemical composition of the material. For this reason the parameters $C^{\alpha}_{ijk\ell}$ will be called the Stiffness Parameters and the function $\hat{C}_{ijk\ell}$ will be called the Stiffness Function. The second set of functions $\hat{c}^{\alpha}$ describes the rate at which the chemical composition of the material changes as a function of the strain and the current chemical composition. Since these changes in the chemical composition are brought about by the remodeling properties of bone, a^{α}_{o}, A^{α}_{ij}, and $B^{\alpha}_{ijk\ell}$ might be termed Remodeling Parameters and the function set $\hat{c}^{\alpha}$ may be said to collectively describe a Remodeling Function.

These equations are similar to those of a classical, linear elastic material except that there now exists an N parameter set $\{\rho^{\alpha}\}$ describing the chemical composition of the elastic material whose values are determined by the conservation of mass equations (82). In fact, in the special case when the Remodeling Function is identically zero, i.e., $\hat{c}^{\alpha} = 0$ for all α, then the chemical composition, as parameterized by the parameter set $\{\rho^{\alpha}\}$ remains fixed and the governing equations reduce to those of a classical linear elastic material. In the case of living bone, however, the Remodeling Function is not zero and this chemical change in the composition allows the material to modify or adapt its physical properties to its ambient loading conditions. Consequently, the governing equations (82) may be said to describe an Adaptive Elastic Material.

II. 6 THE CANCELLOUS BONE MODEL

a. Introduction

In the previous subsection we developed an adaptive elastic model in which there were N "chemical components". In this subsection, we will introduce a model for cancellous bone in which these "chemical components" are rendered equivalent to the trabecular plates that can be observed and

measured anatomically. We will start off in the second subsubsection by equating these N "chemical components" to N infinitesimal trabecular plates oriented normal to N trabecular basis vectors. Since we do not know a priori the spatial orientation of the trabecular basis vectors, we will reformulate the governing equations so that the dependence of the N spatially oriented chemical components is replaced by a trabecular density function whose values will be independent of the N trabecular basis vectors.

In the third subsubsection we will demonstrate that this trabecular density function can be approximately specified by a symmetric, second-rank tensor, $\underset{\sim}{M}$, called the trabecular adaptation tensor. The tensor field $\underset{\sim}{M}$ has a very convenient physical interpretation: Anatomically, the matrix material of cancellous bone is arranged into a structure of mutually orthogonal trabecular plates. The eigen vectors of $\underset{\sim}{M}$ may be interpreted as indicating the normal of each of these trabecular plates, while the eigen value of each of these eigen vectors, indicates the relative thickness of these trabecular plates. In Section IV, we will discuss design of instrumentation which will enable investigators to measure the tensor $\underset{\sim}{M}$ experimentally.

b. The Trabecular Distribution Function

We will begin by associating each of the N "chemical components" of the previous subsection with a trabecular plate whose normal is the unit vector $\underset{\sim}{w}^{\alpha}$. The set of all N $\underset{\sim}{w}^{\alpha}$ may be referred to as the trabecular basis vectors, since they play a role somewhat analogous to the basis vectors in the matrix representation of tensors. The components of any trabecular basis vector in a three-dimensional space can be resolved as

$$\begin{aligned} w_1^{\alpha} &= \cos(\theta^{\alpha}) \sin(\phi^{\alpha}) \\ w_2^{\alpha} &= \sin(\theta^{\alpha}) \sin(\phi^{\alpha}) \\ w_3^{\alpha} &= \cos(\phi^{\alpha}) \end{aligned} \tag{84}$$

where θ^{α} and ϕ^{α} are the longitude and colatitude parameters of conventional spherical polar coordinates. These angles in three-dimensional space, with relationship to the unit vector $\underset{\sim}{w}^{\alpha}$, are illustrated in Figure 7. We will also note, for future reference, that the unit vector $\underset{\sim}{i}_3$ can be rotated into the unit vector $\underset{\sim}{w}^{\alpha}$ by left multiplying by the orthagonal transformation

$$\underset{\sim}{\tilde{Q}}(\theta,\phi) = \underset{\sim}{\bar{Q}}(\underset{\sim}{w}) = \begin{bmatrix} [\cos\theta\cos\phi] & [-\sin\theta\cos\phi] & [-\sin\phi] \\ [\sin\theta] & [\cos\theta] & [0] \\ [\cos\theta\sin\phi] & [\sin\theta\sin\phi] & [\cos\phi] \end{bmatrix} \tag{85}$$

We are now in a position to introduce the trabecular distribution functions $\bar{\nu}(\underset{\sim}{w})$ and $\tilde{\nu}(\theta, \phi)$ which can be used in lieu of the variable set $\{\gamma^{\alpha}\}$. Let us consider a unit sphere covered with a thin shell of mass γ which is composed of material with a uniform mass density of $\bar{\gamma}$. We will further assume that the surface of this unit sphere has been partitioned into N sectors each of which is associated with one of the unit vectors $\underset{\sim}{w}^{\alpha}$. Such a partitioning is illustrated in Figure 8. If we consider the area of each sector to be ΔS^{α} and the mass of the material in each sector to be γ^{α}, then the quotient

$$\nu^{\alpha} = \frac{\gamma^{\alpha}}{\Delta S^{\alpha}} \tag{86}$$

can be considered to be approximately proportional to the thickness of the shell in the sector α. We next observe that the definition (86) will still remain valid regardless of how the sectors are partitioned or even of how the trabecular basis vector set $\{\underset{\sim}{w}^{\alpha}\}$ is selected. This suggests that we consider the set of all ν^{α} depending on $\underset{\sim}{w}^{\alpha}$ as defining a trabecular distribution function $\bar{\nu}(\underset{\sim}{w})$ such that

$$\nu^{\alpha} = \bar{\nu}(\underset{\sim}{w}) \Big|_{\underset{\sim}{w} = \underset{\sim}{w}^{\alpha}} \tag{87}$$

whose domain is the set of all unit vectors $\underset{\sim}{w}$. The trabecular distribution function can also be expressed as a function of the longitude and the colatitude

$$\nu^{\alpha} = \hat{\nu}(\theta, \phi) \Big|_{\substack{\theta = \theta^{\alpha} \\ \phi = \phi^{\alpha}}} \tag{88}$$

Using eq. (86), the expression for the total mass density can be written as

$$\gamma = \sum_{\alpha=1}^{N} \bar{\nu}(\underset{\sim}{w}^{\alpha})\, \Delta S^{\alpha} ; \tag{89}$$

while the expression for the total stiffness, indicating the Stiffness Function, takes the form

$$\hat{C}_{ijk\ell} = \sum_{\alpha=1}^{N} C^{\alpha}_{ijk\ell}\, \bar{\nu}(\underset{\sim}{w}^{\alpha})\, \Delta S^{\alpha} ; \tag{90}$$

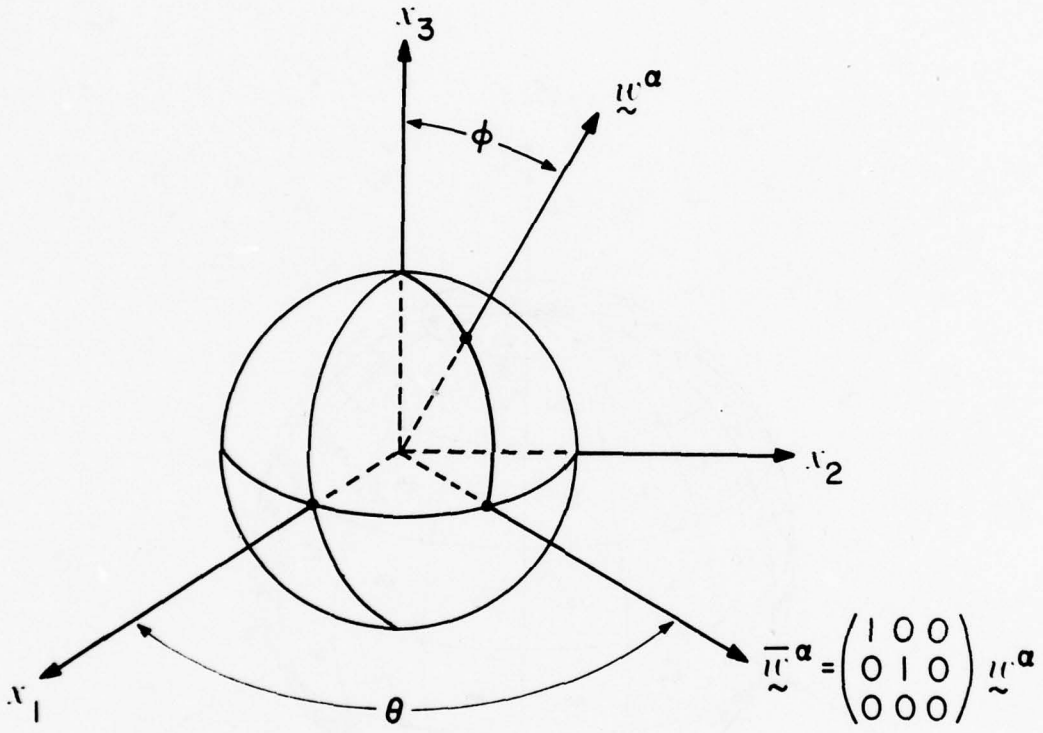

Figure 7. The Longitude and the Colatitude Defining the Trabecular Basis Vector $\underset{\sim}{\omega}^{\alpha}$.

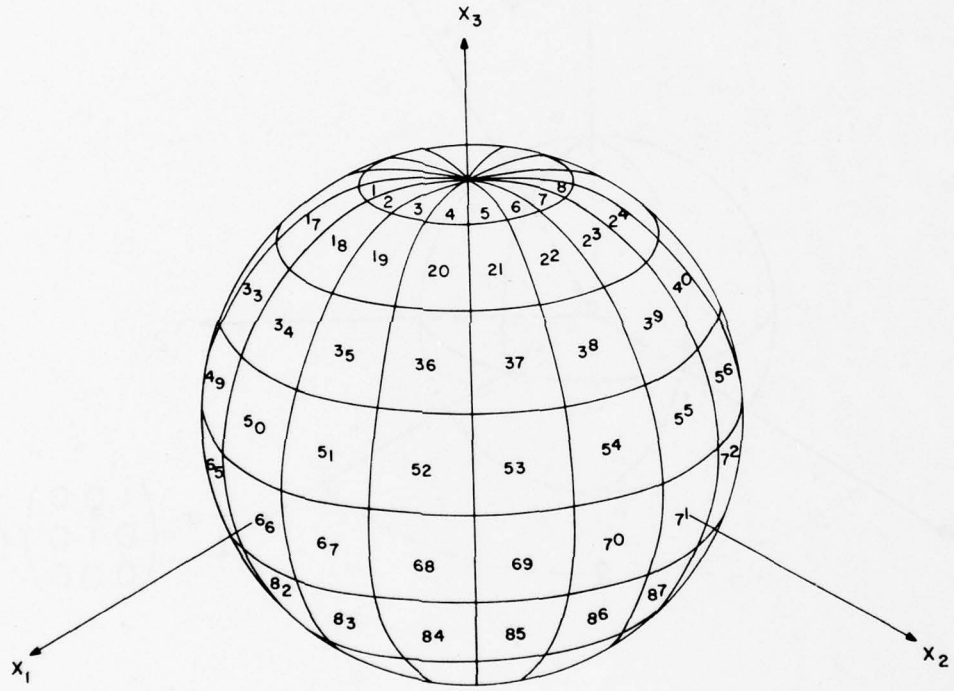

Figure 8. Partitioning of the Unit Sphere into Sectors.

and equations specifying the rate of trabecular adaptation take the form

$$\frac{d}{dt}\left[\bar{\nu}\,(\underset{\sim}{w})\right]\Big|_{\underset{\sim}{w}=\underset{\sim}{w}^{\alpha}} = \left[\frac{1}{\Delta S^{\alpha}}\right]\bar{c}^{\alpha}(E_{ij};\ \Delta S^{1}\nu^{1},\ \Delta S^{2}\nu^{2},\ \Delta S^{3}\nu^{3},\ldots\Delta S^{N}\nu^{N}). \tag{91}$$

As the number of trabecular plates, N , approaches infinity, each segmental area ΔS^{α} becomes incrementally small and the summations (89) and (90) become the surface integral expressions

$$\gamma = \oint_{\underset{\sim}{w}^{\alpha}=1} \bar{\nu}\,(\underset{\sim}{w}^{\alpha})\,dS \tag{92}$$

and

$$\hat{C}_{ijk\ell} = \oint_{\underset{\sim}{w}^{\alpha}=1} C^{\alpha}_{ijk\ell}\,\nu(\underset{\sim}{w}^{\alpha})\,dS \tag{93}$$

Thus, as N approaches infinity, expressions; (89) and (90) and (91) indicate that the values of γ and $\hat{C}_{ijk\ell}$ and $\dot{\bar{\nu}}\,(\underset{\sim}{w})$ depend on <u>every</u> value of the function $\nu\,(\underset{\sim}{w})$ when the argument $\underset{\sim}{w}$ is a unit vector. In general, a function whose value depends on the values of a second function over a given subdomain of this second function is called a functional. The simplest example of a functional is the conventional integral. An integral can be thought of as a function whose value depends on a second function, the integrand, over a subdomain of the integrand as indicated by the limits of integration. Therefore, given that the total bulk mass density and the total stiffness are functionals of the trabecular distribution function, it is not surprising to see them in (87) and (93) expressible in terms of weighted intergrals of the trabecular distribution function for all values of $\underset{\sim}{w}$ such that $|\underset{\sim}{w}'| = 1$.

However, since functionals may not always be expressible as weighted integrals, we now introduce a new notation in which a functional is indicated by an oversized script letter under which is placed an expression containing a dummy variable prescribing the domain of functional dependence of the functional argument. For example, in this notation the expression in eq. (93) can be recast into the form

$$\hat{C}_{ijk\ell} = \underset{|\underset{\sim}{w}'|=1}{\mathscr{C}^{ijk\ell}} \left\{ \overline{\nu}(\underset{\sim}{w}') \right\}, \tag{94}$$

This new notation is necessary to describe the rate of trabecular adaptation. In the case of expression (91), as N approaches infinity, the time derivative of $\overline{\nu}(\underset{\sim}{w})$ depends on not only $\underset{\sim}{w}$ and $\underset{\sim}{E}$ but also on all values of the function $\overline{\nu}(\underset{\sim}{w})$ for $|\underset{\sim}{w}'| = 1$. Thus in the new notation the expression (91) approaches the form

$$\dot{\overline{\nu}}(\underset{\sim}{w}) = \underset{|\underset{\sim}{w}'|=1}{\mathscr{R}} \left\{ \underset{\sim}{w}; \underset{\sim}{E}; \overline{\nu}(\underset{\sim}{w}') \right\} . \tag{95}$$

as N approaches infinity.

The next step in our development of the cancellous bone model is to use a principle of continuum mechanics called material objectivity. In general, material objectivity requires that the governing equations have the same mathematical formulation when written with respect to any arbitrary nonaccelerating coordinate system. In our case, material objectivity requires that equations (93) and (94) will be invariant when rewritten in terms of a new coordinate system obtained from the orthogonal transformation (85). For instance, if the integration of expression (93) is performed with respect to the new coordinate system, the expression for the Stiffness Function takes the form

$$C_{ijk\ell} = \underset{\underset{\sim}{w}=1}{\oint} \overline{\nu}(\underset{\sim}{w})\, Q_{ip}(\underset{\sim}{w})\, Q_{jq}(\underset{\sim}{w})\, Q_{rk}(\underset{\sim}{w})\, Q_{s\ell}(\underset{\sim}{w})\, C^{o}_{pqrs}\, dS \tag{96}$$

where $Q_{ij}(w)$ is given by (85) and C^{o}_{pqrs} describes the stiffness of a single trabecular plate in the x_1, x_2 plane. Likewise, material objectivity requires that the functional expression (95) take the form

$$\dot{\overline{\nu}}(\underset{\sim}{w}) = \underset{|\underset{\sim}{w}'|=1}{\mathscr{R}^{o}} \left\{ Q^{T}(\underset{\sim}{w})\, \underset{\sim}{E}\, Q(\underset{\sim}{w}); \overline{\nu}(Q(\underset{\sim}{w})\, \underset{\sim}{w}') \right\} \tag{97}$$

where

$$\underset{|\underset{\sim}{w}'|=1}{\mathscr{R}^{o}}\left\{\underset{\sim}{E};\nu(\underset{\sim}{w}')\right\} = \underset{|\underset{\sim}{w}'|=1}{\mathscr{R}}\left\{\underset{\sim}{i}_3;\underset{\sim}{E};\nu(\underset{\sim}{w}')\right\} \tag{98}$$

and represents the remodeling function of a trabecular plate in the x_1, x_2 plane. We might also observe that the assumption of quadratic dependence of $\dot{\gamma}^{\alpha}$ on E_{ij} called for in eq. (82) will constrain the functional $\mathscr{R}^{o}$ of (97) to have the form

$$\underset{|\underset{\sim}{w}'|=1}{\mathscr{R}^{o}}\left\{E;\bar{\nu}(\underset{\sim}{w}')\right\} = \underset{|\underset{\sim}{w}'|=1}{\mathscr{F}^{o}}\left\{\bar{\nu}(\underset{\sim}{w}')\right\} + E_{ij}\underset{|\underset{\sim}{w}'|=1}{\mathscr{G}^{ij}}\left\{\bar{\nu}(\underset{\sim}{w}')\right\}$$

$$+ E_{ij}E_{k\ell}\underset{|\underset{\sim}{w}'|=1}{\mathscr{H}^{ijk\ell}}\left\{\bar{\nu}(\underset{\sim}{w}')\right\} \tag{99}$$

where $\mathscr{F}^{o}$, $\mathscr{G}^{ij}$, and $\mathscr{H}^{ijk\ell}$ are functionals on the function $\bar{\nu}(\underset{\sim}{w}')$ over the domain $|\underset{\sim}{w}'|=1$ which are independent of $\underset{\sim}{E}$.

c. The Trabecular Adaptation Tensor

In the previous subsubsection, we discussed how it was possible to specify the trabecular adaptation of cancellous bone using the Trabecular Distribution Function $\bar{\nu}(\underset{\sim}{w})$. In this subsubsection, we will discuss how the Trabecular Distribution Function can be approximately specified by a symmetric, second rank tensor $\underset{\sim}{M}$ called the Trabecular Adaptation Tensor. It will be shown that the Trabecular Distribution Function can be approximated by a quadratic form $\bar{\nu}(\underset{\sim}{w}) \simeq \underset{\sim}{w}\,\underset{\sim}{M}\,\underset{\sim}{w}$ and that the tensor $\underset{\sim}{M}$ is subject to physical interpretation in terms of the anatomical properties of the trabeculae of living cancellous bone.

We will begin by considering how we might approximately specify the Trabecular Distribution Function using a finite number of parameters. Since the function $\hat{\nu}(\theta,\phi)$ is a periodic function in both its arguments, the obvious place to look for such approximating parameters would be in a double Fourier series. Let us consider a double Fourier series for $\hat{\nu}(\theta,\phi)$ truncated at terms of order two, which has the form

$$\hat{\nu}(\theta, \phi) = \sum_{m=0}^{2} \sum_{n=0}^{2} N_{cc}^{mn} \cos m\theta \cos n\phi + \sum_{m=1}^{2} \sum_{n=1}^{2} N_{sc}^{mn} \sin m\theta \cos n\phi$$

$$+ \sum_{m=0}^{2} \sum_{n=1}^{2} N_{cs}^{mn} \cos m\theta \sin n\phi + \sum_{m=1}^{2} \sum_{n=1}^{2} N_{ss}^{mn} \sin m\theta \sin n\phi \qquad (100)$$

where the Fourier coefficients are given by the integrals

$$N_{cc}^{mn} = \left(\frac{1}{\pi^2}\right) \int_{\theta=-\pi}^{\pi} \int_{\phi=-\pi}^{\pi} \bar{\nu}(\theta, \phi) \cos m\theta \cos m\phi \, d\phi \, d\theta$$

$$N_{sc}^{mn} = \left(\frac{1}{\pi^2}\right) \int_{\theta=-\pi}^{\pi} \int_{\phi=-\pi}^{\pi} \bar{\nu}(\theta, \phi) \sin m\theta \cos n\phi \, d\phi \, d\theta$$

$$N_{cs}^{mn} = \left(\frac{1}{\pi^2}\right) \int_{\theta=-\pi}^{\pi} \int_{\phi=-\pi}^{\pi} \bar{\nu}(\theta, \phi) \cos m\theta \sin n\phi \, d\phi \, d\theta$$

and

$$N_{ss}^{mn} = \left(\frac{1}{\pi^2}\right) \int_{\theta=-\pi}^{\pi} \int_{\phi=-\pi}^{\pi} \bar{\nu}(\theta, \phi) \sin m\theta \sin n\phi \, d\phi \, d\theta \qquad (101)$$

It will also prove convenient to express (100) in the form

$$\hat{\nu}(\theta, \phi) = A_0(\theta) + A_1(\theta) \cos \phi + A_2(\theta) \cos 2\phi + B_1(\theta) \sin \phi + B_2(\theta) \sin 2\phi$$

where

$$A_n(\theta) = \sum_{m=0}^{2} \left(N_{cc}^{mn} \cos m\theta + N_{sc}^{mn} \sin m\theta \right)$$

and

$$B_n(\theta) = \sum_{m=0}^{2} \left(N_{cs}^{mn} \cos m\theta + N_{ss}^{mn} \sin m\theta \right). \tag{102}$$

The physical nature of the distribution of the trabeculae places mathematical constraints on the Trabecular Distribution Function which, in turn, constrains the Fourier coefficients. For instance, we can assume that the Trabecular Distribution Function is a continuous function of the longitude θ even at the "north pole" and the "south pole" of the sphere illustrated in Figure 7. This requires that

$$\hat{\nu}(\theta, n\pi) = \text{constant for} \quad n = 0, \pm 1, \pm 2, \ldots \tag{103}$$

In addition, we can observe that a trabecular plate, defined by a unit vector $\underset{\sim}{w}$, will be indistinguishable from a trabecular plate defined by the unit vector $-\underset{\sim}{w}$. This will require that

$$\nu(\underset{\sim}{w}) = \nu(-\underset{\sim}{w})$$

and

$$\hat{\nu}(\theta, \phi) = \hat{\nu}(\theta + \pi, \phi + \pi) \tag{104}$$

When these constraints are applied to the series (102), they take the form

$$A_0(\theta) = A_0(\theta+\pi)$$

$$A_0(\theta) - A_2(\theta) = \text{constant}$$

$$A_1(\theta) = 0$$

$$B_1(\theta) = 0$$

and $$B_2(\theta) = -B_2(\theta+\pi). \tag{105}$$

And when they are applied to the Fourier coefficients they constrain

$$N_{cc}^{22} = -N_{cc}^{20}$$

and (106)

$$N_{sc}^{22} = -N_{sc}^{20}$$

while they require the coefficients N_{cc}^{01}, N_{cc}^{10}, N_{cc}^{11}, N_{cc}^{12}, N_{cc}^{22}, N_{sc}^{10}, N_{sc}^{11}, N_{sc}^{12}, N_{sc}^{21}, N_{cs}^{01}, N_{cs}^{02}, N_{cs}^{11}, N_{cs}^{21}, N_{ss}^{11}, N_{ss}^{12}, N_{ss}^{21}, and N_{ss}^{22} to be equal to zero. This allows us to rewrite the series (100) into the form

$$\hat{\nu}(\theta, \phi) = N_{cc}^{00} + N_{cc}^{02} + \left[N_{cc}^{02} + N_{cc}^{22} \cos 2\theta + N_{sc}^{22} \sin 2\theta\right]\left[\cos 2\phi - 1\right] + \left[N_{cs}^{12} \cos \theta + N_{ss}^{12} \sin \theta\right]\left[\sin 2\phi\right] \tag{107}$$

where there are only six independent Fourier coefficients.

The next step in our development is to consider how the function $\overline{\nu}(\underline{w})$ can be expressed in terms of these Fourier coefficients. If we substitute the definition of the vector components of $\underline{w}$ (84) into the

truncated Fourier series (107), $\bar{\nu}(\underset{\sim}{w})$ can be expressed as a quadratic form

$$\bar{\upsilon}(\underset{\sim}{w}) = M_{ij}\, w_i\, w_j \qquad \text{for} \quad |\underset{\sim}{w}| = 1 \tag{108}$$

where

$$M_{11} = N_{cc}^{00} - N_{cc}^{02} - 2N_{cc}^{22}$$

$$M_{22} = N_{cc}^{00} - N_{cc}^{02} + 2N_{cc}^{22}$$

$$M_{33} = N_{cc}^{00} + N_{cc}^{02}$$

$$M_{23} = M_{32} = N_{ss}^{21}$$

$$M_{13} = M_{31} = N_{cs}^{21}$$

and

$$M_{12} = M_{21} = -2N_{sc}^{22}\,. \tag{109}$$

The extreme simplicity of the expression (108) suggests that we use the tensor $\underset{\sim}{M}$ to specify the trabecular adaptation, in lieu of the Trabecular Distribution Function. We will call the symmetric, second rank tensor $\underset{\sim}{M}$ the Trabecular Adaptation Tensor and observe that it will have the same properties of objectivity and symmetry as the symmetric second rank tensor describing the stress and strain.

Furthermore, like the stress and strain tensors, the Trabecular Adaptation Tensor is subject to physical interpretation. To demonstrate this physical significance, we will first observe that, using integrals (100) and constraints (106), the tensor components of $\underset{\sim}{M}$ can be expressed directly in terms of the function $\bar{\nu}(\underset{\sim}{w})$ by the expression

$$M_{ij} = \left(\frac{1}{\pi^2}\right) \oint_{|\underset{\sim}{w}|=1} w_i\, w_j\, \bar{\nu}(\underset{\sim}{w})\; dS \tag{110}$$

Let us next assume that the material described by this integral possesses, at any given point, only a finite number of trabecular plates. Using definitions (86) and (87) this integral can then be recast as the finite summation

$$M_{ij} = \left(\frac{1}{\pi^2}\right) \sum_{\alpha=1}^{N} w_i^{\alpha} w_j^{\alpha} \gamma^{\alpha} \tag{111}$$

where the integer N now refers to the number of the trabecular plates at the given point. We next remark that anatomical observation of living bone indicates that cancellous bone is generally arranged in a pattern of mutually perpendicular trabecular plates. Consequently, if we define an orthogonal tensor $\underset{\sim}{L}$ as a continuous function of position such that the coordinate axes are always mapped by $\underset{\sim}{L}(\underset{\sim}{x})$ into normals of the trabecular plates, we can express the Trabecular Adaptation Function in the form

$$\underset{\sim}{M} = \underset{\sim}{L}^{t} \begin{bmatrix} \lambda_1 & 0 & 0 \\ 0 & \lambda_2 & 0 \\ 0 & 0 & \lambda_3 \end{bmatrix} \underset{\sim}{L} \tag{112}$$

where λ_1, λ_2 and λ_3 describe the bulk mass density of the trabecular plates normal to the vectors $\underset{\sim}{L}\,\underset{\sim}{i}_1$, $\underset{\sim}{L}\,\underset{\sim}{i}_2$ and $\underset{\sim}{L}\,\underset{\sim}{i}_3$, respectively. If, in addition, we assume that the local mass density of the lamellar bone making up the trabeculae has a uniform mass density, we can make the following physical interpretation of the tensor field $\underset{\sim}{M}$:

1) the eigen vectors of $\underset{\sim}{M}$ represent normals to the trabecular plates of the matrix structure of cancellous bone; and

2) the eigen values, corresponding to these eigen vectors are proportional to the thickness of these trabecular plates.

It therefore can be concluded that the trabecular adaptation of cancellous bone can be described mathematically by evaluating the Trabecular Adaptation Tensor and this Trabecular Adaptation Tensor can be determined by evaluating the fields λ_1 λ_2 λ_3 and $\underset{\sim}{L}$. In Section IV we will discuss procedures by which measurement of these parameters might be effected.

d. The Constitutive Functions and Material Objectivity

At the end of the previous subsection we concluded that in order to quantitatively specify the properties of an Adaptive Elastic Material it would be necessary to specify two sets of functions: A Stiffness Function and a set of Remodeling Functions. In this subsection we demonstrated that it is possible to represent the trabecular adaptation, formerly specified by the parameter set $\{\gamma^{\alpha}\}$, by a symmetric, second-rank Trabecular Adaptation Tensor, $\underset{\sim}{M}$. In this subsubsection we will consider how these Stiffness and Remodeling Functions can be reformulated in terms of the tensor $\underset{\sim}{M}$ and how the spectral decomposition of $\underset{\sim}{M}$ and material objectivity with respect to $\underset{\sim}{M}$ effect this reformulation.

Let us first consider the Stiffness Function, which we wish to evaluate as the function

$$C_{ijk\ell} = \hat{C}_{ijk\ell}(\underset{\sim}{M}) \tag{113}$$

If the objectivity conditions are applied to equation (96), the stiffness tensor takes the form

$$C_{ijk\ell} = \sum_{\alpha=1}^{N} Q_{ip}\, Q_{jq}\, Q_{rk}\, Q_{s\ell}\, \overline{\nu}(\underset{\sim}{Q}\underset{\sim}{w}^{\alpha})\, dS \tag{114}$$

Where $\underset{\sim}{Q}$ is an arbitrary orthogonal transformation and N is the (finite) number of trabecular plates. However, we have already stated that we can consider $N=3$. If we now use the approximation (108) and consider the vectors $\underset{\sim}{Q}\underset{\sim}{w}^{\alpha}$ as being the eigen vectors of M, then eq. (113) takes the form

$$C_{ijk\ell} = \hat{C}_{ijk\ell}(\underset{\sim}{M}) = \sum_{\alpha=1}^{3} \lambda^{\alpha}\, Q^{\alpha}_{ip}\, Q^{\alpha}_{jq}\, Q^{\alpha}_{rk}\, Q^{\alpha}_{s\ell}\, C^{o}_{pqrs} \tag{115}$$

where

$$Q^{1}_{ij} = \begin{bmatrix} L_{33} & L_{31} & L_{32} \\ L_{13} & L_{11} & L_{12} \\ L_{23} & L_{21} & L_{22} \end{bmatrix}$$

$$Q^2_{ij} = \begin{bmatrix} L_{22} & L_{23} & L_{21} \\ L_{32} & L_{33} & L_{31} \\ L_{12} & L_{13} & L_{11} \end{bmatrix} \tag{116}$$

$$Q^3_{ij} \quad \begin{bmatrix} L_{11} & L_{12} & L_{13} \\ L_{21} & L_{22} & L_{23} \\ L_{31} & L_{32} & L_{33} \end{bmatrix}$$

and where λ^{α} and L_{ij} are given in eq. (119) and C^{o}_{pqrs} describes the stiffness of a single trabecular plate in the x_1 x_2 plane.

Let us next consider the equations describing the rate of the chemical reactions. On rewriting (95) in terms of the variable $\underset{\sim}{M}$ the resulting equation would have the form

$$\dot{\underset{\sim}{M}} = \hat{\underset{\sim}{R}} (\underset{\sim}{E}, \underset{\sim}{M}) \tag{117}$$

where the second rank tensor function $\hat{\underset{\sim}{R}}$ can be called the Remodeling Function. The objectivity requirement, in direct notation, takes the form

$$\underset{\approx}{Q}\, \hat{\underset{\approx}{R}} (\underset{\approx}{Q}\underset{\approx}{E}\underset{\approx}{Q}^t ; \underset{\approx}{Q}\underset{\approx}{M}\underset{\approx}{Q}^t)\, \underset{\approx}{Q} = \hat{\underset{\approx}{R}} (\underset{\sim}{E}; \underset{\sim}{M}) \tag{118}$$

We also know that the strain dependence of $\hat{\underset{\sim}{R}}$ is quadratic. Thus, analogous to eq. (99), eq. (117) can be recast into the form

$$\dot{M}_{ij} = \hat{F}^{ij} (M_{ab}) + E_{k\ell}\, \hat{G}^{ij}_{k\ell} (M_{ab}) + E_{k\ell}\, E_{mm}\, \hat{H}^{ij}_{k\ell mm} (M_{ab}) \tag{119}$$

If we now apply the objectivity constraint eq. (118) to this expression, we then have

$$\dot{M}_{ij} = Q_{im} Q_{j n} \hat{F}^{mn}(Q_{ca} Q_{db} M_{cd}) + Q_{im} Q_{jn} Q_{rp} Q_{sq} E_{rs} \hat{G}^{mn}_{pq}(Q_{ca} Q_{db} M_{cd})$$

$$+ Q_{im} Q_{jn} Q_{rp} Q_{sq} Q_{vt} Q_{wu} E_{rs} E_{vw} \hat{H}^{mn}_{pqtu} (Q_{rp} Q_{sq} M_{rs})$$

(120)

for any orthogonal $\underset{\sim}{Q}$. In the special case when $\underset{\sim}{Q}$ equals the tensor $\underset{\sim}{Q}^3_{ij}$ given by the formula in eq. (116), then the arguments of the Functions $\hat{F}^{ij}_{kk}$ $\hat{G}^{ij}_{k\ell}$ and $\hat{H}^{ij}_{k\ell mn}$ become diagonalized. Thus (120) can be recast again in terms of three new functions $\hat{F}^{ij}$, $\hat{G}^{ij}_{k\ell}$ and $\hat{H}^{ij}_{k\ell mn}$ which depends only on the eigen values of $\underset{\sim}{M}$, i.e.

$$\dot{M}_{ij} = Q^3_{im} Q^3_{jn} \hat{F}^{mn}(\lambda_1, \lambda_2, \lambda_3) + Q^3_{im} Q^3_{jn} Q^3_{rp} Q^3_{sq} E_{rs} \hat{G}^{mn}_{pq}(\lambda_1, \lambda_2, \lambda_3)$$

$$+ Q^3_{im} Q^3_{jn} Q^3_{rp} Q^3_{sq} Q^3_{rt} Q^3_{wu} E_{rs} E_{vw} \hat{H}^{mn}_{pqtu} (\lambda_1, \lambda_2, \lambda_3)$$

(121)

Furthermore, if we also consider $\underset{\sim}{Q}^2$ and $\underset{\sim}{Q}^1$ we will have the constraints

$$\hat{R}_{ij}(\underset{\sim}{E}; \underset{\sim}{M}) = Q^1_{im} Q^1_{jn} \hat{F}^{mn}(\lambda_2, \lambda_3, \lambda_1) + Q^1_{im} Q^1_{jn} Q^1_{rp} Q^1_{sq} E_{rs} \hat{G}^{mn}_{pq}(\lambda_2, \lambda_3, \lambda_1)$$

$$+ Q^1_{im} Q^1_{jn} Q^1_{rp} Q^1_{sq} Q^1_{rt} Q^1_{wu} E_{rs} E_{vw} \hat{H}^{mn}_{pqtu} (\lambda_2, \lambda_3, \lambda_1)$$

$$= Q^2_{im} Q^2_{jn} \hat{F}^{mn}(\lambda_3, \lambda_1, \lambda_2) + Q^2_{im} Q^2_{jn} Q^2_{rp} Q^2_{sq} E_{rs} \hat{G}^{mn}_{pq}(\lambda_3, \lambda_1, \lambda_2)$$

$$+ Q^2_{im} Q^2_{jn} Q^2_{rp} Q^2_{sq} Q^2_{rt} Q^2_{wu} E_{rs} E_{vw} \hat{H}^{mn}_{pqtu} (\lambda_3, \lambda_1, \lambda_2)$$

$$= Q^3_{im} Q^3_{jn} \hat{F}^{mn}(\lambda_1, \lambda_2, \lambda_3) + Q^3_{im} Q^3_{jn} Q^3_{rp} Q^3_{sq} E_{rs} \hat{G}^{mn}_{pq}(\lambda_1, \lambda_2, \lambda_3)$$

$$+ Q^3_{im} Q^3_{jn} Q^3_{rp} Q^3_{sq} Q^3_{rt} Q^3_{wu} E_{rs} E_{vw} \hat{H}^{mn}_{pqtu} \ (\lambda_1, \lambda_2, \lambda_3).$$

e. Summary of the Cancellous Bone Model

We began this subsection with a mathematical model for cancellous bone in which the trabecular adaptation was described by a variable set $\{\gamma^\beta\}$ indicating the bulk mass density of a finite number of trabecular plates. This formulation was unsatisfactory, since we did not know a priori the orientation of the trabecular basis by which or through which these trabecular plates were ordered. In the second subsubsection, we replaced dependence on the variable set $\{\gamma^\beta\}$ with dependence on a Trabecular Distribution Function $\overline{\nu}(\underset{\sim}{w})$ which gave our model an infinite trabecular basis. Specification of the trabecular adaptation in terms of the Trabecular Distribution Function did free us from dependence on an arbitrary fixed trabecular basis, but the resulting governing equations were very cumbersome to deploy. In the third subsection, we demonstrated that the Trabecular Distribution Function could be approximated by a quadratic form $\overline{\nu}(\underset{\sim}{w}) = \underset{\sim}{w}\,\underset{\sim}{M}\,\underset{\sim}{w}$ and hence the trabecular adaptation of cancellous bone can be represented by a symmetric, second-rank tensor, $\underset{\sim}{M}$, called the Trabecular Adaptation Tensor. This tensorial representation of the trabecular adaptation in terms of $\underset{\sim}{M}$ is very convenient mathematically, since it allows $\underset{\sim}{M}$ to be subject to the same objectivity and symmetry considerations that apply to the tensors fields $\underset{\sim}{E}$ and $\underset{\sim}{T}$. In addition, the tensor $\underset{\sim}{M}$ has a very convenient physical interpretation: the eigen vectors of $\underset{\sim}{M}$ represent normals to the trabecular plates while the eigen values of $\underset{\sim}{M}$ represent the thickness of these plates.

The governing equations for cancellous bone consist of

a) a definition of the strain tensor in terms of the displacement,

$$E_{ij} = \tfrac{1}{2}\left[u_{i,j} + u_{j,i}\right] \ ; \tag{122}$$

b) a stress-strain relationship

$$T_{ij} = C_{ijk\ell} E_{k\ell} \tag{123}$$

where

$$C_{ijk\ell} = \hat{C}_{ijk\ell}\ (M_{rs})\ ; \tag{124}$$

(c) a rate of reaction equation

$$\dot{M}_{ij} = \hat{R}_{rs}\ (E_{pq},\ M_{rs}) \tag{125}$$

or

$$\dot{M}_{ij} = \hat{F}^{ij}(M_{rs}) + E_{k\ell}\,\hat{G}^{ij}_{k\ell}\ (M_{rs}) + E_{k\ell}E_{mn}\hat{H}^{ij}_{k\ell mn}(M_{rs})\ ;$$

and

(d) a conservation of momentum equation

$$\gamma\,\ddot{u}_i = T_{ij,j} + \gamma\, b_i \tag{126}$$

where

$$\gamma = \frac{1}{\pi^2}\ \mathrm{tr}\ \underset{\sim}{M}\ ; \tag{127}$$

where $\underset{\sim}{M}$ is symmetric and hence can be resolved as

$$\underset{\sim}{M} = \underset{\sim}{L}^t \begin{bmatrix} \lambda_1 & 0 & 0 \\ 0 & \lambda_2 & 0 \\ 0 & 0 & \lambda_3 \end{bmatrix} \underset{\sim}{L} \tag{128}$$

with $$\underset{\sim}{L}\,\underset{\sim}{L}^t = 1\ . \tag{129}$$

To specify a traction boundary value problem, the following data must be given

1) The geometric configuration of the body B and the two constitutive functions, the Stiffness Function (124) and the Remodeling Function (125);

2) The time interval $(0, t_o)$ for which a solution is desired;

3) The body force field, $\underset{\approx}{b}$, acting on the body B;

4) The surface traction $\hat{\underset{\sim}{s}}$ specified on ∂B for $(0, t_o)$, where

$$\hat{s}_i = n_j T_{ij} (\underset{\approx}{x}, t) \text{ for } \underset{\approx}{x} \in \partial B \tag{130}$$

and n_j is a unit normal to the surface ∂B;

5) The continuous initial displacement field $\underset{\sim}{v}^o(\underset{\approx}{x})$, the continuous Initial Trabecular Adaptation Tensor field $\underset{\approx}{\tilde{M}}^o(\underset{\approx}{x})$, and the continuous intital velocity field $\underset{\sim}{v}^o(\underset{\approx}{x})$ for all $\underset{\approx}{x} \in B$ where

$$\underset{\sim}{v}^o(\underset{\approx}{x}) = \frac{\partial}{\partial t} \underset{\sim}{u}(\underset{\approx}{x}, t)\Big|_{t=o} \tag{131}$$

With these data, the traction boundary value problem of quasi-static, isothermal, adaptive elasticity is to determine the fields $\underset{\sim}{\tilde{u}}(\underset{\approx}{x}, t)$, $\underset{\approx}{\tilde{M}}(\underset{\approx}{x}, t)$, $\underset{\approx}{\tilde{E}}(\underset{\approx}{x}, t)$, $\underset{\approx}{\tilde{T}}(\underset{\approx}{x}, t)$ corresponding to b which satisfy:

1) The initial conditions

$$\underset{\sim}{\tilde{u}}(\underset{\approx}{x}, 0) = \underset{\sim}{u}^o(x), \quad \underset{\approx}{\tilde{M}}(\underset{\approx}{x}, 0) = \underset{\approx}{M}^o(\underset{\approx}{x}) \text{ on } B; \tag{132}$$

and

2) The boundary conditions

$$n_j \tilde{T}_{ij}(\underset{\approx}{x}, t) = \hat{s}_i(\underset{\approx}{x}, t) \text{ on } \partial B; \tag{133}$$

and equations (121) through (127).

II. 7 INTERPRETATION OF THE MODEL

Let us now interpret these equations in terms of the observable remodeling properties of cancellous bone. Assuming that bone in a particular region initially has a trabecular adaptation of

$$\underset{\sim}{M}^{o} = \begin{bmatrix} \lambda_1^o & 0 & 0 \\ 0 & \lambda_2^o & 0 \\ 0 & 0 & \lambda_3^o \end{bmatrix} \tag{134}$$

when expressed in the appropriate coordinate system. We will first consider the behavior of the system under uniaxial loading $T_{ij}^{o} = -P^{o}\,\delta_{i3}\,\delta_{j3}$ whose magnitude P^{o} (>0) is such that the total rate of remodeling on all trabeculae is zero. Physiologically, a zero rate of remodeling on all trabecular plates may be termed homeostasis and occurs when the net rate a bone accreation on each trabecular plate exactly cancels the rate of bone resorption. Mathematically, homeostasis requires that the strain E^{o} have a value such that $T_{ij}^{o} = C_{ijk\ell}(\underset{\sim}{M}^{o})\; E_{k\ell}^{o}$ and that $\underset{\sim}{\hat{R}}(\underset{\sim}{E}^{o}; \underset{\sim}{M}^{o}) = 0$. We will also note in passing that the symmetry will require that $\lambda_1^o = \lambda_2^o$.

Let us next consider what would happen if the load were increased, i.e., the value of $\underset{\sim}{T}$ were modified to $T'_{ij} = T_{ij}^{o} - \Delta\,\delta_{i3}\,\delta_{j3}$. Provided $\Delta > 0$, the absolute value of the strain will increase, and, in particular, the negative value of the strain component E_{33} will become more negative. Physiologically, an increase in the axial compressive strain might be expected to stimulate osteoblastic activity in the trabecular plates which run along the x_3 axis, i.e., the plates which are perpendicular to the x_1 and x_2 axes. Mathematically, a more negative component, E_{33}, will cause the R_{11} and R_{22} components of the remodeling function to become positive and the M_{11} and M_{22} components of the trabecular adaptation tensor to have larger positive values. As the two trabecular plates normal to the x_1 and x_2 axes become thicker, the strain, induced by the loading T'_{ij} tends to decrease and the net rate of bone accreation tends to decrease. Mathematically, this means that as M_{11} and M_{22} increase, E_{33} becomes less negative and the R_{11} and R_{22} components of the remodeling function, which bring about the trabecular thickening, also decrease. Thus, as long as the load T'_{ij} continues to be applied, the trabecular plates continue to be thickened, but at a progressively slower rate. Mathematically, we can say that the system asymptotically approaches a new state of homeostasis for the ambient loading T'_{ij} in which the trabecular adaptation tensor has the form

$$\underset{\sim}{M} = \underset{\sim}{M}' = \begin{bmatrix} \lambda'_1 & 0 & 0 \\ 0 & \lambda'_2 & 0 \\ 0 & 0 & \lambda'_3 \end{bmatrix} \tag{135}$$

where $\lambda'_1 > \lambda^o_1$, $\lambda'_2 > \lambda^o_2$, $\lambda'_3 \geq \lambda^o_3$. In addition, symmetry again requires that $\lambda'_1 = \lambda'$ physiologically, the attainment of this new state of homeostasis corresponds to an increase in the axial loading, causing an increase in the thickness of the trabeculae supporting the axial load. The effect of increased loading is schmatically described in the second frame of Figure 9.

Likewise, we can expect that the system will respond to a decrease in axial loading in an analogous fashion: Given a system where the trabecular adaptation tensor is initially M^o given by (130) and where the loading is decreased to the value $T''_{ij} = T^o_{ij} - \Delta \delta_{i3} \delta_{j3}$ with $\Delta < 0$, the system can be expected to approach a new state of homeostasis in which the trabecular adaptation tensor will have the form

$$\underset{\sim}{M} = \underset{\sim}{M}'' = \begin{bmatrix} \lambda''_1 & 0 & 0 \\ 0 & \lambda''_2 & 0 \\ 0 & 0 & \lambda''_3 \end{bmatrix} \tag{136}$$

where $\lambda''_1 = \lambda''_2 < \lambda^o_1 = \lambda^o_2$ and $\lambda''_3 \leq \lambda^o_3$. Physiologically, this corresponds to a decrease in the axial loading, causing a decrease in the thickness of the trabeculae supporting this axial load. The effect of a decreased load on the trabeculae normal to the x_2 axis is schematically illustrated in the third frame of Figure 9.

Finally, we will consider the response of the system to a shear loading. Let us consider the system, initially with a trabecular adaptation $\underset{\sim}{M}^o$ given by (130), in which the load is of the form

$$\underset{\sim}{T}^* = -P^0 \begin{bmatrix} 0 & 0 & 0 \\ 0 & [\sin^2 \theta] & [\sin \theta \cos \theta] \\ 0 & [\sin \theta \cos \theta] & [\cos^2 \theta] \end{bmatrix} \tag{137}$$

where $P > 0$. It is not difficult to demonstrate that this load is nothing more than the uniaxial load $\underset{\sim}{T}^o = P \delta_{i3} \delta_{j3}$ rotated θ radians around the x_i axis. If θ is small, $\cos^2 \theta \approx 1$ and $\sin^2 \theta$ is negligible and thus the principal difference between the load $\underset{\sim}{T}^o$ and the load $\underset{\sim}{T}^*$ is the presence of the shear component T_{23} and T_{32} in the latter. These shear stress components will, in turn, cause the off-diagonal components of the remodeling function $\hat{R}_{23}$ and $\hat{R}_{32}$ to be nonzero. Physiologically, the appearance of a shear load can be observed to induce remodeling of the trabecular structure whose net effect

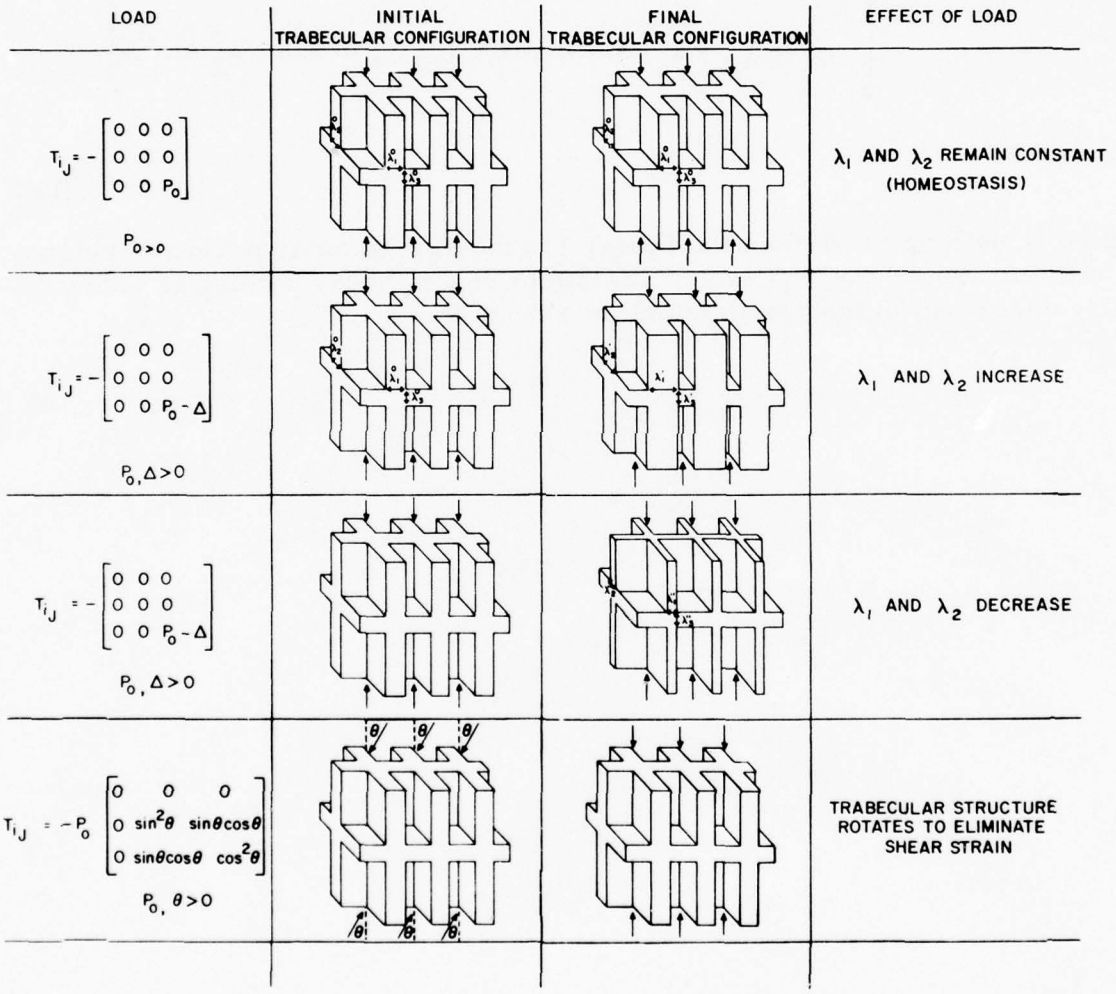

Figure 9. Trabecular Configuration Under Various Loading Conditions.

is to eliminate the shear strain. This can be accomplished if this remodeling caused reorientation of the trabecular structure so that the principal axis of the tensor $\underset{\sim}{M}$ is made to coincide with the principal axis of the ambient strain tensor. This means we can expect that the Trabecular Adaptation Tensor will asymptotically approach the value

$$\underset{\sim}{M}^* = \underset{\sim}{M} = \begin{bmatrix} \lambda_1^o & 0 & 0 \\ 0 & [\lambda_2^o \cos^2\theta + \lambda_3^o \sin^2\theta] & [(\lambda_3^o - \lambda_2^o) \sin\theta \cos\theta] \\ 0 & [(\lambda_3^o - \lambda_1^o) \sin\theta \cos\theta] & [\lambda_3^o \cos^2\theta + \lambda_2^o \sin^2\theta] \end{bmatrix} \tag{138}$$

which is nothing more than the initial Trabecular Adaptation Tensor rotated θ radians around the x_1 axis. The effect of this shear loading is schematically described in the fourth frame of Figure 9.

SECTION III

THE PROBLEM OF TWO-DIMENSIONAL STRESS-ADAPTATION AND ITS NUMERICAL APPROXIMATION

III.1 INTRODUCTION

The previous section developed a mathematical model for cancellous bone. This section will demonstrate its application. However, any demonstration of this model will require that we first must solve the governing equations (122) - (126). Because of the complexity of solving a system of nine partial differential equations in nine unknowns (three displacement and six trabecular adaptation components) we would be well advised to seek plausible methods of simplifying their solution. In subsection III. 2, we will introduce two methods of simplification: the two-dimensionalization and finite element approximation of the governing equations. The former simplification is motivated by the fact that it is possible in Classical Elasticity to reformulate a number of technically important boundary value problems in only two dimensions. Finite element approximation allows us to avoid the virtually impossible task of finding an analytic solution.

However, the use of numerical techniques has one distinct disadvantage: In order to solve the simplified governing equations that are developed in Subsection III. 2 we must have explicit formulations for the analogs of the constitutive functions (124) and (125). Although there are a number of sources from which one might plausibly estimate the form of the stiffness function (124), there is, with a single exception, nothing in the literature from which one might determine the form of the remodeling function. This single exception is the author's dissertation (Hegedus 1976), in which a special case of the stress-adaptation of cortical bone was analyzed. In his analysis the author used certain well-documented qualitative properties of bone remodeling to obtain phenomenological constraint on the remodeling function. With these phenomenological constraints it was possible to obtain an analytic solution to the problem of the stress-adaptation of cortical bone in the special case of uniform uniaxial stress.

In subsection III. 3, we will introduce finite element techniques and use these techniques to argue that cancellous bone may be approximated as a pinned triangular structure whose structural cross-members (trabecular links) behave mechanically as miniature copies of the cortical bone analyzed in the author's dissertation. In subsection III. 5 we will discuss the organization and application of a series of computer programs which simulate the stress-adaptation properties of cancellous bone, using the model subject to the above approximations.

We will show that the model predicts that an initially homogeneous adaptive elastic body, in the shape of a human femur, subject to the boundary traction analogous to that of a human femur will develop values for the tensor field $\underset{\sim}{M}$ which correspond to the trabecular patterns which are visible in the human femur in situ.

III. 2 PLANE STRESS

As mentioned above, in classical elasticity it is possible to reduce a number of technically important boundary value problems in terms of governing equations of only two dimensions. One of the best examples of such a reduction in dimensions occurs in the case of Plane Stress . Plane Stress (in the $x_1 x_2$ -plane) is said to occur if the stress tensor components T_{13} , T_{23} , and T_{33} vanish for all $\underset{\sim}{x}$ and t. The conditions of plane stress are most easily demonstrated under the following circumstances:

Let us consider a generalized cylinder, as illustrated in Figure 10, with a generator parallel to the x_3 axis and with bases in the planes $x_3 = \pm h$. This body can be said to be 'thin' in the x_3 direction, provided that the height of the cylinder, 2h, is small compared to the linear dimensions of the generator. Let us now assume that all boundary forces applied to the surface of the cylinder ∂B are applied only to its lateral surface $\partial B'$ and that these forces exist only in the $x_1 x_2$- plane and are uniform with respect to the variable x_3 . Let us further assume that the inertial and body forces are negligible and that the material composing the cylinder is also uniform and symmetric with respect to the x_3 axis. Under these circumstances, if we define the two-dimensional "reduced" stiffness tensor

$$\overline{C}_{abcd} = C_{abcd} - \frac{C_{ab33}\, C_{cd33}}{C_{3333}} \tag{139}$$

and the two-dimensional "average" displacement vector

$$\overline{u}_a = \overline{u}_a(x_1, x_2; t) = \frac{1}{2h} \int_{x_3=-h}^{x_3=+h} u_a(x_1, x_2, x_3; t)\, dx_3 \tag{140}$$

where the indices a, b, c and d take on only the values 1 and 2 ; then it is possible to show that the governing equations (122) and (123) reduce to the set

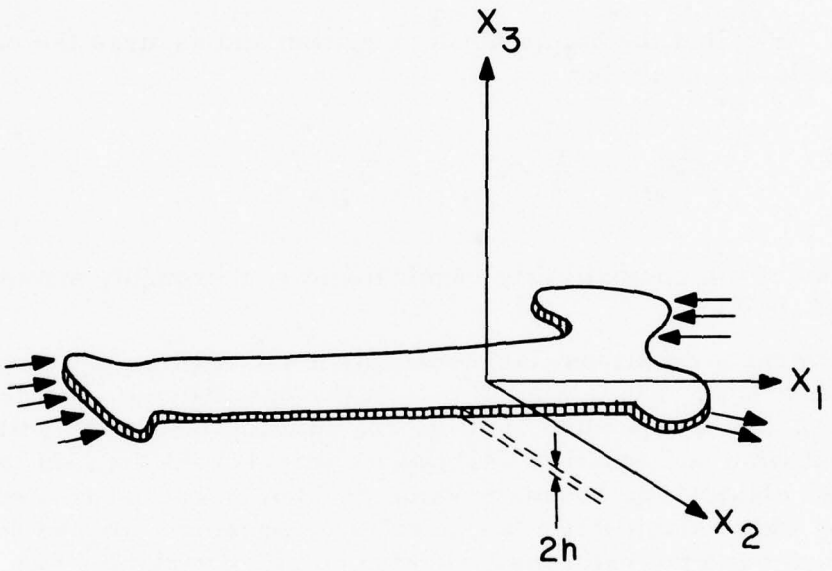

Figure 10. Plane Stress Applied to a 'Thin' Generalized Cylinder.

$$(\bar{C}_{abcd}\bar{E}_{cd})_b = 0$$

and

$$2\,\bar{E}_{12,12} = \bar{E}_{11,22} + \bar{E}_{22,11} \tag{141}$$

while the boundary conditions (133) can be written in the form

$$(C_{abcd}E_{cd}h_b)\Big|_{x\in\partial B'} = s_a(\underset{\sim}{x};t)\Big|_{x\in\partial B'} \tag{142}$$

Equation (141) is called the compatibility equation and assures the existence of a vector field $\bar{u}_a$ such that

$$\bar{E}_{ab} = \frac{1}{2}\,(\bar{u}_{a,b} + \bar{u}_{b,a})\,. \tag{143}$$

The derivation of the compatibility requirement is thoroughly discussed in Sokolnikoff (1956).

The governing equations (141) constitute a set of three equations in the three unknowns $\bar{E}_{11}$, $\bar{E}_{12}$, and E_{22}. In the special case when the boundary conditions (142) are independent of time, the solution tensor $\underset{\sim}{\bar{E}}$ will also be independent of time and equation (141) taken with (142) will be said to constitute a plane stress elastostatic boundary value problem. These are a number of techniques by which elastostatic boundary value problems may be solved. One very elegant and powerful method using complex variables was originally suggested by Kolossoff and was subsequently developed by Muskhelishvili (1953). A very readable discussion of the use of complex variables applied to elastostatic boundary value problems is found in Sokolinikoff (1956). Another, even more powerful, albeit less elegant, method of solving the elastostatic boundary value problems may be obtained using finite element approximations. Finite element methods will be discussed in the following two sections. For general references to finite element techniques, the reader is directed to Huebner (1975) and Zienkiewicz (1971).

Let us now consider how the problem of classical plane elastostatics can be generalized to encompass adaptative elastic materials. We will first note that the requirements of symmetry about the x_3 axis will require the trabecular adaptation tensor $\underset{\sim}{M}$ to have the form

$$\underset{\sim}{M} = \begin{bmatrix} M_{11} & M_{12} & 0 \\ M_{12} & M_{22} & 0 \\ 0 & 0 & M_{33} \end{bmatrix} \tag{144}$$

i.e. there exists a trabecular plate normal to the x_3-plane. In order to two-dimensionalize the governing equations (122-126) one must first two-dimensionalize the tensor $\underset{\sim}{M}$ in a manner analogous to the reduction of the stiffness tensor (139). This will require that there exists a function $\underset{\sim}{\bar{H}}$, mapping the set of all three-dimensional second-rank tensors in the form of (144) onto the set of all two-dimensional symmetric second-rank tensors $\underset{\sim}{\bar{M}}$, i.e.

$$\underset{\sim}{\bar{H}} \left(\underset{\sim}{M} \right) = \underset{\sim}{\bar{M}} \tag{145}$$

where this mapping is subject to the constraint that

$$\underset{\sim}{\bar{H}} \begin{bmatrix} M_{11} & M_{12} & 0 \\ M_{12} & M_{22} & 0 \\ 0 & 0 & 0 \end{bmatrix} = \begin{bmatrix} M_{11} & M_{12} \\ M_{12} & M_{22} \end{bmatrix} \quad \text{for all } M_{33} \tag{146}$$

Having defined such a mapping, the governing equations (122-126) take the form

$$\dot{\bar{M}}_{ab} = \hat{\bar{R}}_{ab} \left(\underset{\sim}{\bar{E}} , \underset{\sim}{\bar{M}} \right)$$

$$\left[\hat{\bar{C}}_{abcd} (\underset{\sim}{\bar{M}}) \, \bar{E}_{cd} \right]_{,b} = 0 \tag{147}$$

and

$$2 \bar{E}_{12,12} = \bar{E}_{11,22} + \bar{E}_{22,11}$$

and are subject to the initial conditions

$$\underset{\sim}{\bar{M}} (\underset{\sim}{x} , t) \Big|_{t=0} = \underset{\sim}{\bar{M}}^{\circ} (\underset{\sim}{x}) \tag{148}$$

and the boundary conditions

$$\hat{s}_a(\underset{\sim}{x},t)\Big|_{\underset{\sim}{x}\in B'} = \bar{C}_{abcd}[M(\underset{\sim}{x},t)]\;\bar{E}_{cd}(\underset{\sim}{x},t)\,n_b\Big|_{\underset{\sim}{x}\in\partial B'} \tag{149}$$

while the stiffness and remodeling functions are subject to the constraints,

$$\hat{C}_{abcd}[\bar{\underset{\sim}{H}}(\underset{\sim}{M})] = \hat{C}_{abcd}(\underset{\sim}{M}) - \frac{\hat{C}_{ab33}(\underset{\sim}{M})\,\hat{C}_{cd33}(\underset{\sim}{M})}{C_{3333}(\underset{\sim}{M})} \tag{150}$$

and

$$\hat{\bar{R}}_{ab}[\bar{\underset{\sim}{E}},\bar{\underset{\sim}{H}}(\underset{\sim}{M})] = \frac{\partial H_{ab}}{\partial M_{ij}}\;\hat{R}_{ij}[\underset{\sim}{E},\underset{\sim}{M}] \tag{151}$$

respectively, where

$$\bar{\underset{\sim}{E}} = \begin{bmatrix} \bar{E}_{11} & \bar{E}_{12} \\ \bar{E}_{12} & \bar{E}_{22} \end{bmatrix} = \begin{bmatrix} 1 & 0 & 0 \\ 0 & 1 & 0 \end{bmatrix} \begin{bmatrix} E_{11} & E_{12} & 0 \\ E_{12} & E_{22} & 0 \\ 0 & 0 & E_{33} \end{bmatrix} \begin{bmatrix} 1 & 0 \\ 0 & 1 \\ 0 & 0 \end{bmatrix} \tag{152}$$

Let us now consider the physical significance of these two-dimensional approximations. The existence of the mapping $\hat{\bar{H}}(\underset{\sim}{M})$ implies that for any three-dimensional trabecular structure whose trabecular adaptation tensor can be described by (144), there must exist an equivalent "reduced" trabecular structure in which the trabeculae normal to the x_3 axis have been removed, i.e., one for which the trabecular adaptation tensor has the form

$$\begin{bmatrix} \bar{M}_{11} & \bar{M}_{12} & 0 \\ \bar{M}_{12} & \bar{M}_{22} & 0 \\ 0 & 0 & 0 \end{bmatrix}. \tag{153}$$

The constraint on the stiffness function (150) implies that, for the "reduced" trabecular structure. The remaining two sets of trabeculae which run along the x_3 axis have been strengthened appropriately so that the stress-strain relationship of the original three-dimensional trabecular structure is equivalent to the stress-strain relationship of plane stress. Likewise, the constraint on the remodeling function (151) implies that the "reduced" trabecular structure remodels in a manner exactly equivalent to that of the original three-dimension trabecular structure, when the latter is subjected to plane stress.

At this point we should make the obvious comment that the assumptions necessary in these two-dimensional approximations of the governing equations will not necessarily be satisfied exactly in the case of the living bone that we wish to consider. We might expect that the two-dimensional governing equations will describe behavior different from that occurring in the three-dimensional living bone, whenever and wherever one of the simplifying assumptions discussed above is violated. For example, the violation of the constraints (150) and (151) should become most manifest in a region in which there exist large variations in the value of M_{33}. In the case of the human femur, which will be discussed in subsection III. 6, the M_{33} component will vanish in an anatomical region called "Ward's Triangle". It is in the region of Ward's Triangle that the two-dimensional governing equations developed here will prove least satisfactory in describing the trabecular adaptation of the human femur.

III. 3 NUMERICAL TECHNIQUES

a. General Plan of Solution

We have already stated that adaptive elasticity may be regarded as a generalization of classical elasticity in which the elastic modulii are considered to be functions of the strain-history. This property has an important application in the case of an elastostatic boundary value problem. Given that the boundary conditions are not a function of time, the solution of $(147)_2$ and $(147)_3$ for the strain field $\underset{\sim}{E}$ at the time $t=0$ can be readily obtained by setting the field $\underset{\sim}{M}$ equal to the values given by (148) and then considering the solution of equations $(147)_2$ and $(147)_3$ for the field $\underset{\sim}{E}$ as equivalent to the solution of the classical plane elastostatic boundary value problem (141). Having obtained the strain field $\underset{\sim}{E}$, the change in the trabecular configuration in some time interval Δt can be calculated by numerical integration in time of the governing equation containing remodeling function $(147)_1$. The value of the trabecular adaptation at the time $t+\Delta t$ can then be used to solve $(144)_2$ and $(144)_3$ for the strain field $\underset{\sim}{E}$ at time $t+\Delta t$ and this process can be continued indefinitely. In this way one can reduce the problem of two dimensional adaptive elastostatics into two simpler problems: (1) solve equations $(147)_2$ and $(147)_3$ to determine the strain field as a function of space, and (2) use Picard integration of $(147)_1$ to determine the trabecular adaptation field $\underset{\sim}{M}$ as a function of time.

b. Solution for the Strain Field

The solutions of equations $(147)_2$ and $(147)_3$ can be effected by the method of finite element approximations. In its simplest form the finite element method resolves to the following technique: We divide the body into a system of ν triangular elements at whose vertices reside a total of N nodes. Next we approximate the governing equations by assuming that the strain and the physical properties of the material within each of these ν elements are uniform. Since the strain and stiffness of each element are uniform, it follows that the stress within each element is uniform. It is possible to resolve the

internal stress of the κ-th element as three two-dimensional forces $(f_i^{\kappa x}, f_i^{\kappa y})$, $(f_j^{\kappa x}, f_j^{\kappa y})$ and $(f_k^{\kappa x}, f_k^{\kappa y})$ acting at the node vertices i, j, and k, respectively. In a similar manner, it is possible to resolve the strain on the κ-th element in terms of the three vectors (u_i^x, u_i^y), (u_j^x, u_j^y) and (u_k^x, u_k^y), which describe the two-dimensional displacement of the three vertices of the κ-th triangular element. Using the stress-strain relations, it is then possible to write the force-displacement relation for the κ-th element in the form

$$\begin{bmatrix} f_i^{\kappa x} \\ f_i^{\kappa y} \\ f_j^{\kappa x} \\ f_j^{\kappa y} \\ f_k^{\kappa x} \\ f_k^{\kappa y} \end{bmatrix} = \begin{bmatrix} A_{ii}^{\kappa xx} & A_{ii}^{\kappa xy} & A_{ij}^{\kappa xx} & A_{ij}^{\kappa xy} & A_{ik}^{\kappa xx} & A_{ik}^{\kappa xy} \\ A_{ii}^{\kappa xy} & A_{ii}^{\kappa yy} & A_{ij}^{\kappa xy} & A_{ij}^{\kappa yy} & A_{ik}^{\kappa xy} & A_{ik}^{\kappa yy} \\ A_{ji}^{\kappa xx} & A_{ji}^{\kappa xy} & A_{jj}^{\kappa xx} & A_{jj}^{\kappa xy} & A_{jk}^{\kappa xx} & A_{jk}^{\kappa xy} \\ A_{ji}^{\kappa xy} & A_{ji}^{\kappa yy} & A_{jj}^{\kappa xy} & A_{jj}^{\kappa yy} & A_{jk}^{\kappa xy} & A_{jk}^{\kappa yy} \\ A_{ki}^{\kappa xx} & A_{ki}^{\kappa xy} & A_{kj}^{\kappa xx} & A_{kj}^{\kappa xy} & A_{kk}^{\kappa xx} & A_{kk}^{\kappa xy} \\ A_{ki}^{\kappa xy} & A_{ki}^{\kappa yy} & A_{kj}^{\kappa xy} & A_{kj}^{\kappa yy} & A_{kk}^{\kappa xy} & A_{kk}^{\kappa yy} \end{bmatrix} \begin{bmatrix} u_i^x \\ u_i^y \\ u_j^x \\ u_j^y \\ u_k^x \\ u_k^y \end{bmatrix} \tag{154}$$

The body is nonaccelerating and each of its component nodes is nonaccelerating. Consequently, the total effective force applied to each node must be zero. The total force of the i-th node equals the total of the equivalent forces arising from the internal stress in each of the elements contingent on the i-th node, $(f_i^{\mu x}, f_i^{\mu y})$, plus the forces from the boundary traction applied to the i-th node. (We recall that we have assumed that the body force is zero.) If we write the boundary traction force on the i-th node with the array $-(f_i^x, f_i^y)$, then nonaccleration of the i-th node implies that

$$f_i^x = \sum_{\mu} f_i^{\mu x}$$

and

$$f_i^y = \sum_{\mu} f_i^{\mu y} \tag{155}$$

If one then uses linear superposition of equation (154) with equation (155), one can then write the boundary forces in terms of the displacements by the linear relation

$$\begin{bmatrix} f_1^x \\ f_1^y \\ f_2^x \\ f_2^y \\ \cdot \\ \cdot \\ \cdot \\ f_N^x \\ f_N^y \end{bmatrix} = \begin{bmatrix} A_{11}^{xx} & A_{11}^{xy} & A_{12}^{xx} & A_{12}^{xy} & \cdot & \cdot & \cdot & A_{1N}^{xx} & A_{1N}^{xy} \\ A_{11}^{xy} & A_{11}^{yy} & A_{12}^{xy} & A_{12}^{yy} & \cdot & \cdot & \cdot & A_{1N}^{xy} & A_{1N}^{yy} \\ A_{21}^{xx} & A_{21}^{xy} & A_{22}^{xx} & A_{22}^{xy} & \cdot & \cdot & \cdot & A_{2N}^{xx} & A_{2N}^{xy} \\ A_{21}^{xy} & A_{21}^{yy} & A_{22}^{xy} & A_{22}^{yy} & \cdot & \cdot & \cdot & A_{2N}^{xy} & A_{2N}^{yy} \\ \cdot & \cdot & \cdot & \cdot & \cdot & \cdot & \cdot & \cdot & \cdot \\ \cdot & \cdot & \cdot & \cdot & \cdot & \cdot & \cdot & \cdot & \cdot \\ \cdot & \cdot & \cdot & \cdot & \cdot & \cdot & \cdot & \cdot & \cdot \\ A_{N1}^{xx} & A_{N1}^{xy} & A_{N2}^{xx} & A_{N2}^{xy} & \cdot & \cdot & \cdot & A_{NN}^{xx} & A_{NN}^{xy} \\ A_{N1}^{xy} & A_{N1}^{yy} & A_{N2}^{xy} & A_{N2}^{yy} & \cdot & \cdot & \cdot & A_{NN}^{xy} & A_{NN}^{yy} \end{bmatrix} \begin{bmatrix} u_1^x \\ u_1^y \\ u_2^x \\ u_2^y \\ \cdot \\ \cdot \\ \cdot \\ u_N^x \\ u_N^y \end{bmatrix} \tag{156}$$

where

$$A_{ij}^{xx} = \sum_{\mu} A_{ij}^{\mu xx}$$

$$A_{ij}^{xy} = \sum_{\mu} A_{ij}^{\mu xy} \tag{157}$$

and

$$A_{ij}^{yy} = \sum_{\mu} A_{ij}^{\mu yy}$$

However, the boundary traction forces $(f_1^x, f_1^y, \ldots f_N^x, f_N^y)$ can be resolved in terms of the boundary tractions described in equation (149). Consequently, using finite element approximations one can reduce the solution of equations $(147)_2$ and $(147)_3$ for $\underset{\sim}{E}$ into the solutions of the linear equation (156) for the displacements $(u_1, v_1), (u_2, v_2), \ldots\ldots (u_N, v_N)$. Having determined the displacements, the strain field $\overline{\underset{\sim}{E}}$ can be calculated directly.

Before we consider the solution of (156) for the displacement, two comments are in order with respect to the arrays $(f_1^x, f_1^y, \ldots\ldots f_N^x, f_N^y)$ and $(u_1^x, u_1^y, \ldots\ldots\ldots, u_N^x, u_N^y)$. First we will observe that the boundary forces depicted by $(f_1^x, f_1^y, \ldots\ldots\ldots, f_N^x, f_N^y)$ are not linearly independent. Since the body is in static equilibrium, the sum of all external (boundary) forces must equal zero, thus

$$0 = \sum_{i=1}^{N} f_i^x \quad .$$

$$0 = \sum_{i=1}^{N} f_i^y \tag{158}$$

Also the sum of the moments about some arbitrary point (x_o, y_o) must be zero, thus

$$0 = \sum_{i=1}^{N} \left[(y_i - y_o) f_i^x - -(x_i - x_o) f_i^y \right] \qquad (159)$$

where the position of the i-th node is given by the array (x_i, y_i). Consequently, in programming any solution of (156), one must install error-detecting subroutines that will verify the validity of constraints (158) and (159). Otherwise boundary data violating these constraints can be inadvertently entered, causing the program to yield spurious results.

The second observation is that the solution of the boundary value problem described by equations (155) through (159) will not be unique. It can be demonstrated that the solution of equation (157) will be indeterminate within a uniform translation and a rigid rotation. In order to render the solution of (157) unique, we must make the following two assumptions: First, let us constrain translation by assuming that one of the internal nodes (i.e., a node which is not on the boundary) has a zero displacement and the ordering of the nodes is such that this stationary node has the index of N. This will mean that

$$\text{and} \qquad \begin{aligned} u_N^x &= 0 \\ u_N^y &= 0 \end{aligned} \qquad (160)$$

Secondly, we will constrain rotation by assuming that one other internal node can move only in the x-direction and that this second constrained node has the index of N-1. This will mean

$$u_{N-1}^y = 0 \qquad (161)$$

It is assumed that there are no body forces and that the nodes of indices N-1 and N are not on the boundary. This will mean that

$$f_{N-1}^y = f_N^x = f_N^y = 0 \qquad (162)$$

When these constraints and the constraints (160) are substituted into (156) we will have the 2N equations in 2N-3 variable, which can be expressed by the matrix relation

$$
\begin{bmatrix} f_1^x \\ f_1^y \\ \cdot \\ \cdot \\ \cdot \\ f_\ell^x \\ f_\ell^y \\ f_m^x \\ 0 \\ 0 \\ 0 \end{bmatrix} = \begin{bmatrix} A_{11}^{xx} & A_{11}^{xy} & \cdots & A_{1\ell}^{xx} & A_{1\ell}^{xy} & A_{1m}^{xx} \\ A_{11}^{xy} & A_{11}^{yy} & \cdots & A_{1\ell}^{xy} & A_{1\ell}^{yy} & A_{1m}^{xy} \\ \cdot & \cdot & \cdots & \cdot & \cdot & \cdot \\ \cdot & \cdot & \cdots & \cdot & \cdot & \cdot \\ \cdot & \cdot & \cdots & \cdot & \cdot & \cdot \\ A_{\ell 1}^{xx} & A_{\ell 1}^{xy} & \cdots & A_{\ell\ell}^{xx} & A_{\ell\ell}^{xy} & A_{\ell m}^{xx} \\ A_{\ell 1}^{xy} & A_{\ell 1}^{yy} & \cdots & A_{\ell\ell}^{xy} & A_{\ell\ell}^{yy} & A_{\ell m}^{xy} \\ A_{m1}^{xx} & A_{m1}^{xy} & \cdots & A_{m\ell}^{xx} & A_{m\ell}^{xy} & A_{mm}^{xx} \\ A_{m1}^{xy} & A_{m1}^{yy} & \cdots & A_{m\ell}^{xy} & A_{m\ell}^{yy} & A_{mm}^{xy} \\ A_{N1}^{xx} & A_{N1}^{xy} & \cdots & A_{N\ell}^{xx} & A_{N\ell}^{xy} & A_{Nm}^{xx} \\ A_{N1}^{xy} & A_{N1}^{yy} & \cdots & A_{N\ell}^{xy} & A_{N\ell}^{yy} & A_{Nm}^{xy} \end{bmatrix} \begin{bmatrix} u_1^x \\ u_1^y \\ \cdot \\ \cdot \\ \cdot \\ u_\ell^x \\ u_\ell^y \\ u_m^x \end{bmatrix} \tag{163}
$$

where $\ell = N-2$ and $m=N-1$. Of course the array $(u_1^x, u_1^y, \ldots, u_\ell^x, u_\ell^y, u_m^x)$ is over-determined and it is not dificult to demonstrate that the last three equations of (163) can be obtained from the first $2N-3$ using Newton's third law and the conservation of momentum equations (158) and (159). Consequently, the $2N-3$ equations given by the matrix equation

$$
\begin{bmatrix} f_i^x \\ f_1^y \\ \cdot \\ \cdot \\ \cdot \\ f_\ell^x \\ f_\ell^y \\ f_m^x \end{bmatrix} = \begin{bmatrix} A_{11}^{xx} & A_{11}^{xy} & \cdots & A_{1\ell}^{xx} & A_{1\ell}^{xy} & A_{1m}^{xx} \\ A_{11}^{xy} & A_{11}^{yy} & \cdots & A_{1\ell}^{xy} & A_{1\ell}^{yy} & A_{1m}^{xy} \\ \cdot & \cdot & \cdots & \cdot & \cdot & \cdot \\ \cdot & \cdot & \cdots & \cdot & \cdot & \cdot \\ \cdot & \cdot & \cdots & \cdot & \cdot & \cdot \\ A_{\ell 1}^{xx} & A_{\ell 1}^{xy} & \cdots & A_{\ell\ell}^{xx} & A_{\ell\ell}^{xy} & A_{\ell m}^{xx} \\ A_{\ell 1}^{xy} & A_{\ell 1}^{yy} & \cdots & A_{\ell\ell}^{xy} & A_{\ell\ell}^{yy} & A_{\ell m}^{xy} \\ A_{m1}^{xx} & A_{m1}^{xy} & \cdots & A_{m\ell}^{xx} & A_{m\ell}^{xy} & A_{mm}^{xx} \end{bmatrix} \begin{bmatrix} u_1^x \\ u_1^y \\ \cdot \\ \cdot \\ \cdot \\ u_\ell^x \\ u_\ell^y \\ u_m^x \end{bmatrix} \tag{164}
$$

will uniquely determine the array $(u_1^x, u_1^y, \ldots, u_m^x)$. This equation can be solved by conventional numerical methods such as Gauss-Seidel elimination and once the array $(u_1^x, u_1^y, \ldots, u_m^x)$ is determined, appending equations (160) and (161) gives a complete, unique solution for the displacement array $(u_1^x, u_1^y, \ldots, u_N^x, u_N^y)$.

c. Solution for the Trabecular Adaptation Field

Assume that we are given the trabecular adaptation field $\underset{\sim}{M}(x,t)$ for $t=t_n$ and the strain field $\underset{\sim}{E}(x,t)$ during the time interval (t_{n+1}, t_n). Integration of the conservation of mass equation (147) gives us the integral equation

$$\underset{\sim}{M}(\underset{\sim}{x}, t_{n+1}) - \underset{\sim}{M}(\underset{\sim}{x}, t_n) = \int_{t'=t_n}^{t_{n+1}} \underset{\sim}{R}\left[\underset{\sim}{E}(\underset{\sim}{x}, t), \underset{\sim}{M}(\underset{\sim}{x}, t)\right] dt' \qquad (165)$$

This integral equation suggests that if the boundary tractions are fixed and the strain field $\underset{\sim}{E}(x,t)$ can be considered time-invariant during the interval (t_{n+1}, t_n), then one might be able to approximate the trabecular adaptation function at $t=t_{n+1}$ by the expression

$$\underset{\sim}{M}(\underset{\sim}{x}, t_{n+1}) - \underset{\sim}{M}(\underset{\sim}{x}, t_n) = \underset{\sim}{R}\left[\underset{\sim}{E}(\underset{\sim}{x}, t_n), \underset{\sim}{M}(\underset{\sim}{x}, t_n)\right] \Delta t_n \qquad (166)$$

$$\text{where} \quad \Delta t_n = t_{n+1} - t_n$$

and then use the techniques of the previous subsubsection to calculate the strain field at the time $t=t_{n+1}$. Recursion of these two approximation techniques can then be used to calculate the strain and the trabecular adaptation fields at any arbitrary later time increment.

In addition, these numerical methods also allow one to consider the behavior of an adaptive elastic material under even more general conditions. For instance, from the discussion in subsubsection I. 4. d, one might conclude that it might be useful to study the properties of an adaptive elastic material in the case when the boundary tractions are cyclic and the function $\underset{\sim}{s}(x,t)$ as used in equation (149) is periodic, i. e.

$$\underset{\sim}{s}(\underset{\sim}{x}, t) = \underset{\sim}{s}(\underset{\sim}{x}, t+\tau) \text{ for all } \underset{\sim}{x} \in \delta B \qquad (167)$$

If numerical methods are employed, one of the simplest periodic functions which can be studied will be one in which the load cycle of duration τ is divided into two hemicycles of equal duration during which the loading assumes the values of two time-invariant boundary tractions $s^1(\underset{\sim}{x})$ and $s^2(\underset{\sim}{x})$, i.e.

$$s(x,t) = s^1(x)\ \upsilon(t-t_o) + s^2(x)\ \upsilon(t-t_o-\frac{\tau}{2}) \tag{168}$$

where

$$\upsilon(t) = \sum_{m=0}^{\infty} (-1)^{-m}\ u[2(t-m\tau)] \tag{169}$$

and $u(t)$ is the Heavyside unit step function. If we assume that the inertial terms in the conservation of mass equation can still be ignored, the quasi-static problem of the previous subsection resolved into the solution of the two strain fields $\underset{\sim}{E}^1(\underset{\sim}{x}, t_n)$ and $\underset{\sim}{E}^2(\underset{\sim}{x}, t_n)$, corresponding to the strain in the adaptive elastic material, given the trabecular adaptation field $\underset{\sim}{M}(\underset{\sim}{x}, t_n)$ and the boundary traction fields $s^1(\underset{\sim}{x})$ and $s^2(\underset{\sim}{x})$, respectively. One might then argue that integration of the conservation of mass equation allows us to approximate the trabecular adaptation at the time $t-t_{n+1}$ by the expression

$$\underset{\sim}{M}(\underset{\sim}{x}, t_{n+1}) - \underset{\sim}{M}(\underset{\sim}{x}, t_n) = 1/2\ \left[\underset{\sim}{R}[\underset{\sim}{E}^1(\underset{\sim}{x}, t_n),\ \underset{\sim}{M}(\underset{\sim}{x}, t_n)] + \underset{\sim}{R}(\underset{\sim}{E}^2(\underset{\sim}{x}, t_n),\ \underset{\sim}{M}(x, t_n))\right] \Delta t_n \tag{170}$$

In closing, we might comment as to the final form the trabecular adaptation function field $\underset{\sim}{M}(\underset{\sim}{x}, t)$ will take as $t \to \infty$. When bone is subjected to static or cyclic loading conditions, one of two things can be observed to happen physiologically: (1) the bone will remain physiologically stable and asymptotically enter a condition of homeostasis, or (2) the bone will become physiologically unstable and enter a pathological condition (such as overstrain necrosis) leading to structural failure. In terms of the model, structural failure of bone corresponds to the strain or trabecular adaptation fields attaining values outside of the normal, nonpathological, physiological range. Such conditions of instability can be described quite rigorously in mathematical terms using the concepts of mathematical stability introduced by Lyapunov. The problem of stability and concomitant structural failure was the subject of considerable discussion in the author's dissertation.

The condition of homeostasis corresponds to the conditions which can be expected of bone with a normal remodeling function subject to a normal loading configuration. Under conditions of homeostasis, the trabecular adaptation field $\underset{\sim}{M}$ will have attained values such that the ambient loading will cause exactly the right amount of strain so that average value of the remodeling function $\underset{\sim}{R}(\underset{\sim}{E}, \underset{\sim}{M})$ over the loading cycle is zero for every point in the body. This trabecular configuration can be termed the homeostatic trabecular configuration. For example, the trabecular configuration illustrated in Figure 4 corresponds to the homeostatic trabecular configuration for a human femur subject to normal loading on a human femur. Determination of the homeostatic trabecular configuration for a given remodeling function and load configuration can be considered the single most important computational result of the computer simulation of an adaptive elastic material.

III. 4 APPLICATION OF THE CORTICAL BONE MODEL IN THE EVALUATION OF THE CONSTITUTIVE FUNCTIONS

a. Introduction

As mentioned previously, the distinct disadvantage of numerical methods is that in order to solve the governing equations that simulate an adaptive elastic material one must first have explicit formulations for the constitutive functions. Unfortunately, quantitative experimental data for such evaluation is nonexistant since there has never, heretofore, existed a coherent mathematical model into which such data might be integrated. However, the author, in his dissertation, has successfully described the remodeling properties of cortical bone using well-established qualitative observations to obtain useful constraints on the remodeling function.

In the following two subsubsections, we will summarize the basic features of the cortical bone model as discussed in the author's dissertation. After that we will apply this model to the evaluation of the constitutive functions of cancellous bone.

b. Cortical Bone: The Basic Model

In this subsubsection, results of the author's dissertation will be reviewed and summarized. In this summary, it will be convenient to modify some of the notation and terminology from that which appears in the dissertation, not only for brevity and simplicity of discussion but also so as not to conflict with the notation and terminology used in the current discussion.

The mechanical properties of either cortical or cancellous bone are essentially identical to the mechanical properties of the extracellular material composing the cortical or cancellous bone. In cancellous bone this matrix structure roughly approximates orthogonal sets of trabecular plates. In cortical bone, this matrix structure consists basically of cylindrically shaped osteons whose long axes run parallel to the long axis of the bone itself. As cortical bone "adapts" to its strain environment, the porosity and radiographic opaqueness of these osteons can be observed to change (Amtmann, 1971). In

his dissertation, (Hegedus, 1976) the author simulated the stress-adaptation of cortical bone by assuming that this adaptation could be simulated by the variation of a single scalar parameter γ analogous to one of the zero-strain mass density parameters introduced in Section II. Let us refer to the parameter γ as the osteonal adaptation parameter and let us assume that its magnitude has been normalized so that its values must lie within the unit interval, i.e. $\gamma \in (0,1)$.

Under these circumstances, the isothermal, elastostatic governing equations for cortical bone consist of a conservation of mass equation,

$$\dot{\gamma} = \hat{c}(\underset{\sim}{E}, \gamma) \tag{171}$$

a stress-strain relation

$$T_{ij} = \hat{C}_{ijk\ell}(\gamma) E_{k\ell}$$

and a conservation of momentum equation

$$T_{ij,j} = 0$$

and a compatibility equation

$$E_{ij,k\ell} + E_{k\ell,ij} - E_{ik,j\ell} - E_{j\ell,ik} = 0$$

that are subject to initial conditions on the osteonal adaptation

$$\gamma(\underset{\sim}{x}, t)\Big| = \gamma^{o}(\underset{\sim}{x})$$

and the boundary conditions on the boundary tractions

$$\underset{\sim}{T}_{ij}(x,t) \Big|_{x \in \partial B} = s_i n_j$$

For further development it will be useful to point out the existence of an auxiliary constitutive function, the compliance function $\hat{K}_{ijk\ell}(\gamma)$, which can be formulated in lieu of the stiffness function $\hat{C}_{ijk\ell}(\gamma)$. For each value of the stiffness function γ, the value of the compliance function $\hat{K}_{ijk\ell}(\gamma)$ will be defined as the fourth rank tensor inverse of the fourth rank tensor value of the stiffness function $\hat{C}_{ijk\ell}(\gamma)$. This will mean that the compliance function will allow the strain components to be expressible as linear combinations of the stress components, i.e.

$$E_{ij} = \hat{K}_{ijk\ell}(\gamma) T_{k\ell}. \tag{172}$$

In the dissertation, the stress-adaptation of cortical bone was investigated in the special case of uniaxial compression of magnitude P(t) applied to an initially uniform hollow cylinder. These boundary and initial conditions very roughly approximate the conditions prevailing on a bone such as the diaphysis of the tibia during normal bipedal activity such as walking. Given that the material (and therefore the osteonal adaptation) is uniform, i.e. $\boldsymbol{\gamma}(\underset{\sim}{x}, 0) = \boldsymbol{\gamma}^{o}$, the governing equations $(171)_2$ through $(171)_4$ are satisfied by spatially uniform stress, strain and volume fraction fields which have the form

$$T_{33} = -P(t)\ \delta_{i3}\ \delta_{j3}$$

$$E_{ij} = \hat{K}_{ijk\ell}(\boldsymbol{\gamma})\ P(t)$$

and

$$\boldsymbol{\gamma}(\underset{\sim}{x}, t) = \tilde{\boldsymbol{\gamma}}(t) \tag{173}$$

where $\tilde{\boldsymbol{\gamma}}(t)$ is the solution to the equation

$$\dot{\tilde{\boldsymbol{\gamma}}} = g(P(t), \tilde{\boldsymbol{\gamma}}) \tag{174}$$

where $\tilde{\boldsymbol{\gamma}}(t)$ is subject to the initial conditions

$$\tilde{\boldsymbol{\gamma}}(t)\Big|_{t=0} = \boldsymbol{\gamma}^{o} \tag{175}$$

and where the stress remodeling function $g(P, \boldsymbol{\gamma})$ is defined by the relation

$$g(P, \boldsymbol{\gamma}) = \hat{c}(-\hat{K}_{ij33}(\boldsymbol{\gamma})P, \boldsymbol{\gamma}) \text{ for all } P \text{ and } \boldsymbol{\gamma} \tag{176}$$

c. Cortical Bone: Phenomenological Constraints

At this point in the development we are left in a situation somewhat similar to that encountered in the previous subsection in the analysis of cancellous bone: a constitutive function of two variables, for which there exists no quantitative data. However, there do exist a number of well-documented qualitative descriptions of the phenomena of bone remodeling from which one can derive constraints for the stress-remodeling function, $g(P, \boldsymbol{\gamma})$. These phenomenological constraints can be summarized as follows:

(1) There Exists a Compressive Stress for Which the Rate of Remodeling is Zero

Matrix material is constantly being deposited and resorbed, but, under normal loading conditions, the net osteonal adaptation does not change. The normal ambient loading of cortical bone is compressive, thus we will postulate the existence of some ambient compressive stress $P_o > 0$, such that with a given osteonal adaptation $\boldsymbol{\gamma}_o$, the rate of remodeling is zero, i.e.

$$0 = g(P_o, \boldsymbol{\gamma}_o) \tag{177}$$

(2) A Negative Slope with Respect to γ_o at the Point of Zero Remodeling.

The most important feature of the remodeling of living bone is its ability to maintain homeostasis stably. One can assume that the application of the compressive stress P_o will cause the adaptive elastic material to remain stable at the osteonal adaptation γ_o. Thus if γ were to increase slightly from γ_o, $g(P_o, \gamma_o)$ must become negative in order to force the osteonal adaptation to decrease. Likewise, if γ_o were to increase slightly from γ_o, $g(P_o, \gamma_o)$ must become negative. Mathematically, this condition of stability requires that

$$\frac{\partial}{\partial \gamma} g\,(P_o, \gamma)\Big|_{\gamma = \gamma_o} < 0 \tag{178}$$

We will digress for a moment from our discussion of the phenomological restrictions of the modeling function in order to introduce some important definitions. In general, we will define a combination (P_h, γ_h) of axial stress P_h and osteonal adaptation γ_h such that

$$g\,(P_h, \gamma_h) = 0$$

$$\frac{\partial}{\partial \gamma} g\,(P_h, \gamma')\Big|_{\gamma' = \gamma_h} < 0 \tag{179}$$

as a point of homeostasis. The particular point of homeostasis consisting of the volume fraction γ_o and the axial loading P_o will be called the homeostatic datum.

Under normal loading conditions living bone reacts to an increase in loading by becoming stiffer and less porous. A point of homeostasis consisting of a compressive stress P_h and an osteonal adaptation γ_h will be said to be a normal point of homeostasis if we have

$$\frac{\partial}{\partial P} g\,(P, \gamma_h)\Big|_{P_h = P} > 0 \tag{180}$$

for $P_h > 0$ in addition to conditions (177) and (178). For instance, given that $\gamma = \gamma_o$, we might expect that if the stress were to increase slightly from that of the homeostatic datum, matrix accretion would occur and the net rate of reaction would become positive. Similarly, if this stress were decreased slightly below that of the homeostatic datum, matrix material would be resorbed and the rate of reaction would be negative.

On the other hand, in certain pathological conditions such as overstrain necrosis, bone reacts to an increased load by becoming more porous, i.e.

$$\frac{\partial}{\partial P}\, g(P, \gamma_h)\Big|_{P = P_h} < 0 \tag{181}$$

for $P_h < 0$, in this case, the material will be said to be at a paradoxical point of homeostasis. Finally, we should note that in the case of tensile stress, ($P < 0$) the definitions (180) and (181) for normal and paradoxical points of homeostasis will be reversed.

We will now return to our discussion of the phenomenological constraints on the remodeling function. In terms of the definitions given above, the stress-remodeling function $g(P, \gamma)$ has the following additional property:

(3) The Homeostatic Datum is a Normal Point of Homeostasis.

This means

$$\frac{\partial}{\partial P}\, g(P, \gamma)\Big|_{P = P_o} > 0 \tag{182}$$

(4) Disuse Resorption Occurring at $\gamma = 0$

It is observed clinically that if bone of average porosity is subjected to zero loading conditions, bone matrix will be resorbed. This means that unstrained matrix material undergoes a type of "disuse atrophy" and thus

$$g(0, \gamma) < 0 \tag{183}$$

(5) The Maximum Rate of Remodeling is Small

Bone remodeling is a very slow process. Bone labeling studies by Frost (1969) indicate typical remodeling rates on the order of months. Even under extreme conditions such as weightlessness, two weeks are required to effect changes in skeletal mass on the order of 10%. We can thus conclude that the values of the material parameters which determine the remodeling function have values such that the quantity

$$\frac{1}{g(P, \gamma)} \tag{184}$$

will be of the order of several weeks, i.e. 10^7 seconds.

d. Cancellous Bone: Approximation as a Pinned Triangular Structure

Anatomically, there does not exist any sharp lineof demarcation between a region of cortical bone and a region of cancellous bone. Furthermore, since the histological distinction between cortical bone and cancellous bone is more one of the structural arrangement of the lamellar bone composing the matrix, one can assume that the remodeling properties, as indicated by the stiffness and remodeling functions of cortical cancellous bone, are comparable if not identical. In fact, cancellous bone might be thought of as a structural rearrangement of cortical bone into trabecular patterns which optimize the load-carrying properties.

It was already stated in the previous subsection that the field equations (171) describing cancellous bone can be approximated by assuming material uniformity over a finite triangular region. Let us now assume that these uniform properties can be simulated by a pinned triangular structure extending along the boundaries of each element and each one of these structural members will be termed a trabecular link, or more simply, a link. Let us further assume that each of these trabecular links is mechanically equivalent to a small uniform portion of cortical bone whose properties have been described in the author's dissertation and assume that the trabecular links composing this structure are of uniform length and thus form an equilateral triangular structure. We recall that in the cortical bone model, the index of osteonal adaptation was a single scalar field γ proportional to the zero strain mass density of cortical bone. Assuming that cancellous bone is composed of an equilateral triangular structure of trabecular links whose properties are identical to cortical bone, is equivalent to assuming that the osteonal adaptation of cancellous bone can be described by the three scalar fields γ^1, γ^2, and γ^3, representing the trabecular adaptation of the trabecular links along the trabecular basis vectors $w^1 = (1, 0)$, $w^2 = 1/2\,(1, \sqrt{3})$ and $w^3 = 1/2\,(-1, \sqrt{3})$, respectively. Using equation (112) one can then express the effective trabecular adaptation tensor in terms of these three scalar fields by the relation

$$\underset{\sim}{M} = \frac{1}{\pi^2} \left\{ \begin{bmatrix} 1 & 0 \\ 0 & 1 \end{bmatrix} \gamma^1 + \frac{1}{4} \begin{bmatrix} 1 & \sqrt{3} \\ \sqrt{3} & 3 \end{bmatrix} \gamma^2 + \frac{1}{4} \begin{bmatrix} 1 & \sqrt{3} \\ \sqrt{3} & 3 \end{bmatrix} \gamma^3 \right\} \quad (185)$$

In this subsection we will dispense with the bar to indicate two-dimensionalization of the parameters $\underset{\sim}{T}$, $\underset{\sim}{E}$, and $\underset{\sim}{M}$.

The next step will be to consider the constitutive functions. To facilitate this discussion, let us consider two new physical parameters that can be associated with each trabecular link. The first of these new parameters will be termed the trabecular strain, ε^{α}, and will indicate the material strain along the trabecular links parallel to the trabecular basis vector $\underset{\sim}{w}^{\alpha}$. In terms of the displacement, the trabecular strain on a trabecular link connecting the i-th and j-th nodes of an equilateral triangular trabecular structure will have the form

$$\varepsilon^{\alpha} = \frac{1}{\ell}\left[w_1^{\alpha}\,(u_1^i - u_1^j) + w_2^{\alpha}\,(u_2^i - u_2^j)\right] \tag{186}$$

where ℓ is the uniform length of the trabecular links and the unstrained position of the j-th node equals the unstrained position of the i-th node plus the vector $\ell \underset{\sim}{w}^{\alpha}$. Using the kinematic definitions of continuum mechanics, it is possible to express ε^{α} in terms of the strain $\underset{\sim}{E}$ by the relation

$$\varepsilon^{\alpha} = \underset{\sim}{w}^{\alpha}\,\underset{\sim}{E}^{\alpha}\,\underset{\sim}{w}^{\alpha} \tag{187}$$

The second new parameter will be termed the trabecular stress σ^{α} and will indicate the tension (or compression) in the trabecular links parallel to the trabecular basis vector $\underset{\sim}{w}^{\alpha}$. In terms of the two-dimensional stress $\underset{\sim}{T}$ (whose dimensions are force per unit length) the trabecular stress can be expressed by the relation

$$\sigma^{\alpha} = \ell\,\underset{\sim}{w}^{\alpha}\,\underset{\sim}{T}\,\underset{\sim}{w}^{\alpha} \tag{188}$$

e. Cancellous Bone: The Constitutive Functions

We are now in a position to discuss the constitutive functions themselves. For simplicity, we will assume that the stiffness of any one of these trabecular links is directly proportional to the osteonal adaptation along the axis of that particular trabecular link. We might note that the assumption that the stiffness of the trabecular link is directly proportional to the osteonal adaptation γ^{α} is equivalent to assuming that the material composing each trabecular link is uniform and the osteonal adaptation is directly proportional to the effective thickness of each trabecular link. This implies that

$$\sigma^{\alpha} = \kappa_o \gamma^{\alpha} \varepsilon^{\alpha} \tag{189}$$

where κ_o is a material constant with the dimensions of force per unit length. It is then possible to demonstrate that the force-displacement relationship for the trabecular link parallel to $\underset{\sim}{w}^{\alpha}$ connecting the i-th and j-th nodes will have the form

$$\begin{bmatrix} f_i^{\Lambda x} \\ f_i^{\Lambda y} \\ f_j^{\Lambda x} \\ f_j^{\Lambda y} \end{bmatrix} = K_o \begin{bmatrix} [w_1^\alpha]^2 & [w_1^\alpha w_2^\alpha] & -[w_1^\alpha]^2 & -[w_1^\alpha w_2^\alpha] \\ [w_1^\alpha w_2^\alpha] & [w_2^\alpha]^2 & -[w_1^\alpha w_2^\alpha] & -[w_2^\alpha]^2 \\ -[w_1^\alpha]^2 & -[w_1^\alpha w_2^\alpha] & [w_1^\alpha]^2 & [w_1^\alpha w_2^\alpha] \\ -[w_1^\alpha w_2^\alpha] & -[w_2^\alpha]^2 & [w_1^\alpha w_2^\alpha] & [w_2^\alpha]^2 \end{bmatrix} \begin{bmatrix} u_i^x \\ u_i^y \\ u_j^x \\ u_j^y \end{bmatrix} \tag{190}$$

Since the structural members are pinned, the force exerted by each trabecular link will depend on only the displacement of the two end points of that trabecular link. Consequently, the force-displacement matrix for the structure as a whole can be obtained by summing the expression (190) over each trabecular link Λ in the structure.

Let us now consider the remodeling function: Let us suppose that the remodeling occurring in any given trabecular link depends only on the physical conditions within that particular link. This will mean that the rate of reaction of a trabecular link will depend on only the trabecular strain ε^α and the trabecular adaptation γ^α. Consequently, the conservation of mass equation will take the form

$$\dot{\gamma}^\alpha = \tilde{\tilde{c}}^\alpha(\varepsilon^\alpha, \gamma^\alpha) \tag{191}$$

where the link remodeling function $\tilde{\tilde{c}}^\alpha(\varepsilon^\alpha \gamma^\alpha)$ can be expressed in terms of the remodeling function $\hat{R}(\underset{\sim}{E}, \underset{\sim}{M})$ by the expression

$$\tilde{\tilde{c}}^\alpha(\varepsilon^\alpha, \gamma^\alpha) = w_i^a \, R_{ij}(\underset{\sim}{E}, \underset{\sim}{M}) \, w_j^\alpha \tag{192}$$

where

$$\begin{aligned} \gamma^\alpha &= \pi^2 \, w_i^\alpha \, M_{ij} \, w_j^\alpha \\ \varepsilon^\alpha &= w_i^\alpha E_{ij} \, w_j^\alpha \end{aligned} \tag{193}$$

Let us further suppose that in view of the quadratic dependence of the remodeling function discussed in section II, the link remodeling function is a quadratic function of both the trabecular strain and the trabecular adaptation, i.e.,

$$\tilde{\tilde{c}}^\alpha(\varepsilon, \gamma) = a_0 + a_1\varepsilon + a_2\gamma + a_3\varepsilon^2 + a_4\varepsilon\gamma + a_5\gamma^2 \tag{194}$$

where a_o, a_1, a_2, a_3, a_4, and a_5 are material constants. We might also note that the link remodeling function used in equation (194) can also be recast in terms of the link stress σ^α. This allows us to recast (191) into the form

$$\dot{\gamma}^{\alpha} = g^{\alpha}(\sigma^{\alpha}, \gamma^{\gamma}) \tag{195}$$

where

$$g(\sigma, \gamma) = a_0 + a_1 \frac{\sigma}{\kappa_o \gamma} + a_2\gamma + a_3\left(\frac{\sigma^2}{\kappa_o^2\gamma^2}\right) + a_4\left(\frac{\sigma}{\kappa_o}\right) + a_5\gamma^2 \tag{196}$$

We can now assume that the stress-remodeling function $g(\sigma,\gamma)$ is exactly analogous to the stress-remodeling function defined by equation (176), which describes the remodeling properties of cortical bone, *except for the sign of its first* argument.

Let us now consider the restrictions of $g(\sigma,\gamma)$ that are imposed by the phenomenological constraints. First of all, let us assume that the force and displacement variables have been normalized so that we can set the material constant $\mathbf{K}_o$ equal to unity. Next let us assume that the compressive homeostatic datum, introduced previously has the values of $\sigma=-1$ and $\gamma=1$ and hence,

$$g(-1,1) = 0 \tag{197}$$

Next we will observe that the stability of the compressive point of homeostasis will require that

$$\frac{\partial}{\partial\gamma} \; g(-1,\gamma)\Big|_{\gamma=1} < 0 \tag{198}$$

In addition, we can also assume that the compressive point of homeostasis is a normal point of homeostasis, hence

$$\frac{\partial}{\partial\delta} \; g(\sigma, 1)\Big|_{\sigma=-1} < 0 \tag{199}$$

The particular nature of cancellous bone implies further constraint. It has long been accepted that the trabeculae of cancellous bone are capable of maintaining homeostasis under tensile loads. In fact, in the human femur, whose trabecular patterns are illustrated in Figure 4, two of the five major trabecular groups carry tensile loads and in fact are referred to as the Principal and Secondary Tensile Groups. The arguments in favor of tensile conditions of homeostasis also have indirect evidence. It is well known that moderate cyclic loading will cause greater trabecular development than static loading of the same average magnitude. In his dissertation, the author demonstrated that this phenomenon would occur if and only if there existed both compressive and tensile points of homeostasis and the coefficients of the remodeling function were such that

$$\frac{\partial^2}{\partial \sigma^2} g(\sigma, \gamma)\Big|_{\sigma=-1} > 0 \qquad (200)$$

In closing, it is important to cite on additional constraint on the remodeling function of cancellous bone, which was not mentioned in our earlier discussion of the phenomenological constraints for cortical bone: We will require that the remodeling function of cancellous bone must depend on the trabecular adaptation tensor $\underset{\sim}{M}$, i.e.

$$\frac{\partial}{\partial M} \hat{\underset{\sim}{R}}(\underset{\sim}{E}, \underset{\sim}{M}) \neq 0 . \qquad (201)$$

The proof of this constraint can be summarized as follows: As mentioned previously, normal bone, subject to normal loading conditions can always be observed to remodel in such a way as to asymptotically tend to a condition of homeostasis. We might further expect that such a condition of homeostasis would be attainable under any loading configuration, provided that loading configuration were within the physiological bounds for that particular bone. In particular, a static load will cause bone to asymtotically approach conditions of homeostasis for which the strain and the trabecular adaptation approach time-invariant homeostatic values E^o and M^o, such that

$$\hat{\underset{\sim}{R}}(\underset{\sim}{E}^o, \underset{\sim}{M}^o) = 0 . \qquad (202)$$

For a two-dimensional strain field, $\underset{\sim}{E}$ has only three degrees of freedom. If inequality (201) is not valid, and the remodeling function $\hat{\underset{\sim}{R}}$ depends only on $\underset{\sim}{E}$, the conditions of homeostasis (202) will cause the field $\underset{\sim}{E}$ to be subject to three constraints. Consequently, if inequality (201) is not valid, the strain field at homeostasis E^o can only have a finite number of values. However, the material must also satisfy the conditions of compatability, which in two dimensions take the form

$$E_{11,22} + E_{22,11} = 2 E_{12,12} . \qquad (203)$$

Obviously, the compatibility equation (203) and the conditions of homeostasis cannot be satisfied simultaneously if the boundary conditions are such that the strain cannot be uniform.

In retrospect, this constraint appears obvious. However, if one were to attempt an ad-hoc computer simulation of cancellous bone without thoroughly investigating the mathematical nature of this simulation, there would be a strong temptation to overlook dependence of the trabecular adaptation in the remodeling function and perhaps a tendency to not fully appreciate the significance of the compatibility equation. There is in the literature some indirect evidence that this oversight has in fact occurred.

III. 5 THE PROGRAMMING PACKAGE

a. Introduction

In this subsection we will discuss the organization and application of a programming package that simulates an adaptive elastic material using the numerical techniques introduced in the three previous subsections. This programming package was designed for use on the SCOPE operating system (a time-shared CDC 6600), which was available at the Aerospace Medical Research Laboratory (AMRL) Initial input data and program control information are punched in on standard 80 column cards read through a Model 305 High-Speed Card Reader located at the AMRL computer terminal. Program output as well as diagnostic error messages are printed out on an off-line 132-character line printer which is also located on-site. The program instructions are written in FORTRAN EXTENDED VERSION 4 and utilize the standard scientific subroutine package which is built into the SCOPE compiler. In its output operations, the programming package can also employ an 11-inch CALCOMP incremental plotter which is also located at the computer terminal. The use of the CALCOMP plotter requires implementation of auxiliary software which is stored in permanent files on the SCOPE operating system.

As developed previously, an adaptive elastic system is approximated as an equilateral triangular structure with N nodes. The main limitation of the present programming package to simulate this structure lies in its ability to solve eq. (164) for the nodal displacement. This solution requires the storage of a (2N x 2N) array representing the force-displacement relation. On the SCOPE operating system the maximum total effective core memory available is 165K(octal) for daytime runs (800-1600 hrs.), 250K for evening runs (2nd shift from 1600 to 2400 hrs.), and 310K for night runs (3rd shift from 2400 hrs. to 0800 hrs.). The memory capacity of 310K has the decimal equivalent of 102400 or $(320)^2$ the computer could conceivably store a force-displacement array for a 160-node structure. However, since some of the memory must be used to store also the programming instructions, the practical limit of nodal capacity was found to be 128 nodes for over-night runs and 80 nodes for daytime runs.

b. Organization

In order to reduce the memory requirement that must be used for programming instructions during the critical phase of the calculations (the solution of (164)) the calculation sequence has been broken up into a series of distinct programs that must be executed sequentially, with intermediate results stored on magnetic tapes. This sequence of programs will be called a programming package and it will have the following four components:

AD-A057 330 DAYTON UNIV OHIO RESEARCH INST F/G 6/16
A MATHEMATICAL MODEL OF BONE REMODELING.(U)
MAY 78 D M HEGEDUS F33615-75-C-5054
UNCLASSIFIED AMRL-TR-76-40 NL

2 OF 2
AD
A057330

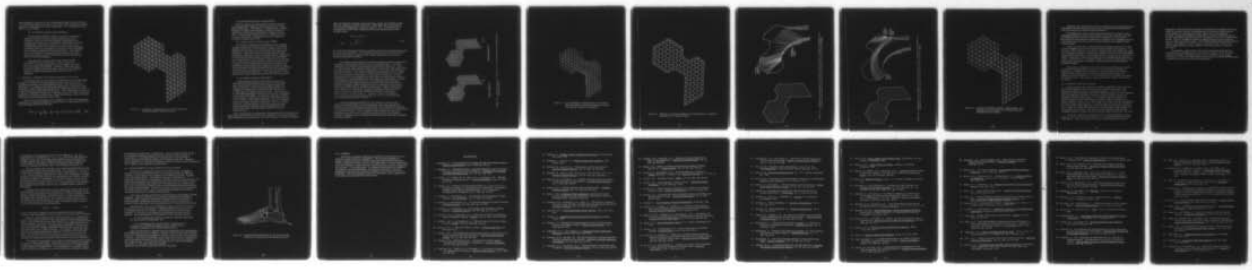

END
DATE
FILMED
9-78
DDC

date nonuniform values of $\underset{\sim}{M}$, but redesigning the input format of INPUTR to accommodate nonuniform values of $\underset{\sim}{M}$ would render its already complex input data configuration even more complicated. To accomplish the same effect, we can employ:

(4) An Auxilary Program Called MODIFIR

The program MODIFIR allows us to consider nonuniform initial values of $\underset{\sim}{M}$ using a relatively simple, fool-proof technique: Initial values of the trabecular configuration are obtained from taped records of the final, homeostatic trabecular configuration in a previous calculation. A new value of the remodeling function can be read-in, if desired, and the boundary conditions in the new calculation are read-in as scalar multiples of the boundary conditions of the old calculation. The output of the new calculation is recorded on logical tape unit 12, using exactly the same data format that had been used on logical tape unit 6 for the old calculation.

This uniformity of output between the output of MAIN and MODIFIR has two advantages. First, it allows the direct use of the output program RERUN to display the results of the calculations in MODIFIR. Secondly, it allows the final trabecular configuration with another calculation with MODIFIR using yet another remodeling function and/or boundary configuration.

c. Application: Simulation of the Stress-Adaptation of the Femur

In this subsection we will consider the application of the programming package to simulate the stress-adaptation of the human femur in situ. As mentioned previously, the programming package, in its present state of development, is capable of calculating the adaptation of a structure of only 128 nodes. Figure 11 illustrates the geometric configuration that was used to approximate the shape of the human femur. This configuration was selected as the best compromise between the conflicting desires to include as much as possible of the distal end of the femur, while representing as fine a structure as possible for the proximal end of the femur.

The first set of calculations to be considered calculated the trabecular adaptation of an initially homogeneous model femur. In the program INPUTR the remodeling function took the form

$$\underset{\sim}{c}^{\alpha}(\varepsilon,\gamma) = \frac{1}{\tau_o}\left(\bar{a}_0 + \bar{a}_1\varepsilon + \bar{a}_2\gamma + \bar{a}_3\varepsilon^2 + \bar{a}_4\varepsilon\gamma + \bar{a}_5\gamma^2\right) \qquad (204)$$

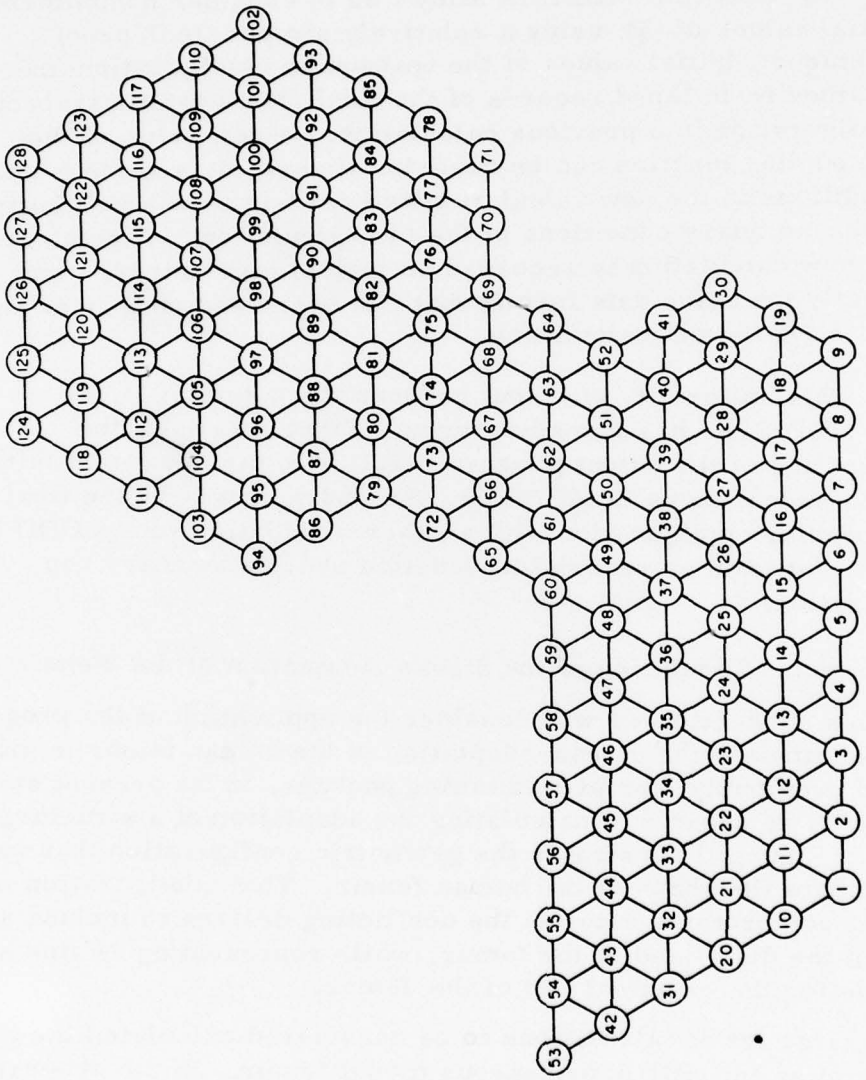

Figure 11. Geometric Configuration of a 128-Node Structure Approximating the Proximal Femur.

(1) An Initializing Program called INPUTR

INPUTR reads in the data from the punched cards and issues diagnostic messages if it detects any errors on the punched data input. For instance, it will print out a warning diagnostic message if the boundary conditions (149) fail to satisfy the conservation of momentum equations (158) and (159). If the program INPUTR detects no explicit error on the punch data input, a predigested form of the input data is stored on logical tape unit 4.

(2) A Main Iterative Program Called MAIN

The Program MAIN takes the predigested data residing on logical tape unit 4 and performs the iterative calculations outlined in Section III. First it solves equation (164) for the displacement and strain on each trabecular link during each hemicycle. If the strain on any one of the trabecular links during either hemicycle exceeds a predetermined compressive or tensile strain limit, further calculations are terminated and an appropriate error message is issued by the line printer. If the strain on each trabecular link is within bounds, the conservation of mass equation (191) is utilized to determine the appropriate osteonal adaptation during the time interval Δt. The strain fields are then calculated for the next time increment and the process is repeated for as many time-increments as are called for by the input data. The results of these calculations for each time increment are stored on logical tape unit 6.

(3) An Output Program Called RERUN

A third program takes the information results of the calculations from MAIN which have been stored on logical tape unit 6 and effect tabular and/or graphical display of these calculations. There exist eight output options, any combination of which can be selected by the insertion of a single card read into the 305 card reader. The execution of a full optioned graphical output can be very time consuming on the incremental plotter It often takes upwards of 20 minutes to display a single frame depicting a 128-node structure. For this reason, it is often advisable to conduct the implementation of the output operation in two parts. First, a cursory survey to verify the general form of the results and an unabbreviated output only later, when monopolization of the incremental plotter will not interfere with work of other terminal users.

At the present state of development, the program INPUTR can only consider initial conditions for the Trabecular Adaptation Tensor $\underset{\sim}{M}$ which are scalar multiples of the unit tensor. It would be useful to be able to accommo-

where the material constants $\bar{a}_0, \bar{a}_1, \bar{a}_2, \bar{a}_3, \bar{a}_4$, and $\bar{a}_5$ were read in as data while the auxiliary material constant τ_o, which fixed time normalization, was internally programmed to have the value of 10^3. For the first set of calculations we will let the coefficients of the remodeling function (204) have the values

$$a_0 = a_1 = a_4 = 0$$

$$a_2 = -1 \qquad (205)$$

and $$a_3 = a_5 = 1$$

It is easily demonstrated that these coefficients satisfy the constraints discussed in the previous subsection. The boundary tractions for the first set of calculations are illustrated in Figure 12 and roughly approximate the boundary tractions illustrated in Figure 5.

The program calculated that the model simulating the femur approached conditions of homeostasis after five units of normalized time. The Link Adaptation of the model at homeostasis is illustrated in Figure 13. One of the output options of the program RERUN allows calculation of the eigen values and eigen vectors of the trabecular adaptation tensor $\underset{\sim}{M}$ for each element in the model structure. The results of these eigen value/eigen vector calculations for the model at homeostasis are illustrated in Figure 14. As mentioned previously, the arrangement of these eigen vector and eigen values can be thought of as representing the effective trabecular adaptation of an equivalent orthogonal trabecular structure. The orientation of this effective orthogonal structure obtained from the computer simulation of the human femur is strikingly similar to the patterns of the trabecular structure in a living human femur that are visible in radiographs. Figure 15 illustrates this comparison by copying the computed compressive trabeculae from Figure 14 next to a copy of the anatomically observed compressive trabeculae first shown in Figure 4. Likewise, Figure 16 compares the computed tensile trabeculae from Figure 14 next to the anatomically observed tensile trabeculae of Figure 4.

Using the Program MODIFIR it is also possible to simulate the trabecular dissolution that occurs during disuse and senile osteoporosis. In Figure 17 we have illustrated the homeostatic Link Adaptation that occurs if the remodeling function remains fixed but the boundary forces are diminished by a factor of one-half. These conditions might simulate the trabecular dissolution that could occur when an astronaut is subjected to extended periods of weightlessness or a bedridden convalescent is subjected to extended periods of bedrest.

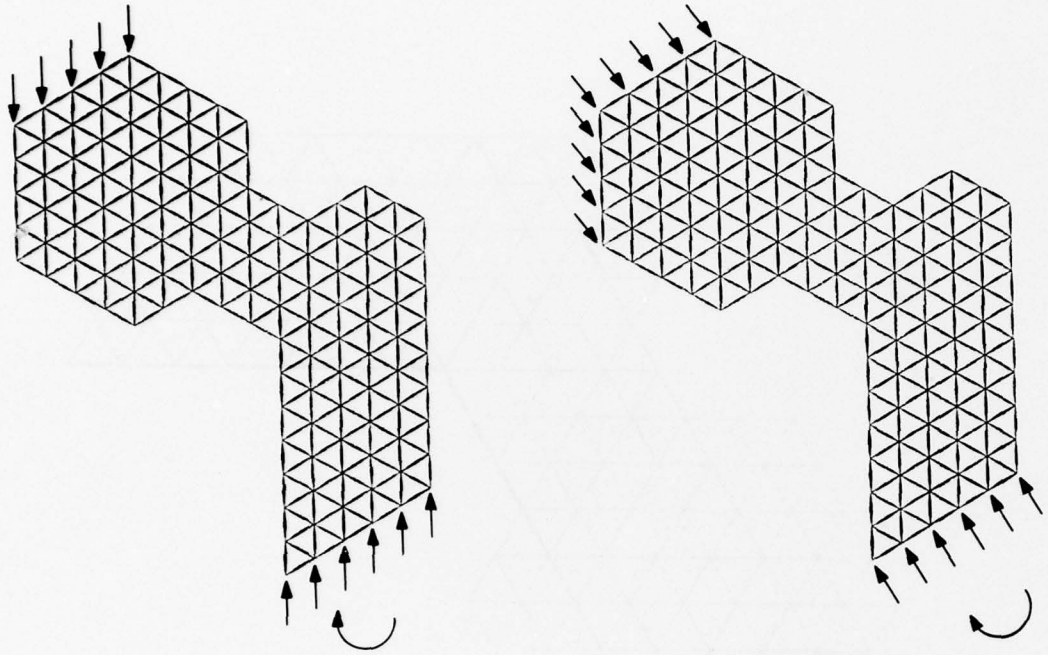

Figure 12. 'Normal' Boundary Tractions on a 128-Node Structure Simulating the Proximal Femur.

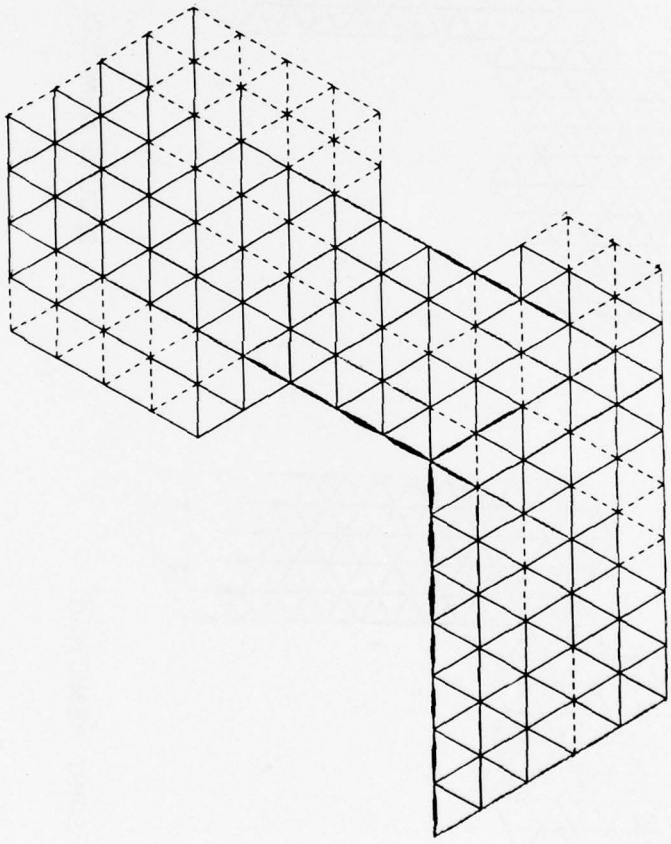

Figure 13. Link Adaptation at Homeostasis of a 128-Node Structure with a 'Normal' Remodeling Function and 'Normal' Boundary Conditions.

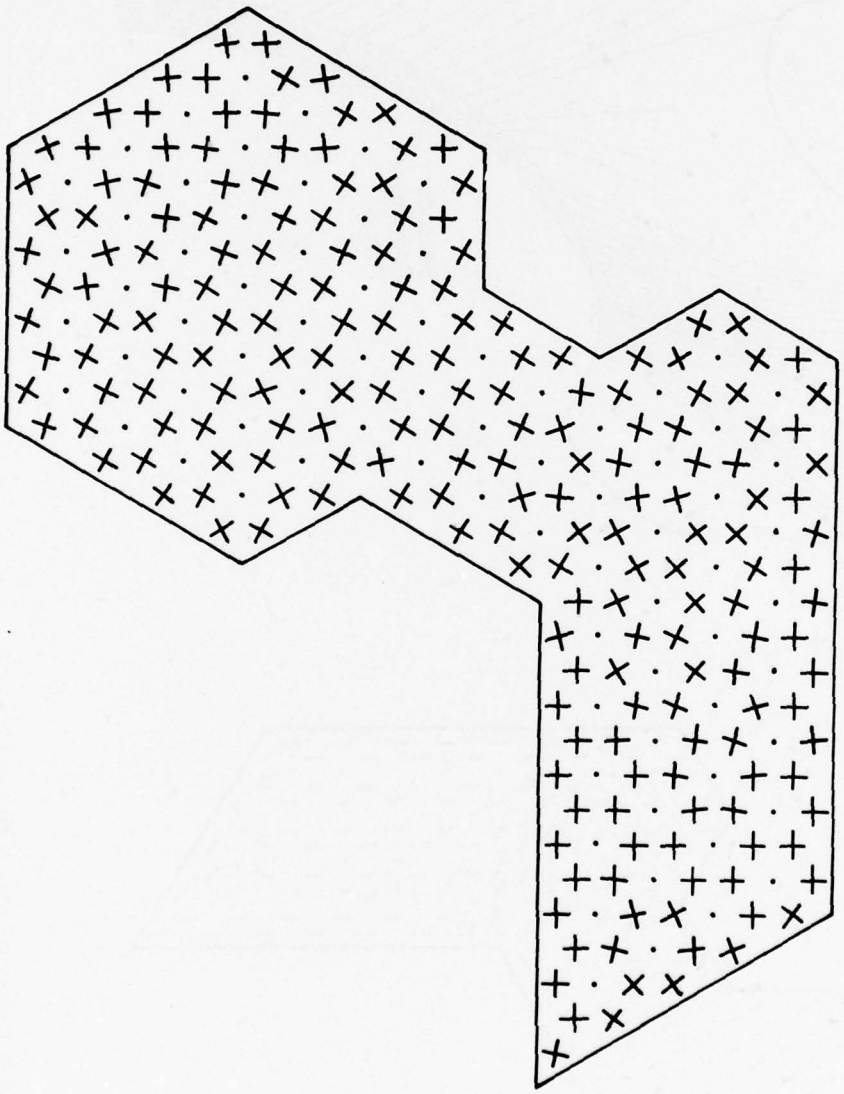

Figure 14. Effective Trabecular Adaptation and Orientation of a Computer Simulation of a 'Normal' Femur.

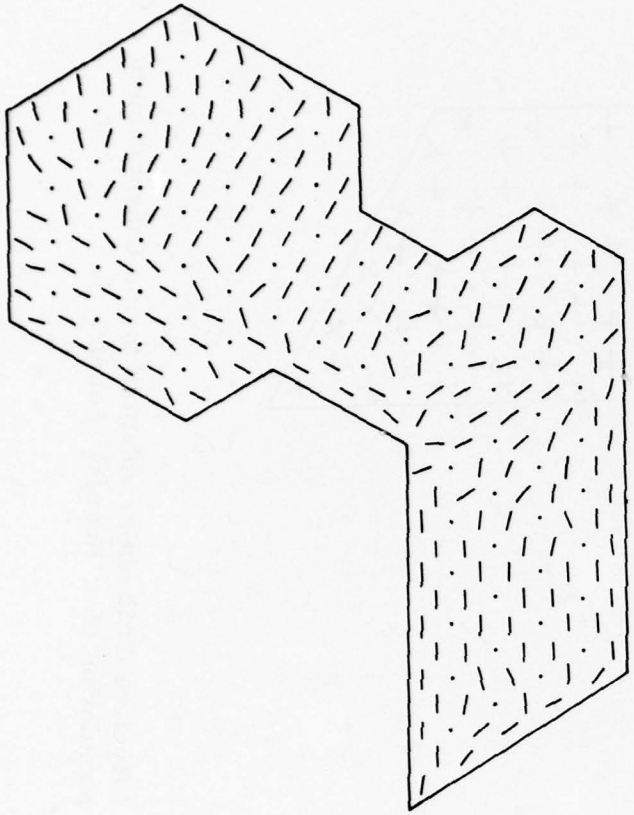

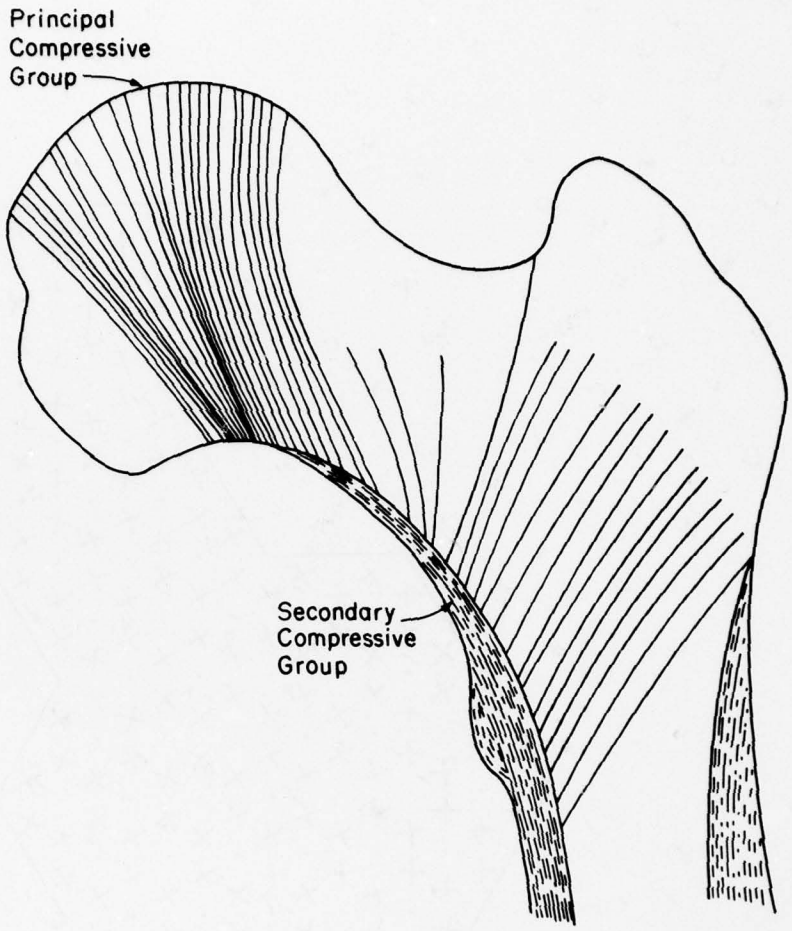

Figure 15. Comparison of the Effective Trabecular Patterns from a Computer Simulation of a 'Normal' Femur and the Compressive Trabeculae of a Living Femur in Vivo.

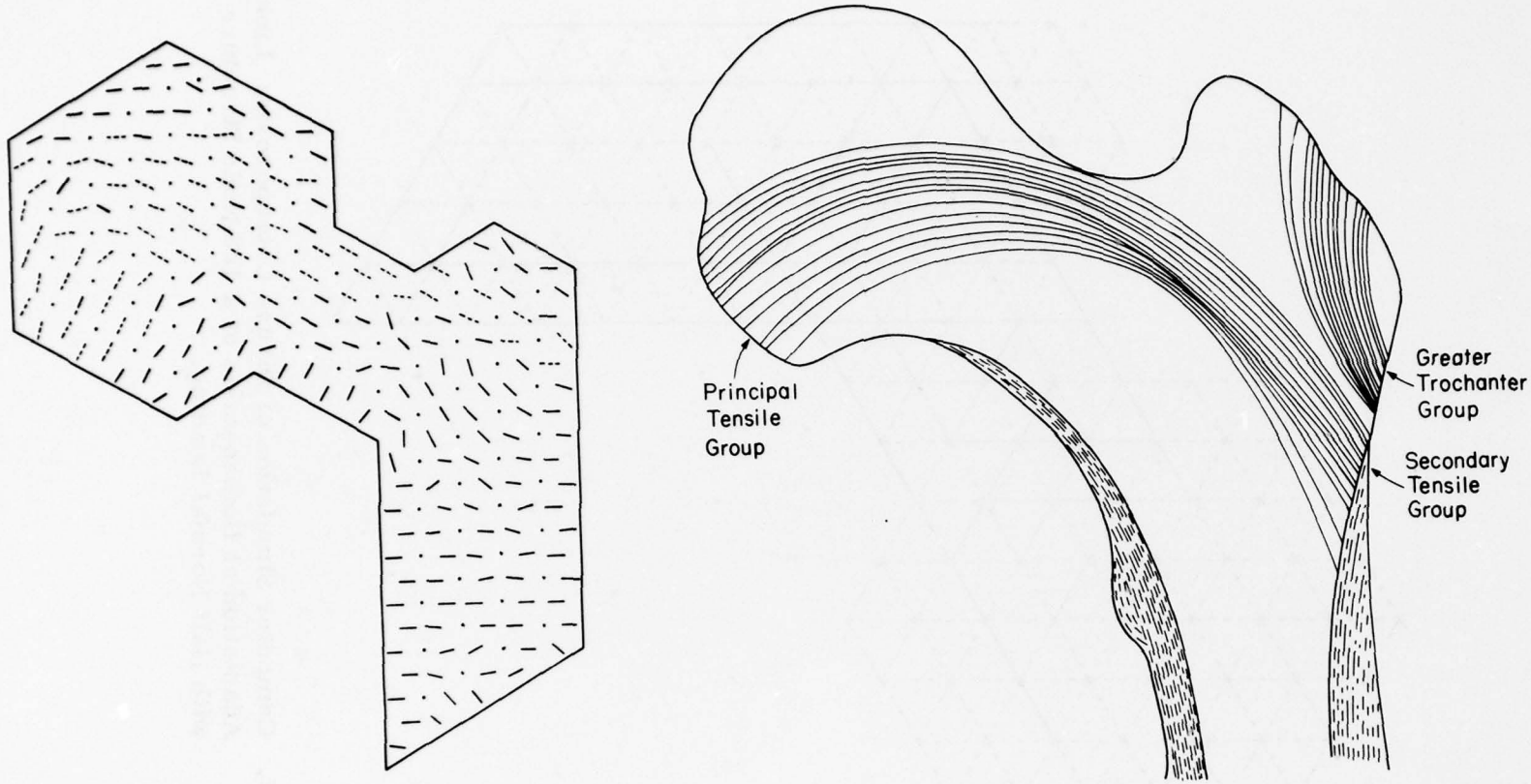

Figure 16. Comparison of the Effective Trabecular Patterns from a Computer Simulation of a 'Normal' Femur and the Tensile Trabeculae of a Living Femur in Vivo.

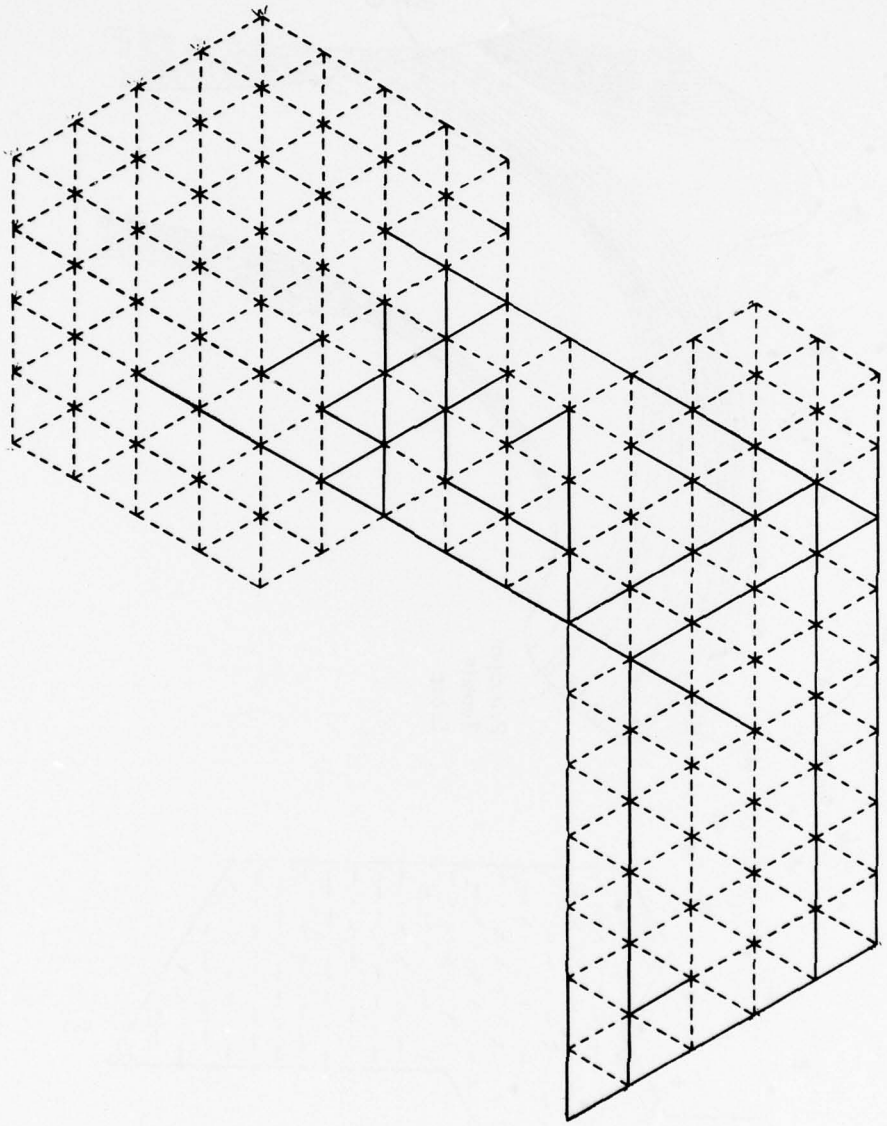

Figure 17. Computer Simulation of Disuse Osteoporosis: Link Adaptation at Homeostasis of a 128-Node Structure with Half Normal Loading.

Clinically, the most important type of osteoporosis is senile osteoporosis. Although the Program MODIFIR can be used to simulate senile osteoporosis, lack of time has so far prevented this simulation.

Physiologically, senile osteoporosis corresponds to a change in the remodeling properties of bone in such a manner that a fixed load will cause the remodeling function to become relatively more negative. In the author's dissertation he demonstrated that this type of change in the remodeling function would cause bone to undergo a loss of matrix material even though the load remained fixed.

There are any number of ways that the remodeling coefficients of (204) could be changed so as to render the remodeling function more negative. For instance, if the coefficient a_0 took on a negative value, this might correspond to a systematic increase in osteoclastic resorption caused by a homonal change in the calcium metabolism. On the other hand, a decrease in the coefficient a_3 might correspond to a decreased sensitivity of the remodeling mechanism to strain. This decrease in sensitivity might be caused by a degeneration of the piezoelectric properties of collagen, stemming from an entirely different hormonal change.

From this, one might conclude that what is presently termed "senile osteoporosis" might actually be two (or even more) distinct pathological conditions, having different etiologies and requiring different treatments. Differentiation of these types of "senile osteoporosis" will require new diagnostic instrumentation that can objectively measure the pattern and degree of trabecular loss. The design of such instrumentation will be described in Section IV.

III. 6 SUMMARY AND CONCLUSIONS

In this section we have discussed computer simulation of the governing equations developed in the previous section, using two techniques: Two-dimensionalization and finite element approximation. There are certain limitations to these techniques and to the computer programs we have employed. The most important limitation is that the numerical solution for the two-dimensional displacement of <u>any</u> N node elastic material, whether it is adaptive elastic or classically elastic, will still require the solution of a linear equation of order 2N and the storage of a 2Nx2N matrix, representing the force-displacement relation. It is obvious that a 128-node representation of a femur only crudely approximates the two-dimensional shape, but direct core storage of its force-displacement matrix will require approximately 10^5 memory storage locations. This memory requirement taxes the storage capabilities of even a relatively large computer system such as the CDC 6600.

There are a number of ways that the effect of these limitations can be reduced. First, it should be possible to use a nonuniform mesh in selecting nodal points. This, for instance in the case of the simulation of femural

adaptation, would allow finer resolution of the trabecular development in areas of special interest, such as the proximal end of the femur, without wasting nodal capacity on uninteresting uniform regions such as the diaphysis. Secondly, it might be possible to employ more economical methods of matrix storage which exploit the symmetry and "bandedness" of the force-displacement matrix. Finally, it might be possible to employ auxiliary memory devices, such as a high-speed disc memory. The SCOPE OPERATING SYSTEM MANUAL alludes to the existence of such a feature, called the ECM, however this feature apparently has not been installed in the SCOPE system available at the AMRL.

Nevertheless, albeit limited, the present programming package has demonstrated the feasibility of the cancellous bone model. It has predicted trabecular adaptation strikingly similar to that of a human femur in situ. Furthermore, it has even demonstrated the feasibility of simulating pathological conditions such as senile and disuse osteoporosis.

SECTION IV

SUGGESTIONS FOR FUTURE WORK

IV.1 INTRODUCTION

The most serious difficulty in our development of a theory of the adaptive remodeling in bone tissue has been the scarcity of quantitative data, particularly with respect to the rate of matrix apposition and resorption as a function of the loading. Consequently, we have had to depend exclusively on qualitative descriptions of bone remodeling. This lack of data is understandable historically. Systematic experiments to accurately measure the elastic modulii of structural materials had to be preceded by the development of a mathematical theory of elasticity. The development of a mathematical theory of elasticity was, in turn, motivated by a desire to systematize experimental observations of the behavior of these structural materials. Likewise, experimental and clinical observations of stress-controlled remodeling of living bone has motivated a theory of adaptive elasticity.

The quantification of the stress-adaptation properties of cancellous bone can be effected in two steps:

(1) Develop experimental techniques and instrumentation to measure the Trabecular Adaptation $\underset{\sim}{M}$ for a given sample of bone

(2) Determine the Constitutive Functions $C_{ijk\ell}(\underset{\sim}{M})$ and $\underset{\sim}{R}(\underset{\sim}{E}, \underset{\sim}{M})$.

These two steps will be the subjects of the following two subsections:

IV.2 MEASUREMENT OF TRABECULAR ADAPTATION TENSOR, $\underset{\sim}{M}$

The concept developed in this paper of using a second-rank tensor to quantify the trabecular adaptation of cancellous bone is new. However, there do exist in the literature reports by workers who have attempted to quantify the trabecular adaptation of cancellous bone, tensorial nature notwithstanding. Rockoff (1968) gave a semiquantitative description of the trabecular structure of a vertebral body using straightforward dissection techniques. Also recently, Raux et al (1975) have given a quantitative description of the trabecular structure of the human patella using the techniques of statistical microscopy described in Underwood (1970). Nevertheless, the dissection/microscopic techniques described by these authors are extremely time-consuming and consequently would render experimental data reduction prohibitively expensive.

We will now consider methods of measuring the trabecular structure of bone from radiographs. Radiographic measurements are desirable not only because they are nondestructive, but also, as we shall see, they can easily be automated. As mentioned previously, the trabecular plates of cancellous bone are often visible on radiographs. They become particularly clear if one of the trabecular plates runs normal to the axis of the X-ray beam. In this case, the trabecular plate normal to the beam axis will appear as only a change in the X-ray density, while the other two trabecular plates, which run parallel to the axis of the beam, would clearly stand out in a radiograph as "trabecular lines".

These patterns of "trabecular lines", indicating the direction and thickness of the trabecular plates, can be measured quantitatively on a device called a polarimeter, which works on the principle of Moire interference. A trabecular line at the angle θ will be transmitted through a polarimeter oriented at the angle θ^{α} by an amount linearly related to the quantity $\cos^2(\theta - \theta^{\alpha})$. If we consider the transmission factors at the angles $\theta^1 = 0^o$, $\theta^2 = 120^o$, and $\theta^3 = 240^o$ as proportional to the trabecular adaptation parameters γ^1, γ^2, and γ^3, respectively, then employing eq. (185) determines the value of $\underset{\sim}{M}$ for each point of the radiograph.

Since the polarimeter is coming into more frequent use at a number of research institutions, it is important to point out a possible error in the experimental protocol of its use: Some researchers have attempted to collect radiographic data on the trabecular structure of cancellous bone using only two polarimetric readings. In view of the tensorial nature of the trabecular structure of cancellous bone, data gathered in this manner will of necessity be incomplete. This error is exactly analogous to someone attempting to completely specify the strain state of a plane elastic body using only two strain gauges.

We will next consider how the trabecular patterns that are visible on a radiograph and measurable on a polarimeter can be analyzed mathematically. First of all, let us assume that the sample of bone under measurement has a trabecular structure symmetric about the axis of the X-ray beam. If the effect of the trabecular plate normal to the X-ray beam were subtracted out, the resulting radiograph would represent a two-dimensional structure similar to that introduced in Section III, which could be evaluated by a two-dimensional symmetric tensor M_{ij}. This tensor can be uniquely resolved as the sum of a scalar times the unit tensor plus an isochoric tensor, i.e.

$$\begin{bmatrix} M_{11} & M_{12} \\ M_{12} & M_{22} \end{bmatrix} = \begin{bmatrix} 1 & 0 \\ 0 & 1 \end{bmatrix} \phi + \begin{bmatrix} u & v \\ v & -u \end{bmatrix} \tag{206}$$

where

$$\begin{aligned} \phi &= 1/2 \operatorname{tr} M = 1/2 \left[M_{11} + M_{22} \right] \\ u &= 1/2 \left[M_{11} - M_{22} \right] \end{aligned} \tag{207}$$

and

$$v = M_{12} \ .$$

We should mention two important properties of the isochoric tensor $\begin{bmatrix} u & v \\ v & -u \end{bmatrix}$. First, the eigen vectors of $\begin{bmatrix} u & v \\ v & -u \end{bmatrix}$ exactly coincide with those of the tensor $\underset{\sim}{M}$. Secondly, the mathematical properties of $\begin{bmatrix} u & v \\ v & -u \end{bmatrix}$ with respect to additionaand multiplication are exactly equivalent to those of the complex number

$$\psi = u + i v \tag{208}$$

Consequently, if we consider the plane of the radiograph $x_1 - x_2$ to be equivalent to the complex plane $x = x_1 + i x_2$, the value of the trabecular adaptation tensor $\underline{M}$ can be uniquely represented by the real function of a complex variable $\phi(z)$ and a complex function of a complex variable $\phi(z)$. It is not difficult to demonstrate that the orthogonality of the trabecular structure constrains the function $\psi(z)$ to be an analytic function of z.

The two functions $\theta(z)$ and $\psi(z)$ can be interpreted physically in terms of the trabecular structure of cancellous bone. If we consider k_1 and k_2 are arbitrary real constants, then the function $\psi(z)$ maps the lines $z = k_1$ and $z = ik_2$ into the trabecular lines that are visible on the radiograph. We might therefore conclude that the function $\psi(z)$ parametrizes the shape of the trabecular plates visible on a radiograph. Furthermore, from eq. (207), we see that the value of ϕ is equal to half the trace of M and thus ϕ also equals the average of the two eigen values of M. We might therefore conclude that $\phi(z)$ parametrizes the mean thickness of the trabecular plates visible on a radiograph.

We might note in passing that an interesting parallel exists between our formulation of $\underline{M}$ in terms of two functions of a complex variable ϕ and ψ and an analogous formulation of the stress tensor $\underline{T}$ used in complex variable analysis of plane elastostatics (Sokolnikoff, 1956). In plane elastostatics the analog of the complex function $\psi_\sigma(z)$ represents the shear stress while the analog of the real function $\phi_\sigma(z)$ represents the hydrostatic stress. If we claim that at homeostasis the trabeculae of an adaptive elastic material do not carry shear loads, this will imply that

$$\text{Arg}(\psi) = \text{Arg}(\psi_\sigma) . \tag{209}$$

At some later time it might be possible to generalize classical complex analysis of plane elastostatics so as to include the effects of adaptive elasticity.

However, the formulation of the trabecular patterns on a radiograph in terms of two analytic functions is more than simply an elegant mathematical theory: It has extremely practical implications in the design of instrumentation. If the polarimeter is used in conjunction with an image digitalization device, such as a flying-spot scanner, the mathematical formulation discussed above can be used to devise computer algorithms with which data can be "fit" and from which data "noise" might be filtered. A "smoothed" evaluation of $\phi(z)$ will give a continuous quantification of the mean thickness of the trabecular plate. This smoothed data will not only allow a much clearer view of the trabecular structure, but more importantly, for the first time will give an objective and experimental repeatable quantification of trabecular adaptation.

The design and development of an automatic polarimeter will have clinical as well as research applications. Presently, the most sophisticated method of clinically evaluating the degeneration of osteoporosis is a semiquantitative method introduced by Singh (1970). The development of an automatic polarimeter would give the clinician a more accurate and more objective criterion

for diagnosing osteoporosis. Furthermore, we have already pointed out that the mathematical analysis suggests that there are more than one type of osteoporosis. These different types of osteoporosis can be expected to induce quantitatively different osteoporotic trabecular patterns. Therefore the development of an automatic polarimeter would be of great clinical importance in the diagnosis and treatment of osteoporosis.

IV. 3 MEASUREMENT OF THE CONSTITUTIVE FUNCTIONS

There are two constitutive functions to be determined: the Stiffness Function and the Remodeling Function. Let us first consider the Stiffness Function. At first glance, the evaluation of the Stiffness Function $\hat{C}_{ijk\ell}(\underset{\sim}{M})$ seems formidable indeed. The stiffness tensor has 21 independent parameters that depend on 6 independent variables. However, the symmetry and objectivity relationships discussed in Section II yield the formula (115), which reduces the formulation of the stiffness of cancellous bone (as a whole tissue) down to the considerably simpler problem of determining the stiffness function of a single trabecular plate. There are a number of researchers, among them Townsend and Rose (1975), who are presently investigating the problem of the elastic properties of a single trabecular plate.

Let us next consider the problem of determining the Remodeling Function $\hat{R}_{ij}(\underset{\sim}{E}, \underset{\sim}{M})$. Again the objectivity and symmetry relationships developed in Section II yield a simplified formulation (120) which reduce the problem of determining the remodeling function of cancellous bone as a whole into a problem of determining the remodeling properties of a single trabecular plate.

Unfortunately, since bone remodeling can only occur with the action of living bone cells, the measurement of the Remodeling Function can only be accomplished with in-vivo testing. At the present time, the most likely candidate as a site for in-vivo testing is the calcaneus (or heel bone) of a primate. This experimental site is desirable for the following reasons:

(1) the calcaneus has distinctive trabecular patterns which show up very clearly on radiographs, and

(2) the loading patterns and geometric configuration of a calcaneus are such that the adaptive elastic problem may be considered symmetric in the medial-anterior plane.

Figure 18 illustrates an experimental test configuration for measuring the Remodeling Function of the calcaneus. One foot is immobilized from the ankle down and a calibrated load is applied to the heel, while the other foot is used as a control. Periodically radiographs can be taken and an automatic polarimeter used to determine the strain in each region of the calcaneous as a function of the calibrated load. Observing the rate change in the trabecular adaptation tensor $\dot{\underset{\sim}{M}}$ as a function of the strain and the adaptation, one can then evaluate the function $\hat{R}_{ij}(\underset{\sim}{E}, \underset{\sim}{M})$.

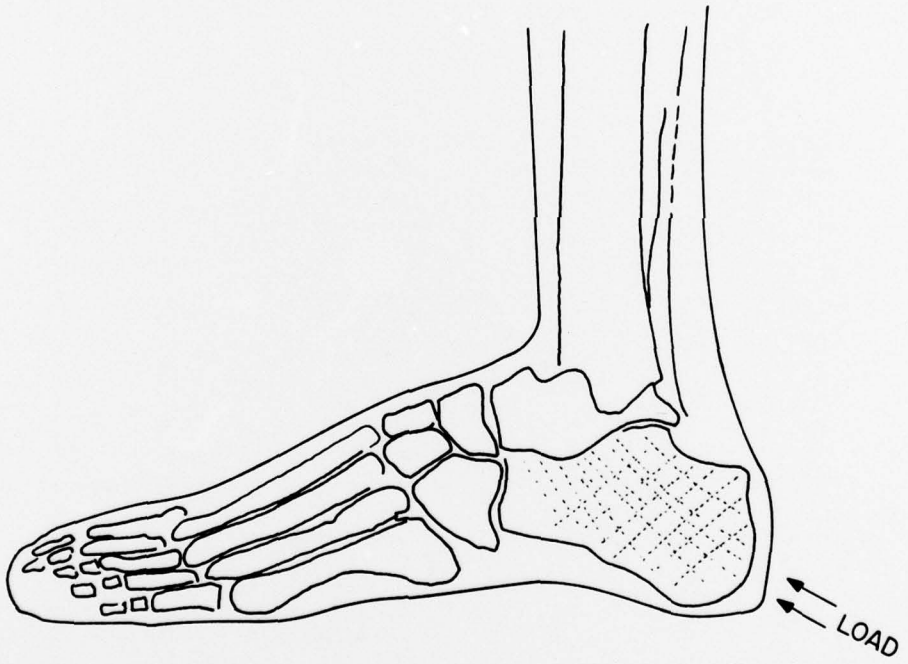

Figure 18. Experimental Configuration for the Loading of the Calcaneus to Determine the Remodeling Function.

IV.4 CLOSURE

The Theory of Adaptive Elasticity presented here should prove to be a useful tool in the practice of orthopedics. The governing equations of Adaptive Elasticity not only model the important physiological phenomena of stress-adaptation of bone, but they also might enable a clearer understanding of the etiology of certain muscular-skeletal disorders such as osteoporosis and scoliosis. As an added bonus, our mathematical analysis has suggested the design of new instrumentation, an automatic polarimeter, which can quantitatively measure the trabecular adaptation of cancellous bone from a radiograph. This instrumentation would have immediate clinical applications in the diagnosis and treatment of osteoporosis.

REFERENCES

1. Amtmann, E., "The Distribution of Breaking Strength in the Human Femur", Journal of Biomechanics, Vol. 1, 1968, pp. 271-277.

2. Amtmann, E., "Mechanical Stress, Functional Adaptation and the Variation Structure of the Human Femur Diaphysis", Ergebnisse der Anatomie und Entwicklungsgeschichte, Vol. 44, 1971, pp. 7-89.

3. Arnold, J.S., Bartley, M. H., Tont, S. A., and Jenkins, D.P., "Skeletal Changes in Aging and Disease", Clinical Orthopedics, Vol. 49, 1966, pp. 17-38.

4. Arnold, J.S., "External and Trabecular Morphologic Changes in Lumbar Vertebrae in Aging", in Proceedings of the Conference: "Progress in Methods of Bone Mineral Measurements", U.S. Government Printing Office, Washington, D.C., 1968, pp. 352-409.

5. Ascenzi, A., and Bonnucci, E., "The Ultimate Tensile Strength of Single Osteons", Acta Anatomica, Vol. 58, 1964, pp. 160-183.

6. Ascenzi, A., and Bonnucci, E., "The Tensile Properties of Single Osteons", Anatomical Record, Vol. 158, 1967, pp. 375-386.

7. Ascenzi, A., and Bonucci, E., "The Compressive Properties of Single Osteons", Anatomical Record, Vol. 161, 1968, pp. 377-392.

8. Basset, C.A.L., and Becker, R.O., "Generation of Electric Potential in Bone in Response to Stress", Science, Vol. 137, 1962, pp. 1063-1064.

9. Basset, C.A.L., and Pawluk, R.J., "Effect of Electric Currents on Bone in Vivo", Nature, Vol. 204, 1964, pp. 652-653.

10. Basset, C.A.L., "Electrical Effects in Bone", Scientific American, Oct. 1965, pp. 18-25.

11. Bazant, Z.P., "Thermodynamics of Interacting Continua with Surfaces and Creep Analysis of Concrete Structures", Nuclear Engineering and Design, Vol. 20, 1972, pp. 477-505.

12. Becker, R.O., and Murray, D.G., "The Electrical Control System Regulating Fracture Healing in Amphibians", Clinical Orthopedics, No. 73, 1970, pp. 169-198.

13. Behrens, J.C., Walker, P.S., and Shoji, H., "Variations in Strength of Cancellous Bone at the Knee", Journal of Biomechanics, Vol. 7, 1974, pp. 201-207.

14. Bellman, R., Stability Theory of Differential Equations, McGraw-Hill, New York, 1953.

15. Birkhoff, G., and Rota, G., Ordinary Differential Equations, Ginn, Boston, 1962.

16. Bonfield, W., and Li, C.H., "Deformation and Fracture of Bone", Journal of Applied Physics, Vol. 37, 1966, pp. 869-875.

17. Bonfield, W., and Li, C.H., "Anisotrophy of Non-Elastic Flow in Bone". Journal of Applied Physics, Vol. 38, 1967, pp. 2450-2455.

18. Bonnucci, E., and Ascenzi, A., "Density of Osteoid Tissue and Osteons at Different Stages of Calcification", Calcified Tissue Research, Vol. 5, 1970, pp. 100-107.

19. Bowen, R.M., "Thermochemistry of Reacting Materials", Journal of Chemical Physics, Vol. 49, 1968, pp. 1625-1637.

20. Bowen, R.M., Continuum Theory of Mixtures, Ballistics Research Laboratory Report No. 45, RDT&E No. 1b062113A660, Aberdeen Proving Ground, Maryland, June 1971.

21. Brannon, E.W., Rockwood, C.A., Potts, P., "The Influence of Specific Exercises in the Prevention of Debilitating Musculoskeltal Disorders", Aerospace Medicine, Vol. 34, 1963, pp. 900-906.

22. Brockett, R.W., Finite Dimensional Linear Systems, Wiley, New York, 1970.

23. Cesari, L., Asymptotic Behavior and Stability Problems, Springer, Berlin, 1959.

24. Chamay, A., "Mechanical and Morphological Aspects of Experimental Overload and Fatigue in Bone", Journal of Biomechanics, Vol. 3, 1970, pp. 263-270.

25. Coddington, E.A., and Levinson, N., Theory of Ordinary Differential Equations, McGraw-Hill, New York, 1955.

26. Coleman, B.D., and Noll, W., "The Thermodynamics of Elastic Materials with Heat Conduction and Viscosity", Archives of Rational Mechanics and Analysis, Vol. 13, 1963, pp. 167-178.

27. Coleman, B.D., and Gurtin, M.E., "Thermodynamics with Internal State Variables", Journal of Chemical Physics, Vol. 47, 1967, pp. 597-613.

28. Coleman, B.D., and Mizel, V.J., "Existence of Caloric Equations of State in Thermodynamics", Journal of Chemical Physics, Vol. 40, 1964, pp. 1116-1125.

29. Coletti, J.M., "Effects of Sustained Compression Loading of Cortical Bone in Vivo", Surgical Forum, Vol. 20, 1969, pp. 471-473.

30. Cowin, S.C., and Hegedus, D.M., "Bone Remodeling I: A Theory of Adaptive Elasticity", to appear in the Journal of Elasticity, Vol. 6, 1976, pp. 313-325.

31. Currey, J.D., "Strength of Bone", Nature, Vol. 195, 1962, pp. 513-514.

32. Currey, J.D., "The Adaptation of Bones to Stress", Journal of Theoretical Biology, Vol. 20, 1968, pp. 91-106.

33. Currey, J.D., "The Mechanical Consequences of Variation in the Mineral Content of Bone", Journal of Biomechanics, Vol. 2, 1969, pp. 1-11.

34. Currey, J.D., "Technical Note: The Relationship Between the Stiffness and Mineral Content of Bone", Journal of Biomechanics, Vol. 2, 1969, pp. 477-480.

35. Denbigh, K., The Principles of Chemical Equilibrium, Cambridge, 1968.

36. Dietrick, J.E., Whedon, G., and Shorr, E., "Effects of Immobilization upon Various Metabolic and Physiological Functions of Normal Men", American Journal of Medicine, Vol. 4, 1948, pp. 3-36.

37. Eggers, G.W.N., Shindler, T.O., and Pomerat, C.M., "The Influence of the Contact-Compression Factor on Osteogenesis in Surgical Fractures", Journal of Bone and Joint Surgery, Vol. 31-A, 1949, pp. 693-716.

38. Evans, F.G., Stress and Strain in Bones, C.C. Thomas, Springfield, Ill, 1957.

39. Evans, F.G., "Bibliography on the Physical Properties of the Skeletal System", Artificial Limbs, Vol. 11, 1967, pp. 48-66.

40. Evans, F.G., and Bang, S., "Difference and Relationships between the Physical Properties and the Microscopic Structure of Human Femural, Tibial, and Fibular Cortical Bone", American Journal of Anatomy, Vol. 120, 1967, pp. 79-88.

41. Evans, F.G., and Vinentelli, R., "Relation of Collagen Fiber Orientation to Some Mechanical Properties of Cortical Bone", Journal of Biomechanics, Vol. 2, 1969, pp. 63-71.

42. Friedenberg, Z.B., and French, G., "The Effects of Known Compression Forces on Fracture Healing", Surgery, Gynecology and Obstetrics, Vol. 97, 1952, pp. 743-748.

43. Frost, H.M., "Dynamics of Bone Remodeling", Frost, H.M., ed., Bone Biodynamics, Little and Brown, Boston, 1964, pp. 315-333.

44. Frost, H.M., The Laws of Bone Structure, ed., C.C. Thomas, Springfield, Ill., 1964.

45. Frost, H.M., "Tetracycline-based Histological Analysis of Bone Remodeling", Calcified Tissue Research, Vol. 3, 1969, pp. 211-237.

46. Fukada, E., and Yasuda, I., "On the Piezoelectric Effect of Bone", Journal of the Physical Society of Japan, Vol. 12, 1957, pp. 1158-1162.

47. Fukada, E., "Mechanical Deformation and Electrical Polarization in Biological Substances", Biorheology, Vol. 5, 1968, pp. 199-208.

48. Gardner, E., Gray, D.J., O'Rahilly, R., Anatomy, W.B. Saunders, Philadelphia, 1969.

49. Gjelsvik, A., "Bone Remodeling: I," Journal of Biomechanics, Vol. 6, 1973, pp. 69-77.

50. Gjelsvik, A., "Bone Remodeling - II", Journal of Biomechanics, Vol. 6, 1973, pp. 187-193.

51. Glegg, R.E., Leblond, C.P., "Pressure as a Possible Cause of Dissolution and Redeposition of Bone and Tooth Crystals", Canadian Journal of Medical Science, Vol. 31, 1953, pp. 202-206.

52. Glucksmann, A., "Studies on Bone Mechanics in Vitro - I: Influence of Pressure on Orientation of Structure", Anatomical Record, Vol. 72, 1938, pp. 97-115.

53. Glucksmann, A., "Studies of Bone Mechanics in Vitro - II: Role of Tension and Pressure in Chondrogenesis", Anatomical Record, Vol. 73, 1939, pp. 39-55.

54. Glucksmann, A., "The Role of Mechanical Stress in Bone Formation in Vitro", Journal of Anatomy, Vol. 76, 1942, pp. 231-239.

55. Goodman, M.A., "A Continuum Theory for Granular Materials", Archives for Rational Mechanics and Analysis, Vol. 44, 1972, pp. 249-266.

56. Goss, C.M., Gray's Anatomy of the Human Body, 26th Edition, Lea and Febiger, Philadelphia, 1954.

57. Grant, J.C.B., Grant's Atlas of Anatomy, Williams and Wilkins, Baltimore, 1962.

58. Hattner, R., Epker, B.M., and Frost, H.M., "Suggested Sequential Mode of Control of Changes in Cell Behavior in Adult Bone Remodeling", Nature, Vol. 206, 1965, pp. 489-490.

59. Hahn, W., Stability of Motion, trans., A.P. Baartz, Springer, New York, 1967.

60. Hermann, G., and Liebowitz, H., "Mechanics of Bone Fracture", in Fracture: An Advanced Treatise, Vol. VII, Liebowitz, H., ed., Academic Press, New York, 1972, pp. 771-840.

61. Hegedus, D., and Cowin, S., "Constitutive Relations for Wolff's Law", Proceedings 1973 Biomechanics Symposium, AMD Vol. 2, Fung, Y.C., and Brighton, J.A., eds. American Society of Mechanical Engineers, New York, 1973, pp. 77-78.

62. Hegedus, D.M., and Cowin, S.C., "Bone Remodeling II: Small Strain Adaptive Elasticity", Journal of Elasticity, Vol. 6, 1976, pp. 337-352

63. Hegedus, David M., Bone Remodeling: A Theory of Adaptive Elasticity, Dissertation at Tulane University, to be published at University Microfilms, Ann Arbor, 1976.

64. Hoyte, D.A.N., and Enlow, D., "Wolff's Law and the Problem of Muscle Attachments", American Journal of Physical Anthropology, Vol. 24, 1966, pp. 205-213.

65. Huebner, K.H., The Finite Element Method for Engineers, Wiley, New York, 1975.

66. Ince, E., Ordinary Differential Equations, Dover, New York, 1956.

67. Jahn, Theodore L., "A Possible Mechanism for the Effect of Electric Potentials on Apatite Formation in Bone", Clinical Orthopedics, Number 56, 1968, pp. 261-273.

68. Justus, R., and Luft, J.H., "A Mechanochemical Hypothesis for Bone Remodeling Induced by Mechanical Stress", Calcified Tissue Research, Vol. 5, 1970, pp. 222-235.

69. Kazarian, L. E., and Van Gierke, H. E., "Bone Loss as a Result of Immobilization and Chelation", Clinical Orthopedics, No. 65, 1969, pp. 67-75.

70. Kelly, P. D., "A reacting Continuum:, International Journal of Engineering Science, Vol. 2, 1964, pp. 129-153.

71. Kiselev, A. I., Kransnov, M. L., and Makarenko, G. I., Ordinary Differential Equations, Trans. E. J. F. Primrose, Frederick Ungar, New York, 1967.

72. Knops, R. J., and Payne, L. E., Uniqueness Theorems in Linear-Elasticity, Springer, New York, 1971.

73. Koch, J. C., "Laws of Bone Architecture", American Journal of Anatomy, Vol. 21, 1917, pp. 177-293.

74. Kraus, H., "On the Mechanical Properties and Behavior of Human Compact Bone", Advances in Engineering and Medical Physics, Vol. 2, Interscience, New York, 1968, pp. 169-204.

75. Kummer, B. K., "Biomechanics of Bone", Biomechanics, ed. Fung, Y. C., Prentice Hall, New Jersey, 1972, pp. 237-271.

76. La Salle, J., and Lefschtz, S., Stability by Liapunov's Direct Method with Applications, Academic Press, New York, 1961.

77. Lang, S. B., "Elastic Coefficients of Animal Bone", Science, Vol. 165, 1969, pp. 287-288.

78. Lang, S. B., "Ultrasonic Method for Measuring Elastic Coefficients of Bone and Results on Fresh and Dried Bovine Bone", Institute of Electrical and Electronic Engineers Transactions, BME-17, No 2, April 1970, pp. 101-105.

79. Lekhnitski, S. G., Theory of Anisotropic Elastic Body, Trans., Fern, R., and Brandstatter, J. J., Holden-Day, San Francisco, 1963.

80. Lura, H. E., "Tissue Reactions of Bone Upon Mechanical Stress", American Journal of Orthodonics, Vol. 38, 1952, pp. 453-459.

81. Martin, R. B., A Model for Bone and Other Porous Materials, Dissertation West Virginia University, Order Number 69-3082, University Microfilms, Ann Arbor, 1970.

82. Martin, R. B., "The Effects of Geometric Feedback in the Development of Osteoporosis", Journal of Biomechanics, Vol. 5, 1972, pp. 447-455.

83. Mack, P. B., and LaChance, P. L., "Effects of Recumbancy and Space Flight on Bone Density", American Journal of Clinical Nutrition, Vol. 20, 1967, pp. 1194-1205.

84. Mack, P. B., LaChange, P. A., Vose, G. P., and Vogt, F. B., "Bone Deminerialization of the Foot and Hand of Geminii IV, V, and VII Astronauts During Orbital Flight", American Journal of Roentgenology, Vol. 100, 1967, pp. 503-511.

85. Marino, A. A., and Becker, R. O., "The Effect of Electrical Current on Rat Tail Tendon Collagen Solution", Calcified Tissue Research, Vol. 4, No. 4, 1970, pp. 330-338.

86. Maximow, A., and Bloom, W., Histology, 7th ed., W. B. Saunders, Philadelphia, 1957.

87. McLean, F. C., "The Ultrastructure of Function of Bone", Science, Vol. 127, February, 2, 1958, p. 451.

88. McLeish, R. D., and Charnley, J., "Abduction Forces in the One-Legged Stance", Journal of Biomechanics, Vol. 3, 1970, pp. 191-209.

89. McLean, F. C., and Urist, M. R., Bone, 3rd ed., University of Chicago, 1968.

90. Muskhelishvili, N. I., Some Basic Problems of the Mathematical Theory of Elasticity, P. Noordhoff, N. V., Groningen, 1953.

91. Neuman, W., and Neuman, M., The Biochemistry of Bone Material, University of Chicago, 1958.

92. Pauwels, F., "Die Bedeutung der Bauprinzipien der unteren Extremität für Beanspruchung des Beinskelettes", Zeitschrift für anatomie und Entwicklungsgeschichte, Vol. 114, 1950, pp. 525-538.

93. Pauwels, F., "Die Bedeutung der Muskelkräfte für die Regelung der Beanspruchung de Rohrenknochens wahrend der Bewegung der Glieder", Zeitschrift für Anatomie und Entwicklungsgeschichte, Vol. 115, 1950, pp. 327-351.

94. Pugh, J. W., Radin, E. L., and Rose, R. M., "Quantitative Studies of Human-Subchondral Cancellous Bone", Journal of Bone and Joint Surgery, Vol. 56-A, 1974, pp. 313-321

95. Rambaut, P. C., Smith, M. C., Mach, P. B. , and Vogel, J. M., "Skeletal Response", Chapter 7 in Biomedical Results of Apollo, NASA SP-368, eds. Johnston, R. S., Dietlein, L. F., and Berry, C. A., Scientific and Technical Office, NASA, Washington, D. C., 1975.

96. Raux, P., Towsend, P. R., Miegel, R., Rose, R. M., and Radin, E. L. "Trabecular Architecture of the Human Patella", Journal of Biomechanics, Vol. 8, 1975, pp. 1-7.

97. Rockoff, S. D., "Radiographic Trabecular Quantitation of Human Vertebrae in Situ: Progress in Development of Methods and Digital Computer Analysis", in Proceedings of the Conference: "Progress in Methods of Bone Mineral Measurements", U. S. Government Printing Office, 1968, pp. 331-351

98. Scott, J. H., "The Mechanical Basis of Bone Formation", Journal of Bone and Joint Surgery, Vol. 39B, 1957, pp. 134-144.

99. Sedlin, E. D., "A Rheological Model for Cortical Bone", Acta Orthopedica Scandinavica, Supplement Number 83, 1965.

100. Seireg, A., and Kempke, W., "Behavior of in Vivo Bone under Cyclic Loading", Journal of Biomechanics, Vol. 2, 1969, pp. 455-461.

101. Singh, M., Nagrath, A. R., and Maini, P. S., "Changes in Trabecular Pattern of the Upper End of the Femur as an Index of Osteoporosis", Journal of Bone and Joint Surgery, Vol. 52-A, 1970, pp. 457-467.

102. Smith, J. W., "The Arrangement of Collagen Fiber in Human Secondary Osteones", Journal of Bone and Joint Surgery, Vol. 42-B, 1960, pp. 588-605.

103. Sokolnikoff, I. S., Mathematical Theory of Elasticity, McGraw-Hill, New York, 1956.

104. Struble, R. A., Non-Linear Differential Equations, Mc-Graw Hill, New York, 1962.

105. Swanson, G. T., and Lafferty, J. F., "Electrical Properties of Bone as a Function of Age, Immobilization and Vibration", Journal of Biomechanics, Vol. 5, 1972, pp. 261-266.

106. Taylor, A. E., Calculus with Analytic Geometry, Prentice-Hall, Englewood Cliffs, New Jersey, 1959, pp. 294-300.

107. Tobin, William J., "An Atlas of the Comparative Anatomy of the Upper End of the Femur: Part I", Clinical Orthopedics, Number 56, 1968, pp. 83-103.

108. Townsend, P. R., Rose, R. M., and Radin, E. L., "Bulking Studies of Human Trabeculae", Journal of Biomechanics, Vol. 8, 1975, pp. 199-201.

109. Truesdell, C., and Toupin, R., Handbook of Physics, Vol. III/I, Springer, New York, 1960.

110. Truesdell, C., and Noll, W., Handbook of Physics, Vol. III/3, "Non-Linear Field Theories", Springer, New York, 1965.

111. Underwood, Ervin E., Quantitative Sterology, Addison-Wesley, Reading Mass., 1970.

112. Vose, G. P., and Kubala, A. L., "Bone Strength: Its Relationship to X-Ray Determined Ash Content", Human Biology, Vol. 31, 1959, pp. 262-270.

113. Welch, D. O., "The Composite Structure of Bone and Its Response to Mechanical Stress", Recent Advances in Engineering Science, A. C. Eringen, ed., Gordon and Breach, New York, 1970, pp. 245-262.

114. Wolff, J., Das Gesetz der Transformation der Knochen, A. Hirschwald, Berlin, 1892.

115. Zienkiewicz, O. C., The Finite Element Method in Engineering Science, 2d ed., McGraw-Hill, New York, 1971.

116. Zubov, V. I., Methods of A. M. Lyapunov and Their Application, trans. A. E. C., ed., L. F. Boron, P. Noordhoff Ltd., Groningen, 1964.

☆U.S.Government Printing Office: 1978 — 757-080/663